

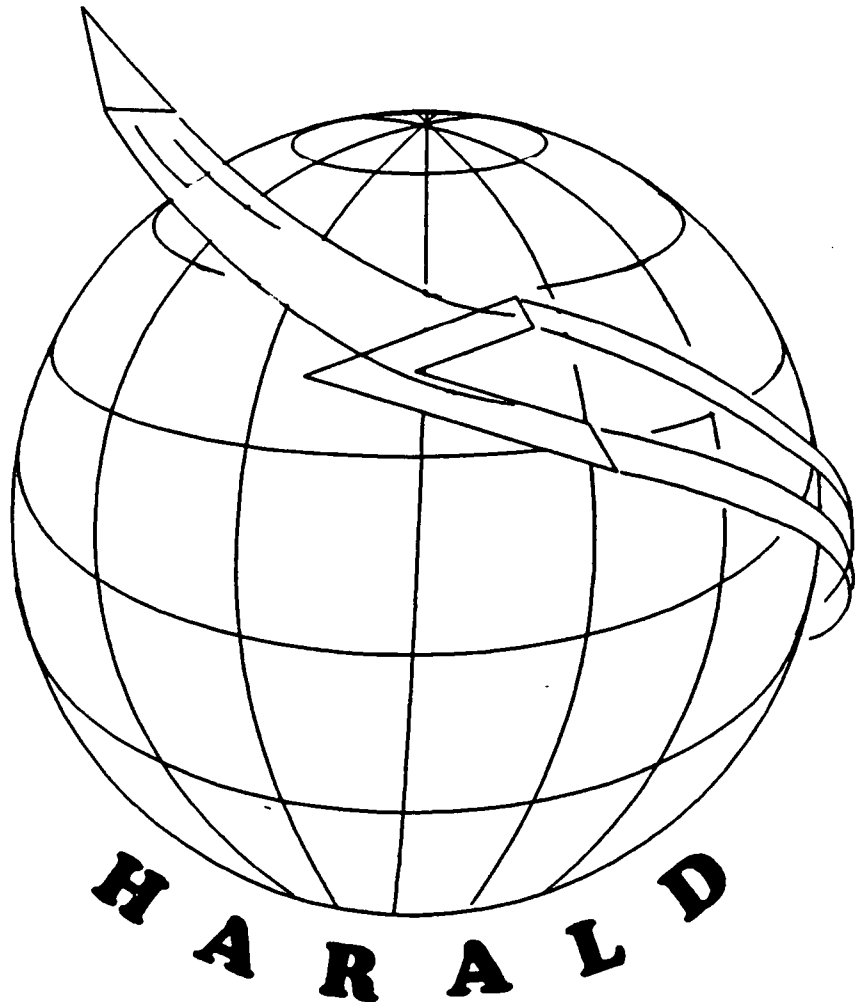
Report LR-764

Hypersonic Airbreathing Reusable Advanced Launcher

A feasibility study

October 1993

J. Bakker / A.R. Kraa (editors)



HARALD

**HYPERSONIC
AIRBREATHING
REUSABLE
ADVANCED
LAUNCHER**

**a feasibility study
under the guidance of
ir. B.T.C. Zandbergen**

October 1993

**Delft University of Technology
Faculty of Aerospace Engineering**

© HARALD, October 1993
In cooperation with *J&A productions*®

No part of this report may be reproduced, stored in a retrieval system,
or transcribed in any language without paying a large sum of money to J&A productions.

Editorial production/supervision : Jorgo Bakker & Adri Kraa
Lay-out : Jorgo Bakker

This report is edited with Wordperfect 5.1. Most illustrations and figures are drawn in Wordperfect Presentation 2.0, AutoCad 12, Lotus 123 and Slide.

Foreword

Since 1988, Delft University of Technology, Faculty of Aerospace Engineering, each year has organised a group-study project in space engineering as part of the third year curriculum in aerospace engineering. This academic year (1992-1993), the feasibility of a low-cost, two-stage-to-orbit aerospace plane type of space launcher with an airbreathing first stage and a rocket-propelled second stage has been selected as the study topic.

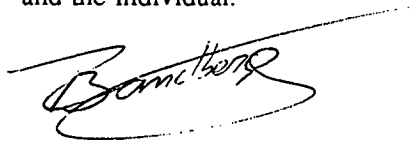
The motivation for this topic is that low cost space launchers are critical for expanding men's current space activities and that the introduction of airplane-like features, hence aerospace planes, like wings and airbreathing jet propulsion, in the design of space launchers presents new ways for reducing costs. However, the US Space Shuttle, which can be seen as the very first aerospace plane, clearly demonstrates that the introduction of airplane-like features also can lead to an increase in costs due to excessively high development and operations costs. This then clearly illustrates the challenge to the aerospace plane designer of finding ways of incorporating airplane-like features in the design without increasing development and operations costs too much.

The design team consisted of 24 students and 4 TWAIO's of the Faculty, who were organized in 8 groups, including management, system engineering, aerodynamics and propulsion. Guidance has been provided by the faculty on project management, system engineering, (progress) reporting, oral presentation, communication in general, and in the specialist disciplines: aerodynamics, propulsion, structures and flight dynamics. In this respect, also the help of specialists from Fokker Space & Systems B.V., Stork Product Engineering B.V., TNO and NLR is gratefully acknowledged.

Initial operations (customer) requirements for the launcher to be designed have been provided by the Faculty. Functional requirements have been derived partially based on a set of requirements generated as part of the national study program on advanced launcher technology; AEOLUS. The design itself has been accomplished in about 30 working days divided over the period starting February 11, 1993 and ending with a formal final presentation on June 30, 1993. Outputs of the design project are:

- 1) a mid-term and a final presentation
- 2) an individual report (20-30 pp.) for each student, and
- 3) a comprehensive overall report (of about 140 pp.).

Considering the efforts of the students, the extent of the work covered in this overall report, and the limited time available in the curriculum (nominal 240 hours per student), I have to congratulate the project team with its design of a Hypersonic Advanced Reusable Airbreathing Launcher Design (HARALD). It is 'HARALD', which clearly demonstrates the learning abilities of both the team, and the individual.



ir. B.T.C. Zandbergen

Delft, May 1994

Thanks

We would like to thank the following persons for providing us with useful advice:

FSS

Herwaarden, van, J.Ph.
Sudmeijer, K.J.
Wegereef, J.W.

NLR-Noordoostpolder

Wolf, de, W.B.

PML-TNO

Elands, P.J.M.
Veraar, R.G.

SPE

Broek, van den, M.J.R.
Dijk, van, M.J.
Nieuwenhuizen, van, M.P.

TUD-LR

Marée, A.G.M.
Rothwell, A.
Wittenberg, H.
Wakker, K.F.
Bannink, W.J.
Mooij, E.
Baten, van, T.J.
Broek, van den, P.Ph.

Project participants

Management

Bakker, J.
Kreuwel, W.H.
Vossepoel, F.C.

System Engineering

Kraa, A.R.
Oving, B.

Mission

Bos, M.S.
Sprenger, M.L.M.
Vorm, van der, P.A.

Costs

Frenken, G.W.R.
Punt, P.C.

Aerodynamics

Broomhead, M.J.
Buyten, A.
Linden, van der, B.J.
Pagen, M.
Spruyt, M.

Propulsion

Mijnen, P.
Verduijn, F.F.
Vliet, van, L.D.
Wiel, van der, R.A.N.

Structures

Boogaard, M.J.
Brinkman, M.R.
Khodaparast, M.
Luipen, van, J.J.W.
Mourik, van, A.

Stability

Cremers, G.
Gastel, van, P.
Kolk, van de, C.B.

Abstract

After the first two and a half years of the study for aerospace engineer at TU-Delft, Faculty of Aerospace Engineering, students specializing in space technology can participate in a group-design exercise of a space vehicle.

The goal of this years exercise has been defined to perform a feasibility study of a space plane. In this respect, attention should be paid to the trajectory, the basic geometry and the weight distribution, the basic avionics, the aero(thermo)dynamic loads, the propulsion system as well as the costs.

To achieve this goal the group of students is subdivided into subgroups with their own specialty, like Management, System Engineering, Mission, Costs, Aero(thermo)dynamics, Propulsion, Structures and Stability.

Each group uses a set of requirements, based on requirements at a higher level in the hierarchy of the project.

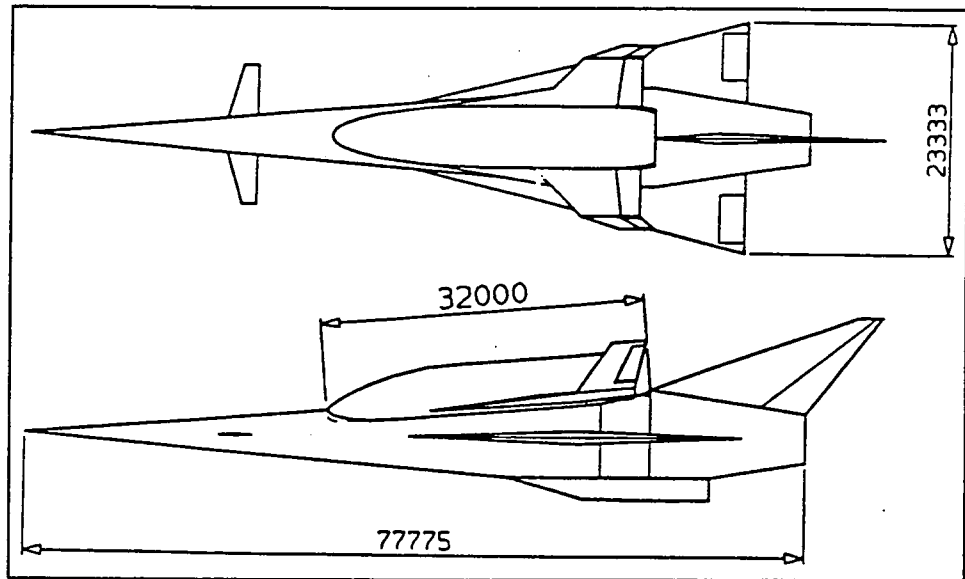
Based on the first level of requirements (the user's or operations requirements), Management and System Engineering formulate the functional requirements, in which starting points and constraints are stated. From this, System Engineering defines the task and output of every group. This output consists of data, that predicts the performance of the chosen baseline vehicle. After combining these data, scaling of the baseline vehicle is applied to meet the specifications.

This has resulted in a vehicle named HARALD, i.e. a reusable two-stage-to-orbit horizontal take-off and landing winged launcher. Some characteristics of HARALD are:

- Geometry of a winged-cone vehicle with a length of 78 meters;
- Total take-off weight of 355 Mg (including second stage);
- Adapted HORUS 3B as the second stage;
- 6 turbo ramjet engines with a total max. thrust of 8700 kN;
- 200 missions per vehicle;
- Development Cost of 4 vehicles of 27,3 billion US\$ (1992);
- Launch Cost of 45 million US\$ (1993);
- Separation of the second stage at an altitude of 32 km at $M=6.6$



Within the scope of this project, HARALD satisfies the user's requirements. In order to design a launch vehicle in more detail, more time to develop accurate prediction models is needed.



Basic geometry of HARALD

WING:

gross area	= 544.4 m ²
span	= 23.33 m
root chord	= 46.66 m
tip chord	= 0 m
MAC	= 31.1 m
taper ratio	= 0
sweep angle	= 76°

angle of incidence = 0°

thickness ratio = 0.04

aspect ratio = 1.0

FUSELAGE:

total length = 77.78 m

maximum height = 10.01 m

maximum width = 10.01 m



Contents

Preface	i
Abstract	ii
1 General Introduction	1.1
1.1 Background	1.1
1.2 Why designing a new launcher	1.1
1.3 Purpose of this project	1.2
1.4 Approach	1.2
1.5 Outline of this report	1.4
1.6 Remarks on this report	1.5
References	1.6
2 Requirements	2.1
2.1 Operational requirements	2.1
2.2 Functional requirements document	2.2
2.2.1 Starting points	2.3
2.2.2 Functional requirements for Subsystems	2.4
2.2.3 Constraints Requirements	2.5
2.2.4 Output of system engineering	2.6
2.3 Functional requirements of the modules	2.6
2.3.1 FRD Aerodynamics	2.6
2.3.2 FRD Propulsion	2.7
2.3.3 FRD Structures	2.8
2.3.4 FRD Stability	2.9
2.3.5 FRD Mission	2.10
2.3.6 FRD Costs	2.10
References	2.11
3 System Engineering	3.1
Abbreviations	3.1
3.1 Introduction	3.2
3.2 Tasks of System Engineering	3.3
3.3 Performance prediction	3.3
3.4 HORUS adaption	3.5
3.5 Photographic scaling	3.8
3.5.1 Scaling model	3.9
3.5.2 Results	3.13
3.6 Conclusions & Recommendations	3.19
3.7 References	3.21



4 Aerodynamics	4.1
Abbreviations	4.1
4.1 Introduction	4.2
4.2 Aerodynamic coefficients	4.3
4.2.1 Liftcoefficient	4.3
4.2.2 Dragcoefficient	4.6
4.2.3 Pitching-momentcoefficient	4.9
4.3 Heat flux	4.12
4.3.1 Flat-plate model	4.12
4.3.2 Stagnation Point	4.13
4.4 Effect of scaling	4.14
4.5 Conclusions & Recommendations	4.14
References	4.16
5 Propulsion	5.1
Abbreviations	5.1
5.1 Introduction	5.2
5.2 Powerplant layout	5.2
5.3 Thrust and specific impulse	5.4
5.3.1 The J. Propulsion model.	5.5
5.3.2 Verification	5.6
5.3.3 Effects of throttling and angle of attack	5.10
5.4 Cooling model for the engines	5.12
5.5 Mass of the propulsion system	5.13
5.6 Conclusions & Recommendations	5.15
References	5.17
6 Structures	6.1
Abbreviations	6.1
6.1 Introduction	6.2
6.2 Mass prediction model	6.2
6.2.1 Mass-breakdown	6.2
6.2.2 Determination of the masses	6.3
6.3 Verification, validation and qualification of the model	6.4
6.4 Adaption of the model for the HARALD	6.5
6.5 Internal layout	6.6
6.5.1 Canard	6.7
6.5.2 Gear	6.7
6.5.3 Flight deck	6.7
6.5.4 Fuel tanks	6.7
6.6 Prediction of the cg-position	6.8
6.7 Results	6.9
6.8 Conclusion & Recommendations	6.12
References	6.13



7 Stability & Control	7.1
Abbreviations	7.1
7.1 Introduction	7.2
7.2 Static stability requirements	7.3
7.2.1 Static longitudinal stability	7.3
7.2.2 Static directional stability	7.5
7.3 Trimmed flight	7.6
7.4 Effects of the canard on stability and control	7.7
7.5 Conclusions & Recommendations	7.10
References	7.11
8 Mission	8.1
Abbreviations	8.1
8.1 Introduction	8.2
8.2 Methods and results	8.3
8.2.1 Take-off	8.3
8.2.2 Ascent of both stages	8.4
8.2.3 Ascent of second stage	8.7
8.3 Effect of scaling	8.10
8.4 Conclusions & Recommendations	8.10
References	8.11
9 Costs	9.1
Abbreviations	9.1
9.1 Introduction	9.2
9.2 The CEMR model	9.3
9.3 The TRANSCOST model	9.5
9.4 Sensitivity analysis	9.8
9.5 Break-even-point	9.10
9.6 Conclusions & Recommendations	9.11
References	9.12

Credits



1 General Introduction

1.1 Background

In the third year of the study program of TU-Delft, Faculty of Aerospace Engineering, students specializing in space technology can participate in a group-design exercise of a space vehicle. Aim of this exercise is to learn to apply and integrate the knowledge and experiences learned so far as well as about aspects concerning team work, coordination of work, progress reporting and so on. This year, the students joined in a group-design study of a space plane (ref. [1.1]).

Since the design team had very little design experience, the depth of the study has been limited to the conceptual design of a single concept. As a result, the project is not complete yet, and a lot of investigation can still be done. This project could be continued for several years as also many points remain for further analysis. With the help of our recommendations, the project can be worked out in more detail.

1.2 Why designing a new launcher

The present generation of space launch vehicles is the generation of expendable launch systems. However, in various countries a lot of research is done on developing new types of space launch vehicles. Why? It is expected that our space activities will expand, and to meet this expansion, it is essential to reduce the launch costs (ref. [1.2]). Furthermore we have to increase the reliability and safety of the launchers.

Modern technology indicates that in the next decade these conditions will be met.

In contrast to the Space Shuttle concept - which is a multi purpose system - we might have to develop different optimal transportation systems: each for different transportation tasks. A vehicle scheme of next generation space launchers can be:

- Heavy-lift Cargo up to 150 tons
- Medium-size Payloads
- Manned Operations and space stations supply



For the last, which has to be the safest configuration because of manned flight, the Horizontal Take-Off and Landing [HTOL] Winged Launch Vehicle is probably the most convenient vehicle. Together with air-breathing engines it provides safe take-off and landing, cruise capability during ascent and landing. It might even use conventional airfields, so no highly-expensive launch areas have to be built. For this last reason, the take-off mass is limited to 400-500 tons, in addition the payload is limited to 3 to 5 tons.

1.3 Purpose of this project

The purpose of this project can be divided in the following:

- To make a design conform the user's requirements.
- To learn about aspects of working in a team.

The goal is to obtain a conceptional design in which the following topics will be paid attention to:

- mission profile and possible trajectory
- basic geometry
- weight and weight distribution
- basic avionics
- aero(thermo)dynamic loads
- lay out of the propulsion system
- costs.

This report describes the work done by 29 students, in various stages of the study, during the first half of 1993 on a HTOL Two Stage To Orbit concept, called HARALD - a Hypersonic Advanced Reusable Air-breathing Launcher Design.

We emphasize the fact that this report is based on the draft results, as they were available at the final presentation, July 1993.

1.4 Approach

Requirements

Requirements allow complete coverage at any level of detail during the project (ref. [1.3]). They show what is wanted and are the communication path between customer, management and designers (see chapter 2 for detailed description of the requirements).

Every individual discipline uses a set of requirements, based on



requirements at a higher level in the hierarchy of the project (figure 1.1).

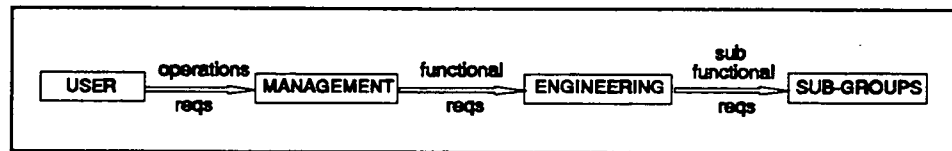


Figure 1.1

requirements documents hierarchy

Breakdown of the team by discipline

The team is divided in several groups (ref. [1.4]), each with a different (technical) discipline and requirements based on that discipline (figure 1.2). In this figure, management stands on top.

The management team consists of:

- a project manager;
- a configuration manager and
- a documentation manager.

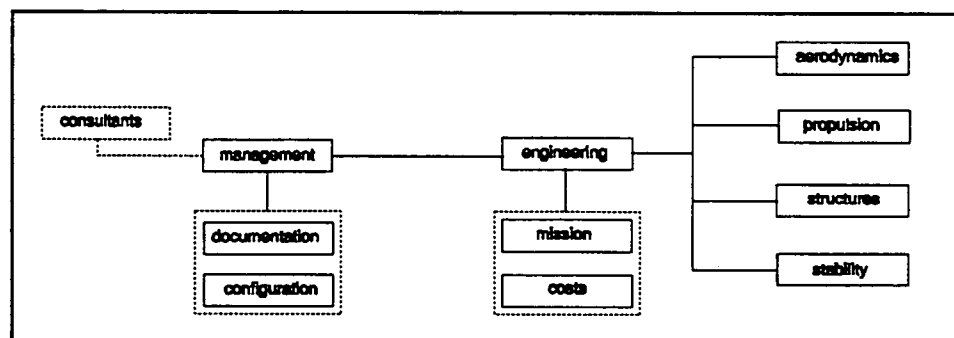


Figure 1.2

team breakdown in modules

The configuration manager keeps control of the configuration control, a document consisting of the latest data of HARALD (ref. [1.5]). The configuration manager also controls the functional requirements document, i.e. the requirements distilled from the operations requirements (see chapter 2).

During this project numerous reports are made. The documentation manager takes care of archiving these, setting up document standards. Also he created a document called Space Directory (ref. [1.6]). This document consists of data of various launchers, existing and conceptual ones. The specialized modules use the data in the Space Directory to verify their models (fig. 1.3).

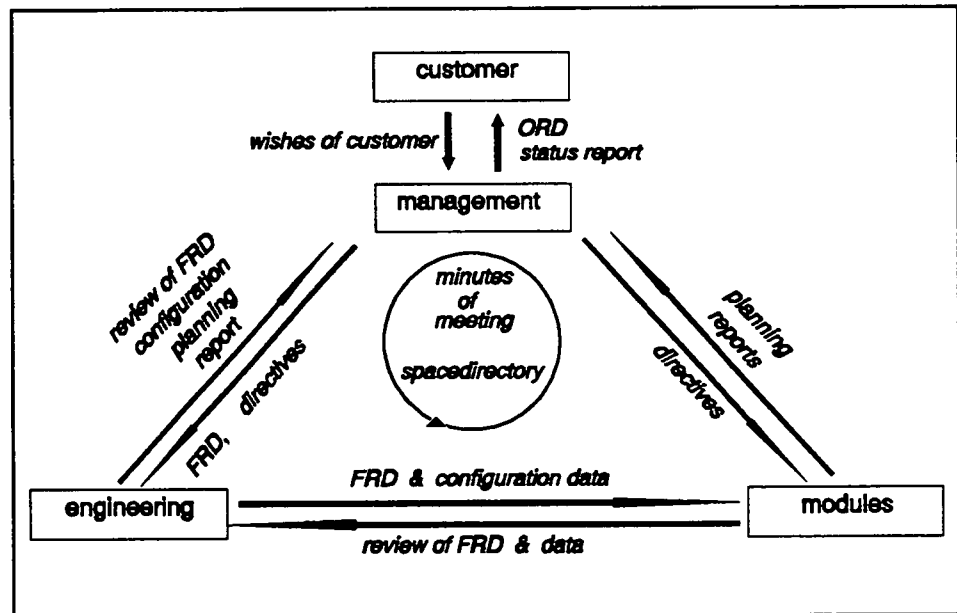


The project manager is responsible for the total project, the results, status report, PR and he also was the chairman of meetings.

Communications

Besides verbal communication, transfer of information took place by:

- a (weekly) technical meeting with management, system engineering and a sub-group;
- progress meeting every two weeks;
- requirements documents and their reviews;
- reports and their reviews;
- data flow between the modules (see chapter 3) and
- presentation of the progress and results: a mid-term and a final review.



Planning of the project in time

A global planning of the project is given in figure 1.3.

1.5 Outline of this report

The students were divided in several groups, each with their own speciality. In this report an overview of the studies performed by these groups is given. In chapter 2, the Operations Requirements [OR] are



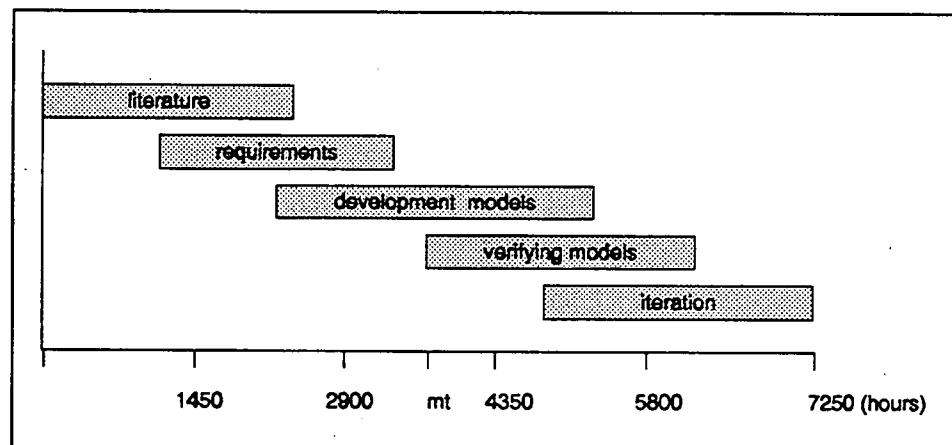


figure 1.3

time planning

given. These are the general specifications from the client (i.e. the project coordinator). Based on the OR more detailed requirements are set up in the Functional Requirements Document (FRD), which contain the requirements for the different subsystems of the spaceplane. A summary of these FRD's can also be found in this part.

Chapter 3 presents the work of the System Engineering group. By getting detailed information of four specialists groups, System Engineering could make their design decisions. These four specialists groups are: Aerothermodynamics (chapter 4), Propulsion (chapter 5), Structures & Materials (chapter 6), and Stability & Control (chapter 7). Also System Engineering was supported by two other specialists groups including the Mission group (chapter 8) and the Costs group (chapter 9).

1.6 Remarks on this report

This report is primarily based on the work documented in the *draft* reports of the different groups contributing to the HARALD-project. These draft reports date back to August-September 1993.

Since that time, some of the groups have improved their models and corrected for some mistakes made during the process of developing their models. However, the time available for this report did not permit to include all these changes, so some errors might exist. The readers of this report, though, have to keep in mind that the main goal of this report is to present a coherent view of the overall project and the total effort involved.



References

- [1.1] Zandbergen, B.T.C. A TSTO horizontal take-off air-breathing space launcher, proposal for a conceptual design study, TU Delft, 1992
- [1.2] Koelle, D.E. Cost-Optimized Launch Vehicle Design, AIAA Paper 92-1281, 1992
- [1.3] Stevens, R.C. Some considerations on requirements for system management, ESA Journal 1991, vol. 15, ESRIN, Italy, 1991
- [1.4] Bakker, J. HARALD Management report, HAR-MAN-001, TU Delft, 1993
- [1.5] Vossepoel, F.C. Configuration Management of a conceptual design, HAR-CON-001, TU Delft, 1993
- [1.6] Kreuwel, W.H. HARALD Documentation Report, HAR-DOC-001, TU Delft, 1993



2 Requirements

Requirements allow complete coverage at any level of detail during the project. They show what is wanted and are the communication path between customer, management and designers (ref. [2.1]). In this chapter the operations and functional requirements are set out.

2.1 Operational requirements

The first requirements to be produced are the operations requirements (OR), defining what the customer want. They describe the problem, not the solution.

The following requirements are the guideline for the HARALD-team. They were accomplished by the customer and management (ref. [2.2]).

OR1 circular orbit, height 200 km, inclined 28.5°

OR2 an unmanned payload of 5000 kg with a volume of 60 m³
The payload will consist of either satellites or parts (units) of a future spacelab.

OR3 cruise capability of 1000 km

OR4 limited development time
The first launch is set for 2010.

OR5 launch & landing site close to the equator
This is the most convenient site, using the earth rotation.

OR6 use of conventional airfields
Because of the number of launches a year, it will be convenient to use conventional airfields. As a result there is no need to build expensive launch sites, but the launcher will have to have a horizontal take-off and landing.

OR7 reusability
In order to keep the productions costs low, as many parts as



possible have to be reusable. The degree of reusability has to be determined.

OR8 40 to 60 launches a year

In the past, launchers were developed for bigger payloads and so the overall costs boomed in order to meet these payloads. OR8 - together with OR2 - will result in a modest payload into LEO but able to fly frequently.

OR9 low costs

- The research and development costs of the prototype launcher will not exceed the maximum of 30 billion US\$ (1992).
- The launch costs may not exceed the launch costs of ARIANE 4

OR10 flexibility

Because of the planned flights a year, the launchers ought to be made operational as quick as possible. In case of rescue missions a launch on demand is required.

OR11 reliability comparable to Ariane 5 (manned version)

A high reliability is required in order to :

- insure the life of the crew
- keep insurance costs low.

2.2 Functional requirements document

The FRD is distilled from the OR's and this FRD is a management tool to control the project development. Moreover it is a guideline for SE.

Functional requirements define what the system must do -without stating how it is to be done; they describe the system. They define the system capability, do not restrict system engineer creativity and allow to make a realistic cost-estimation.

The FRD is divided in four parts (ref. [2.3]):

- starting points;
- sub-systems that has to be examined;
- constraints;



→ the output of SE

2.2.1 Starting points

Starting points are those limitations chosen by management and SE to exclude subjects which the HARALD-team cannot cope with or the team (because of limited time) cannot pay attention to.

The starting points are:

Two Stage to Orbit

Limitation of development time demands the use of recent technology. Single stage to orbit might be a possible design. The technological realisation of it still needs a lot of research, since no SSTO vehicle is already in such a phase of development that realisation before 2010 can be expected. So designing a SSTO vehicle to meet the given operational requirements can not be realised within the given time frame.

A design with a higher number of stages, which may seem attractive because of it's higher payload ratio, is only possible in a different configuration . It remains to be examined if such a configuration can be launched on a conventional airfield without too much extra costs. For reasons of limited time and financial resources, this possibility will not be looked at.

A great advantage of the use of two stages is the possibility it offers for reusability of both stages. As a result flexibility can be realised more easily than with configurations with a higher number of stages. Failure is more likely to happen when the construction becomes more complex, as would be the case with more than two reusable stages.

Air-breathing (First stage)

To bring the vehicle in flight weight should be minimized and thrust should be sufficient to cause enough lift. A way to minimize the weight with a given thrust, is to make use of an oxidator that does not need to be carried along: the oxygen in our atmosphere.

By taking away the need of oxygen tanks the structure can be lighter. Thus the structure can remain simple and costs can be saved.

In contrast with other possible (rocket) engines, reusability can be realised with air-breathing propulsion. Air-breathing engines will not be thrown away after use, but can be used again after some revision.



Take off and landing horizontally (BOTH stages)

Vertical launching requires special equipment, which is not present at most conventional airfields. The adjustments needed for such a launching will take time and money to realize. Also the security measurements of a vertical launching decreases the flexibility of the mission.

The reusability of both launching equipment and vehicle can be realized cheaper with horizontal take off.

The possibility to land on a conventional airfield will increase the flexibility of the mission, since -in case of any abort- landing can take place on different locations, without consequences for the reusability or safety.

Second stage separates at supersonic speed

Since development time is limited, a choice had to be made between sub- and supersonic separation. The choice of supersonic separation enables us to use the reference trajectory of the Sanger.

Baseline design of first stage is winged-cone vehicle

As a result of time restriction a reference vehicle is chosen as a baseline design. With aspect to the take off and landing features, the choice of the winged-cone vehicle is made. Doing so flexibility and reliability are maximized, while costs are kept low.

Second stage will be a scaled version of HORUS 3B

HORUS 3B can meet the requirements of the reusability and the number of launches, since it's configuration offers good possibilities for horizontal take off and landing. The data of the 3B version of the HORUS are most complete,so using those, time and money can be minimized, while requirements of reliability can be met.

To meet the required payload volume and the required orbit, the HORUS 3B only needs to be scaled photographically.

The second stage will be attached to the first one in such a configuration that stability can be realized.

2.2.2 Functional requirements for Subsystems

System Engineering has to take into account the following main subjects: The structural system, the propulsion system, the stability and the aero(thermo)dynamics.



Structural System

- | | |
|----------------|------------------------------------|
| → body | → wings |
| → tail | → canard (extendibility of canard) |
| → landing gear | → fixed equipment |
| → fuel tanks | → power plant |
| → payload | → fuel |

Propulsion System

- air-breathing engine(s) for first stage: turbo-ramjets
- number of engines for first stage
- type of fuel for first stage

Stability

HARALD has to be stable and trimmed during his mission, only static stability will be examined.

Thermo- and Aerodynamics

- temperature/ heat loads
- L over D
- pressures

2.2.3 Constraints Requirements

The importance of putting constraints on the design is obvious: Since time and knowledge are restricted, it will be impossible to give a detailed description of all aspects of the design.

The analysis will be concerned within the following constraints:

- Attention will be limited to the initial phase, so testing as well as failure possibilities will not be considered.
- Propulsion and aerodynamics will only be examined for the first stage (for reasons of time restriction).
- No complex mass estimations will be made.
- The dynamic stability will not be considered.



- Side slip is excluded as a possible avionic parameter.
- Effects on the environment, such as noise and pollution will not be regarded.
- The calculations have to be verified and be correct in a accuracy of 30 %, as only conceptual design is regarded.
- The detailed avionics system, such as the electrical and hydraulic system will not be considered.
- Provisions for manned flight are not examined.
- The operational readiness target can not be specified.
- The atmospherical data are those of the ICAO standard atmosphere.
- Acceleration limited to $a/g = 5$ for the second stage
- Acceleration of the first stage limited to $a/g = 3$.
- The dynamic pressure may not exceed 60 kPa.
- The general lay out should be of such shape that the plane is able to take off and land on an airfield meant for regular aircraft.

2.2.4 Output of system engineering

System engineering has to report the global performance of HARALD to management.

The output of system engineering is defined by :

- general data in tabular and graphical form for typical data of the design characteristics, which are necessary to understand the progress of this design study.
- review on the Functional Requirements
- review on the Constraints Requirements
- status report

2.3 Functional requirements of the modules

Out of the FRD from management to SE, system engineering has built up the detailed functional requirements for the sub-groups.

A short summarize of those FRD's will follow in the next para-graphs.

2.3.1 FRD Aerodynamics

Summarised, the output that has to be delivered should consist of:



-
- O1) The verification of the C_l -of the WCRV report- as function of R1 and R3.
 - O2) The calculation of C_{d0} and as function of R1 and R2.
 - O3) Heatflux (Watt/m^2) as a function of R1 and x-coordinate.
 - O4) Sensitivity study upon the effect of altitude on O1 and O2
 - O5) Accuracy and margins of NLRAERO and EULER

Range of parameters:

- R1) Mach number $0 < M < 7$
- R2) Altitude $0 < h < 35 \text{ km}$
- R3) Angle of attack $-1 < \alpha < 10 \text{ deg}$

Constrained parameters:

- C1) T_{max} of the structure 700 K

The output should be given in graphics and in tabular form to improve comparison between HARALD and other TSTO vehicles.

2.3.2 FRD Propulsion

The propulsion system is defined as to consist of:

- 1) turbo/ramjet engines
- 2) fuel system
- 3) cooling system
- 4) tanks
- 5) propellants

Summarised, the output that has to be delivered should consist of:

- O1) net uninstalled thrust of the turbo/ramjet engine as a function of R1, R2 and R3
- O2) the specific impulse of the turbo/ramjet engine as a function of R2 and R3
- O3) The thrust and the specific impulse when cruising.
- O4) the mass of the engines, the fuel system and the cooling system as a function of R1
- O5) the volume of the two tank options as a function of;
the length to thickness ratio
- O6) the lay out of the integrated turbo/ramjet engines as a function of R1
- O7) an estimation of the accuracy of the output (O1 to O6) that is



required.

(where R_i is defined below)
(i denotes the number)

Range of parameters:

- R1) engine total frontal intake area $23 < A_e < 45 \text{ m}^2$
 R2) number of Mach $0 < M < 7.5$
 R3) Altitude $0 < H < 35 \text{ km}$

Constrained parameters:

- C1) temp.in the ramjet combustion chamber: $T_{cc_{max}} = 3000 \text{ K}$
 C2) temperature of the turbine entrance: $T_{cc_{max}} = 1600 \text{ K}$

The output should be given in graphics and in tabular form to improve comparison between HARALD and other TSTO vehicles.

2.3.3 FRD Structures

Summarised, the output that has to be delivered should consist of :

- O1) A (mass)breakdown in the different subsystems and lay out of these subsystems. Determination of place for retractable canard and landing gear.
 O2) A volume estimate of the subsystems
 O3) Calculation of the centre of gravity of the different subsystems and the integrated system.
 O4) Determine whether to use passive or active TPS. Mass TPS as function of q . Suggestions about the materials (besides Titanium) that should be used.
 O5) Calculation of the moments of inertia for the integrated system.
 O6) Determination of the max fuel weight.
 O7) Determination of fuel tank mass: 4 cylindrical tanks with elliptical ends.

Range of parameters:

- R1) The load factors: $n_{ax} = 1.5$
 $n_{norm} = 3.5 \pm 0.5$

Constrained parameters:



- | | | |
|-----|-----------------------|---------------------------|
| C1) | Tmax of the structure | 700-750 K |
| C2) | Max. heatflux | 2 MWatts/m ² |
| C3) | c.g. | 60% - 70% of total length |

The output should be given in tabular and in graphical form to improve comparison between HARALD and other TSTO vehicles.

2.3.4 FRD Stability

Definition of the Aerodynamic Control Surfaces

- 1) elevons
- 2) rudder
- 3) canards

Summarized, the output that has to be delivered should consist of;

- O1) the longitudinal Static Margin (and C_m -alpha) as a function of R1, R2, R3 and C7.
- O2) the trimmed lift and drag coefficients as a function of R1, R2, R3 and C7.
- O3) the deflections of the elevons and rudder when achieving the trimmed flight condition as a function of C7.
- O4) recommendations of options to improve the Static Margin and to minimize the trimmed drag as a function of C5, C6, C7 and the order of succession of operationable tanks.
- O5) Investigation of the directional Static Margin.
- O6) an estimation of the accuracy of the given output.
- O7) an investigation of the effect of the wake of the HORUS and recommendations to minimize this effect.

Where R_i , C_i are given below.
(i denotes the number)

Range of parameters:

- | | | |
|-----|-------------------|----------------------|
| R1) | Mach number | $0 < M < 7.5$ |
| R2) | Altitude | $0 < H < 35$ |
| R3) | Angle of attack | $-1 < \alpha < 10$ |
| R4) | Centre of gravity | $60\% < c.g. < 70\%$ |

Constrained parameters:

- | | | |
|-----|-------------------|-------------------------------|
| C1) | Rudder deflection | $-20 < \delta_r < 20$ degrees |
| C2) | Elevon deflection | $-20 < \delta_e < 20$ degrees |



C3)	Acceleration	$-3 < a/g < 3$
C4)	Dynamic pressure	$0 < q < 60 \text{ kPa}$
C5)	Position of the canard	$10000 < x\text{-can} < 51400 \text{ mm}$
C6)	Position of the HORUS	$20700 < x\text{-hor} < 62200 \text{ mm}$
C7)	Angle of incidence of canard	$-10 < \delta\text{-c} < 10$
C8)	Static Margin	$SM > -5\%$ of mean aerodynamic chord

The output should be given in graphics and in tabular form to improve comparison between HARALD and other TSTO vehicles.

2.3.5 FRD Mission

Summarised, the output that has to be delivered should consist of:

O1)	trajectory	
O2)	take-off distance	s_{TO}
O3)	landing distance	s_{LA}
O4)	required fuel weight	$W_{f,req}$
O5)	engine cycle transition	M_{ECT}, h_{ECT}

Range of parameters:

R1)	wing loading	$10 \text{ kPa} < W/S < 30 \text{ kPa}$
R2)	thrust-weight ratio	$0,25 < F/W < 1,00$
R3)	lift coefficient	$0,01 < C_L < 1,00$

Constrained parameters:

C1)	max.dynamic pressure	50 kPa
C2)	max. field length	3200 m
C3)	max. acceleration	3 g (first stage) 5 g (second stage)

The output should be given in graphics and in tabular form to improve comparison between HARALD and other TSTO vehicles.

2.3.6 FRD Costs

Summarised, the output that has to be delivered should consist of:



- O1) development costs
- O2) production costs
- O3) operational costs
- O4) revenue
- O5) accuracy of the applied method

As a function of:

Range of parameters:

R1)	max.dynamic pressure	$40 \text{ kPa} < q_{\text{max}} < 80 \text{ kPa}$
R2)	fuel weight	$50 \text{ Mg} < W_f < 200 \text{ Mg}$
R3)	empty weight	$50 \text{ Mg} < W_e < 200 \text{ Mg}$
R4)	take-off weight	$100 \text{ Mg} < W_{\text{to}} < 500 \text{ Mg}$
R5)	take-off thrust	$1000 \text{ kN} < T_{\text{to}} < 5000 \text{ kN}$
R6)	fuel types	LH ₂ and CH ₄
R7)	materials	aluminium, titanium, nickel, steel

Constrained parameters:

C1)	number of launchers	3
C2)	life span	20 years
C3)	number of launches in a launcher's life	200
C4)	max. take-off weight	430 Mg
C5)	max.dynamic pressure	32,6 kPa
C6)	total budget	1992 US\$ 30.000.000.000 + 20%

References

- [2.1] Stevens, R.J. Some considerations on requirements for system management, ESA Journal 1991, Vol. 15 (35-48), ESRIN, Italy, 1991
- [2.2] Bakker, J HARALD management report, HAR-MAN-001, TU Delft, 1993
- [2.3] Vossepoel, F.C. Configuration Management of a conceptual design, HAR-CON-001, TU Delft, 1993



3 System Engineering

Abbreviations

SE	System Engineering
OR	Operational Requirements
FRD	Functional Requirements Document
WCRV	Winged Cone Reference Vehicle
λ_{eng}	scale factor of the total frontal intake area of the engine
λ_{tot}	scale factor of the whole vehicle
κ	$\lambda_{eng} / \lambda_{tot}$
h	altitude
v	velocity
m	mass
M	number of Mach
D	total drag
F_{ws}	thrust without scaling
F_{wp}	thrust without precompression
F	thrust after scaling, with precompression
L	total lift
W,t.o	total take off weight
Mg	Mega gram (1000 kg)
Isp	specific impulse
$C_d \text{ eng}$	percentage of the total drag due to the presence of the nacelle of the engine
$C_d \text{ 2nd}$	percentage of the total drag due to the presence of the second stage
C_{d0}	drag coefficient at zero lift
C_{dl}	drag coefficient due to lift
C_l	lift coefficient
PCM ₇	the amount of precompression at Mach=7
S_{ref}	reference area
S_{wet}	wetted area
M_0	initial mass
M_f	fuel mass
q	dynamic pressure
V_f	volume of fuel
V_{LOX}	volume of liquid oxygen tank
V_{LH2}	volume of liquid hydrogen tank



3.1 Introduction

In the Functional Requirements Document from Management to System Engineering it is stated that SE is responsible for the design of a launch vehicle that is in compliance with the specifications.

This means that first the performance of the launcher has to be predicted, after which this data is integrated in order to check the given specifications. If this check fails, the design is photographically scaled. Since the performance analysis is very elaborate, several groups will execute this task.

In the first paragraph the tasks of SE are stated.

The next paragraphs deal with the performance prediction and the adaption of the HORUS. In the last paragraphs the scaling model is discussed which was used to scale the first stage and some conclusions of SE are given.

Starting points

To make sure that the design of a launch vehicle would be completed within the limited time, starting points were given which would reduce the number of concepts.

The chance that the ultimate design would not be optimal, because of these starting points, was accepted.

Some of the most important starting points, which were stated before the subgroups would commence their work, are given below;

- The second stage will be mounted on top of the first stage. Because the second stage (HORUS 3B) was designed for this concept, no extensive adaptations were expected.
- The powerplant will be mounted underneath the fuselage. This was decided in accordance with 1) and because of the possibility of applying precompression.
- The priority of the prediction of the performance lies at the accent phase.
It was expected that the performance of the vehicle would be vitally during that phase.
- The Winged Cone Reference Vehicle (WCRV), which would serve as the baseline vehicle, will be photographically scaled



with a factor 1.5.

Because the operational requirements of the HARALD (ref. [3.1]) are almost similar to those of Sanger, it was expected that the amount of fuel necessary to reach the specified orbit would also have to be equal.

The volume available for fuel of the WCRV would equal that of Sanger when scaling was applied.

- In accordance with Sanger trajectory the separation speed was chosen to lie at Mach= 6.6 at an altitude of approximately 32 km.

These were the most important starting points.

Furthermore, SE uses Sanger as a guideline when choosing between concepts of a more detailed nature (p.e. number of engines).

3.2 Tasks of System Engineering

The tasks that followed from the requirement of SE being responsible for the design were stated as follows;

- SE should deliver data that predicts the performance of the design.
- SE should combine this data to deliver a semi-optimized design of the launcher which satisfies the Operational Requirements.

The first task could not be conducted by SE alone. Four subgroups will have to produce the necessary data which would then be gathered and checked by SE

In the fulfilment of the second task, SE was assisted by two more subgroups. Because it was decided to scale the vehicle to meet the requirements a semi-optimized design would be delivered. This is discussed later on.

3.3 Performance prediction

When designing a vehicle the performance of the design has to be known. In the conceptual design phase the most important design



drivers, such as the thrust, the weight, the aerodynamics etc. will be examined in order to make conclusions about the capabilities of the design.

Functional requirements

The data which is necessary to predict the performance will be produced by four of the subgroups. SE must decide, in accordance with the FRD from Management (ref. [3.2]), which data should be produced by which subgroup.

In fig 3.1 the data flow scheme is given. It can be seen that some of the output of a given subgroup will serve as a input for another subgroup.

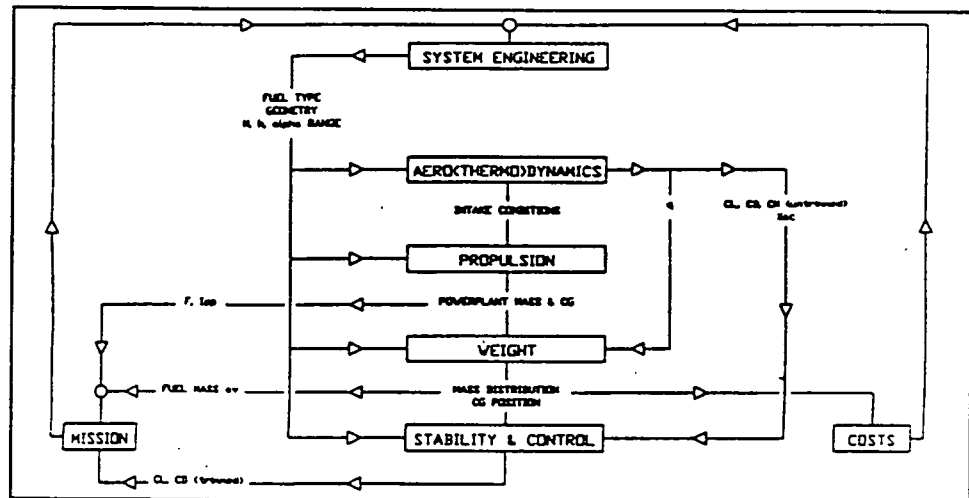


Figure 3.1

Design flow scheme

The means by which SE will fulfil its first task, are the functional requirements documents (FRD) for the subgroups.

To make sure that all the required data is delivered in the right form, SE introduced the functional requirements documents. In these documents it is clearly stated which tasks each subgroup has to perform. In chapter 2.3 a short summarisation of all the FRD.'s is given.

The structure of all these documents is the same.

First it is explained which parameters are important and for what purpose they have to be known. In the documents the constraints of the required data and the form in which they have to be delivered are given.



After this the output as well as the input is clearly specified in a summarisation.

In accordance with the second task of SE the FRD's specified the data which would be dependent on the size of the vehicle. To accommodate the scaling of the vehicle it was required to investigate the influence of scaling on this data.

Results

The most important data which predicts the performance of the launch vehicle are summarized below. These are the data which were delivered by the subgroups for the HARALD 1.5

- The aerodynamic coefficients of the vehicle were taken from the Winged Cone Reference Vehicle Report.
- From a Journal of Propulsion the specific impulse and the thrust for a integrated turbo-ramjet engine were found. For six engines a thrust at sea level of 1837 kN and a specific impulse of 4400 s. was calculated.
- The take off mass of the vehicle, including HORUS was predicted to be 428 Mg.
- A trajectory was delivered that was similar to that of Sanger.
- The development costs were estimated to be 11.9 billion dollars.

A drawing of the HARALD 1.5 and the HORUS 3B is given in figure 3.2

3.4 HORUS adaption

Part of the mission requirements is to bring a payload of 5 tons to a 100 km circular orbit. In the initial phase of the HARALD project the decision was made to emphasize on the first stage and to find and adjust the second stage. HORUS was chosen because it is the second stage of the Sanger which implicates that it is designed for our trajectory.

Since HORUS 3B has (ref. [3.3]) a payload mass of 2-3 Mg and a



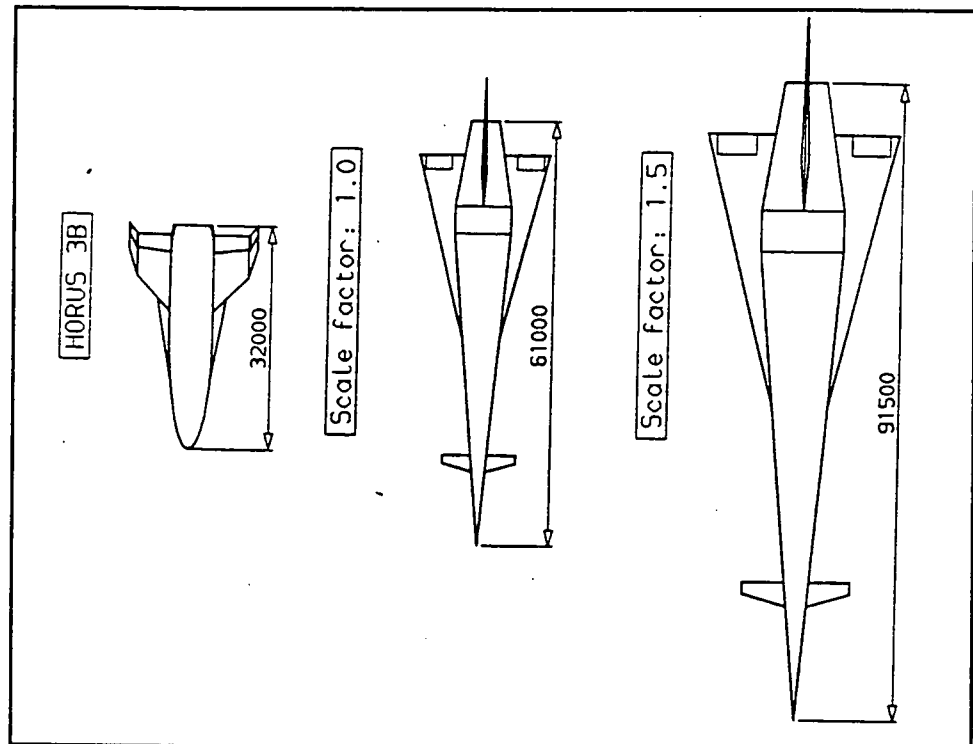


Figure 3.2

WCRV, HARALD 1.5 and HORUS 3B

payload volume of about 170 m^3 (instead of the 5 Mg payload mass and 100 m^3 as dedicated in the mission requirements) HORUS needs an adjustment of the payload mass and thus the propellant mass. After the adaption it should be verified if HORUS still satisfies the mission requirements.

HORUS 3B has an initial mass of 91 Mg and a propellant mass of 65 Mg(LH_2/LOX). Two high-pressure rocket engines with 700 kN each bring HORUS to its circular orbit.

Sizing of the propellant Mass

A simple method to size a launch vehicle is to use the rocket equation derived from Newton's second law with assumption of zero drag and gravity and constant thrust (ref. [3.4]):

$$\Delta V = g \cdot I_{sp} \ln \Lambda \quad [1]$$

where Δv is the velocity imparted to the rocket, I_{sp} is the specific



the vehicle's initial mass to final mass:

$$\Lambda = M_0 / (M_0 - M_f) \quad [2]$$

where M_0 is the initial mass and M_f is the fuel mass.

For HORUS 3B $\Lambda = 91 / (91 - 65) = 3.5$.

A simple method is to keep Λ constant with increasing M_0 , M_f and M_p . It can be expected that when this is done the mission requirements will still be satisfied.

$$M_0' = 91 + \Delta M_f + \Delta M_p \quad [3]$$

With a constant value of Λ ;

$$\Lambda_{\text{new}} = \Lambda_{\text{old}} \quad [4]$$

$$\Lambda = 91 + 2 + \Delta M_f / (91 + 2 - 65) = 3.5 \quad [5]$$

$$\Delta M_f = 5 \text{ Mg}$$

For safety reasons 2 Mg extra Fuel is taken into account. The new M_0 is 100 Mg. (This implicates a small increase of Λ).

The new masses are tabulated in table[1]

Volume

Due to the increase of M_f the LOX and LH₂ tank volumes increase.

$$\Delta V_f = \Delta V_{\text{LH}_2} + \Delta V_{\text{LOX}} \quad [6]$$

where V_f is the fuel volume, V_{LH_2} is the LH₂ tank volume and V_{LOX} is the LOX tank volume.

With a specific density of LOX (1.144 Mg/m³) and LH₂ (0.071 Mg/m³) and a mix ratio (LOX/LH₂) of 0.5 the new tank volumes are calculated with the next formula:

$$\begin{aligned} X (2 \cdot 0.071 + 1.144) &= 7 \text{ Mg} \\ X &= 5.44 \end{aligned} \quad [7]$$



The volume of the LOX tanks increase with 5.44 m^3 and the volume of the LH₂ tanks increase with $2 \times 5.43 = 10.88 \text{ m}^3$.

The total volume increase is 16.32 m^3 . The tank volumes are tabulated in table[2]

The volume increase due to fuel mass increase does not exceed the 70 m^3 , which mission requirements demands.

After a verification by the Mission group, it could be concluded that the adapted HORUS was still able to reach the required orbit.

	HORUS 3B	Resized
M_0	91 Mg	100 Mg
M_f	65 Mg	72 Mg
M_p	3 Mg	5 Mg

Table 3.1 *Mass of HORUS 3B compared to resized mass*

	HORUS 3B	Resized
V_{LOX}	50	55
V_{LH_2}	101	117
V_{TOT}	151	172

Table 3.2 *Tank volume of HORUS 3B compared to resized volume*

3.5 Photographic scaling

Photographic scaling is chosen as the tool for satisfying the OR most optimally (within the scope of the project). After all the performance prediction data is delivered, a scale factor could be necessary to scale the performance.

SE developed a model that indicates the scaling factor necessary.



3.5.1 Scaling model

The scaling model that has been developed is based on an AIAA paper by Chaput (ref [3.8]). This paper assumes that, by applying a photographic scale factor on a given baseline vehicle, it is possible to meet the requirements.

In the model the baseline vehicle is chosen to be the HARALD 1.5 (the WCRV scaled photographically with a factor 1.5). This vehicle will be optimally scaled when the amount of fuel required equals the amount of available fuel. When this is accomplished the model is assumed to be converged.

The required amount of fuel can be found from;

$$W_{i+1} \approx \frac{W_i}{\exp\left(\frac{(\sqrt{v_{i+1}^2 + 2g(h_{i+1} - h_i)} - v_i)}{gI_{sp}\left(1 - \frac{D_i}{F_i}\right)}\right)} \quad [8]$$

The required amount of fuel follows after summation, until the required velocity and altitude are achieved.

When all the parameters in this equation are known the scale factor can be found from;

$$\lambda = \sqrt[3]{\frac{W_{\text{tank}(\text{req.})}}{W_{\text{tank}(\text{avail.})}}} \quad [9]$$

Where the available amount of fuel is calculated from the available volume.

The AIAA paper considers only one scale factor for the entire vehicle (λ_{tot}). Because it was expected that the engines could not deliver sufficient thrust, a second scale factor was introduced in the scaling model. With this scale factor (λ_{eng}) the (total frontal intake area of the) engines, and thus the thrust, could be scaled separately from the



rest of the vehicle.

The scaling model consists of different modules of which a schematic representation is given in figure 3.2.

These modules deliver the parameters necessary to solve equation 8.

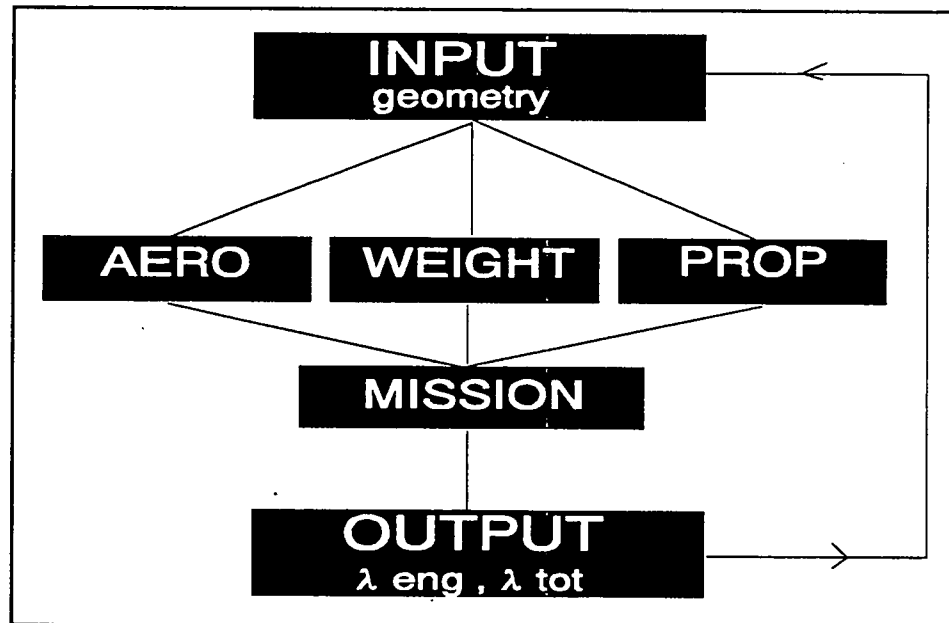


Figure 3.3 *schematic representation of scaling model*

Modules incorporated in the model

Aero module

This module calculates the lift and the drag of the vehicle along the trajectory.

The lift is calculated using a lift-to-weight ratio to velocity approximation (ref. [3.5]) which is accurate for the vehicle at small angles of attack.

Because the geometry of the vehicle is maintained, when scaling is applied, the lift coefficient is not dependent on a scale factor. The lift varies linearly with the wing area, which in turn varies with the square of the scale factor of the total vehicle.



The drag is assumed to consist of two components expressed in coefficient form as;

$$D = q S_{ref} [C_{d_0}(M) + C_{d_l}(M) C_l^2] \quad [10]$$

The drag coefficient at zero lift can be found from the table given by the Aero group. The effect of scaling on this coefficient was found to be neglectable (ref. [3.6]).

Because the drag coefficient due to lift is also independent of the scale factor, since basic wing parameters remain constant, the drag also varies linearly with total wing area (S_{ref}).

Weight module

The mass of the vehicle is calculated using the model developed by the structures group (ref. [3.7]) with some small adaptations.

This model and the effects of scaling on the weight of the vehicle are described in chapter 8.

Propulsion module

The thrust and the specific impulse of the engines are found from the tables delivered by the Propulsion group.

The effect of applying an engine scale factor on the thrust is assumed to be;

$$F_{wp} = F_{ws} \cdot \lambda_{eng}^2 \quad [11]$$

Where F_{ws} is given by the Propulsion group (ref. [3.8])

The specific impulse remains constant when applying a scale factor.

Because of the small thrust-to-weight ratio of the engines, the possibility of applying precompression is included in the Propulsion module.

Due to compression of the flow on the forebody of the vehicle, a larger mass flow is possible which results, for a given intake area, in a higher thrust.

As the amount of precompression is dependent on the angle of attack and the number of Mach, the thrust including precompression (and



scaling) is calculated from;

$$F = F_{wp} \cdot (A + B \cdot M) \quad [12]$$

where;

$$B = \frac{(PCM_7 - 1)}{6} \quad [13]$$

$$A = 1 - B \quad [14]$$

PCM_7 is an input parameter.

It can be assumed that precompression is possible as long as the maximum mass flow with precompression does not exceed the maximum mass flow without precompression. This is to avoid chocking.

Mission module

A trajectory (the velocity as a function of the altitude) was delivered by the Mission group (ref. [3.9]). Together with the output from the other modules equation 1 can be solved for each point of the trajectory.

Hereby a 1962 standard atmosphere is used.

Operation of the model

As the λ_{tot} also scales the engines (together with the rest of the vehicle), the two scale factors are not independent.

Several combinations of the two scaling factors can give convergence. However, it turned out that the lowest take-off weight was reached, for a given data set of the vehicle, when using a constant ratio of λ_{eng} to λ_{tot} . This ratio is called κ

The model works as follows;

A value of κ is given as input and a combination of λ_{eng} and λ_{tot} is calculated.



With these factors the parameters in equation 1 are calculated and the amount of fuel required is compared to the amount of fuel available. When this does not equal one and another a new combination of the two scale factors is determined and another iteration step is made. By altering the value of κ an optimal size (minimal take off weight) of the vehicle can be found.

Corrections on the models

Some corrections are applied on the output of the different modules to increase the accuracy of the final results.

- The effects of trimmed drag,
- effects of the second stage on the drag,
- effects of fuel reserve and
- effects of the engine nacelle on the drag are included.

As explained before, the model also allows the use of precompression. The values of these 'correction parameters', as well as the cruise range, can be varied in the scaling model.

3.5.2 Results

The scale factor that is necessary is, as explained before, dependent on the value of the 'correction parameters'. SE conducted a sensibility study with these parameters. Hereby the parameters that have the highest influence on the final results were examined. The other parameters were kept at a constant value.

The values of two of the parameters were quickly found. It appeared that the influence of the drag due to trimming was rather small. The drag increase resulting from trimming was estimated to be 5 percent of the total drag. According to ref. [3.5] and a verification of this value with the results of the stability group (ref. [3.10]), this is a fair assumption for a conceptual design.

The amount of fuel necessary for the return flight was taken to be 15 percent of the fuel needed for the ascent of the vehicle. As there is a direct relationship between the take off weight and the reserve fuel this parameter is not examined further.



The cruising speed was set to be at $M=4.5$, so the cruising altitude was found to be $h=23$ km. Although this is not completely in accordance with Sanger trajectory, a simpler algorithm could be used.

The cruise range was specified in the OR : 1000 km

The influence of the values of the 'correction parameters' on the total take off weight (the given values of the weight are in Mg * the gravitational constant) is given in figures 3.4 to 3.8.

In figure 3.4 it is shown that the total take off weight varies linear with the value of the drag increase due to the engine (Cd_{eng}).

When the total drag increases due to a larger contribution of the engine drag, the thrust that has to be delivered must also increase.

A higher thrust means a larger engine, which results in an increase of the mass.

To find a fair value of the Cd_{eng} it is assumed that the total drag consists mainly of the drag due to friction.

As the drag due to friction varies linearly with total wetted area, an approximation for Cd_{eng} can be found;

HARALD 1.5:

$$\begin{aligned} S_{wet} \text{ engine} &= 156 \text{ m}^2 \\ S_{wet} \text{ vehicle} &= 3242 \text{ m}^2 \end{aligned}$$

$$Cd_{eng} = S_{wet} \text{ eng} / S_{wet} \text{ veh} = 0.048 \quad [15]$$

A safe approximation for C_{deng} would be 0.05

In figure 3.5 it can be seen that the take-off weight decreases with increasing precompression factor (PCM_7).

When applying more precompression more thrust can be generated.

For a given thrust, the engine can be smaller and thus lighter, which results in a smaller total weight.

From ref. [3.11] it was found that the thrust at Mach=7 can be doubled ($PCM_7=2$) when the engine is placed at an angle of 8 degrees with the oncoming airflow. As the forebody angle is 5 degrees, this value



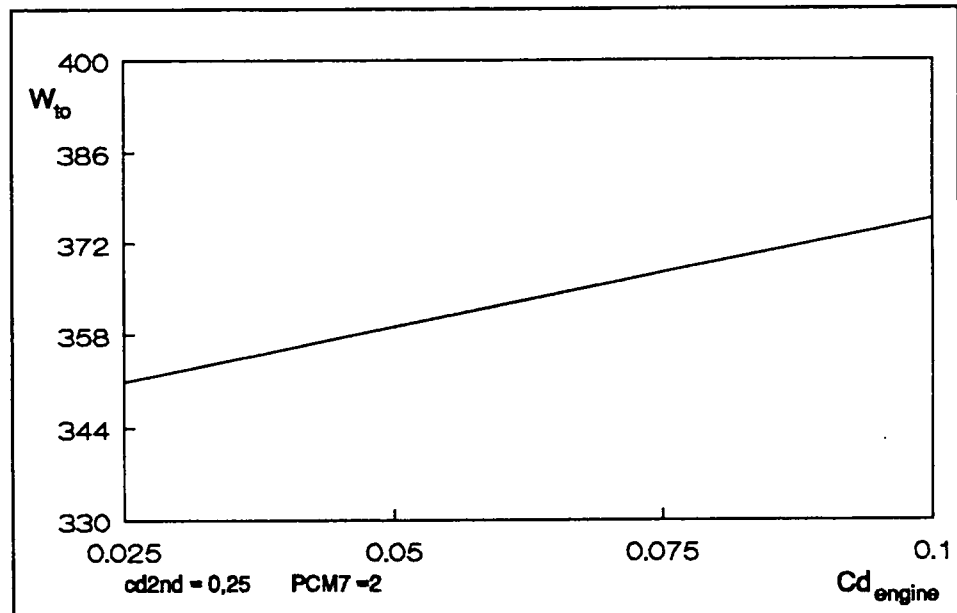


Figure 3.4 Weight versus the drag increase due to the nacelle

seems reasonable.

After verification it was found that the maximum mass flow with precompression does not exceed the maximum mass flow without precompression. Thus, choking is most likely not to occur when applying this value of precompression.

The graph of the weight to the increase of the drag due to the presence of the second stage (C_{d2nd}) does also show a linear relationship. When the drag contribution of the second stage increases, the total drag increases. This results in a larger engine and thus the total weight increases.

In finding the value of C_{d2nd} it was taken into account that the influence of the second stage on the drag will increase when the ratio of the wetted areas of the second stage to the first stage will be higher. So the printed values of the C_{d2nd} are valid for the baseline vehicle of the scaling model (HARALD 1.5).

At this configuration:

$$\begin{aligned} S_{wet \ 1st} &= 3242 \text{ m}^2 \\ S_{wet \ 2nd} &= 750 \text{ m}^2 \end{aligned}$$

So the value of C_{d2nd} was approximated at $3242 / 750 \approx 0.25$ [16]



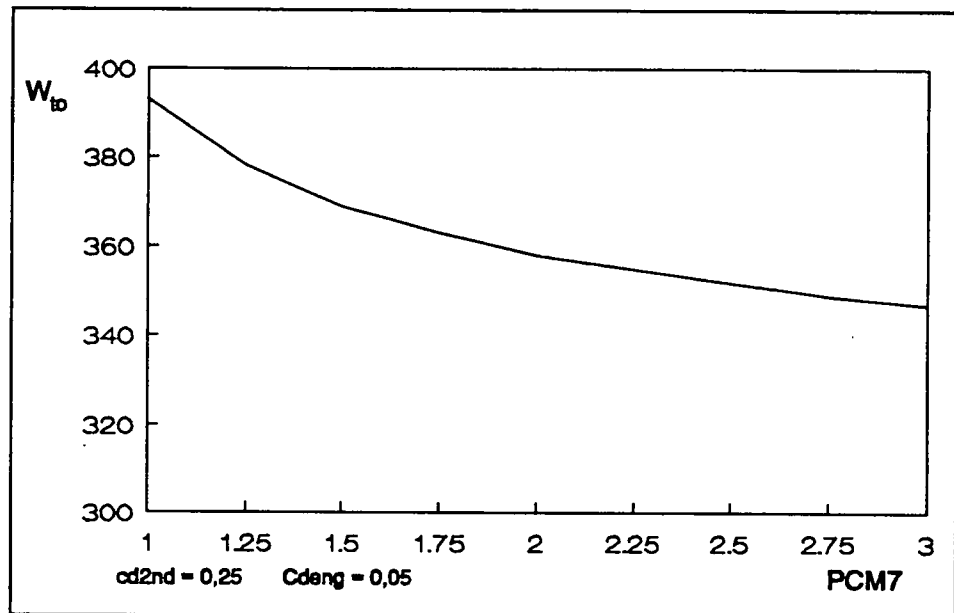


Figure 3.5 Weight versus the applied amount of precompression

It has to be pointed out that only frictional drag is taken into account. Examining the drag due to shock interference etc., which would very likely be apparent, did not lie within the scope of this project.

With these values of the 'correction parameters' a figure could be made of the total weight to the λ_{eng} to λ_{tot} ratio (κ). Figure 3.8 shows a parabolic relationship.

First, the total weight decreases at increasing values of κ . At this part of the graph the whole vehicle becomes smaller (λ_{tot} decreases), which results in a lower weight.

When κ increases even more the weight will also start to increase.

At this part the engine of the vehicle becomes larger (λ_{eng} increases) and thus the weight increases.

It is shown that a minimum weight is reached for a κ between 1.35 and 1.4.

The scaling factor (κ) that was applied on the HARALD 1.5 was chosen to be 1.4.



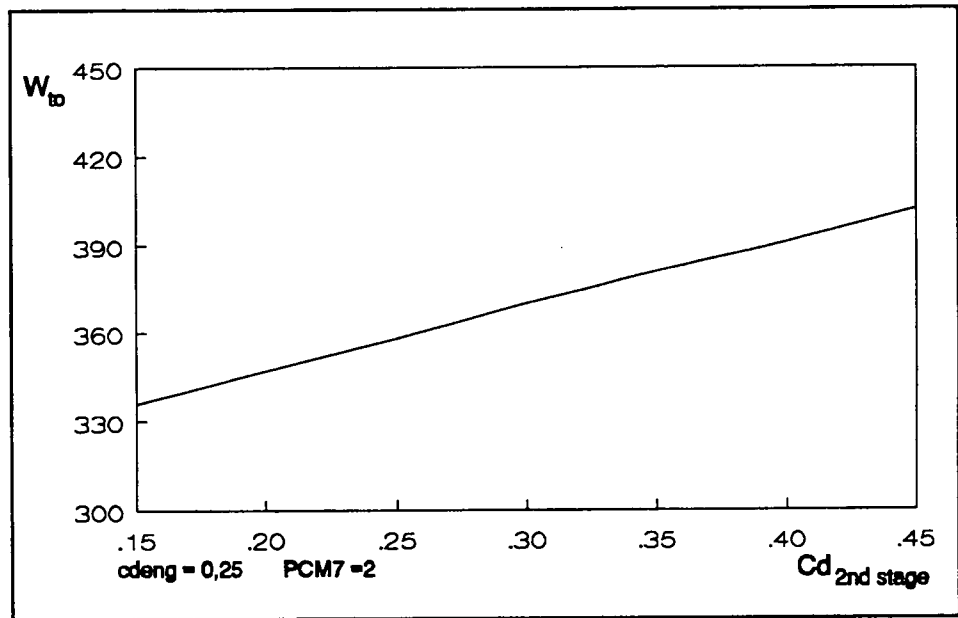


Figure 3.6 Weight versus the increase in drag due to the second stage

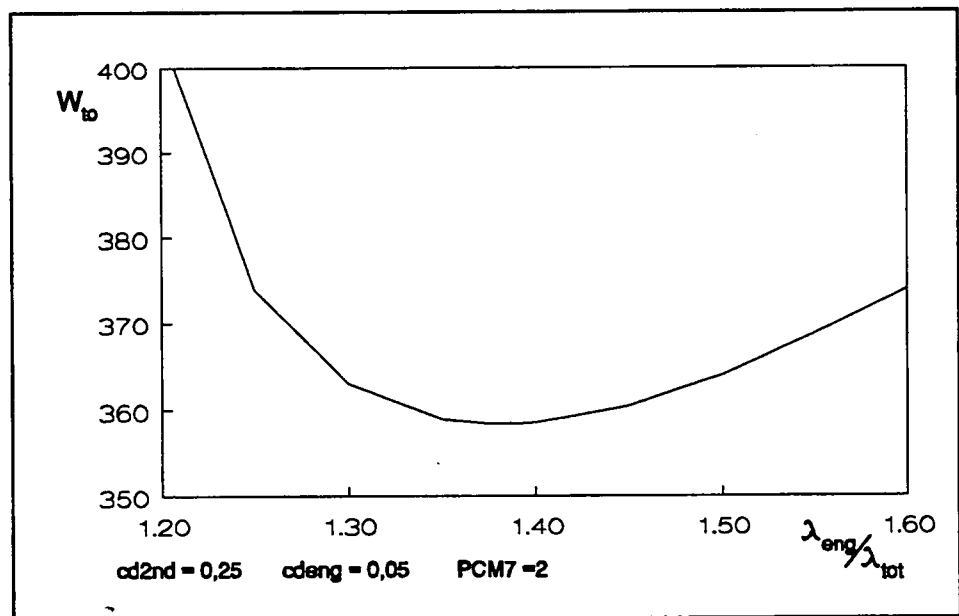


Figure 3.7 Weight versus the scalingfactor (κ)

This meant that the engine was scaled with a factor 1.14 and the whole vehicle with a factor 0.85.



Remarks on results

It was expected that the engine should have to generate more thrust, especially in the trajectory region around Mach=1.

It was however not expected that the whole vehicle could be 'down' scaled. It appeared that the initial scaling factor of 1.5 was over estimated.

It was found that this was due a difference in cruise range of Sanger and the HARALD. Sanger has a cruising capability of 3000 km where as the HARALD is only required to have a cruise range of 1000 km.

The influence of the cruise range on the amount of fuel consumed appeared to be rather large, which was the reason of the over estimation of the scaling factor.

In table 3.3 the most important parameters of the ultimate design are given, which were delivered by the scaling model.

Table 3.3

Some results of the scaling model

L/W	: 2-4	
m,t.o	: 355 Mg	
m fuel	: 78 Mg	
Length	: 77.8 m	
Wing area	: 544 m ²	
F take off	: 2380 kN	
F max.	: 8700 kN	(at M=4.2)
F sep.	: 2200 kN	
Isp	: 4000 sec.	(along trajectory)
	: 2000 sec.	(at separation)
Dyn. press.	: 59 kPa	(along trajectory)
	: 26 kPa	(at separation)
Mcr	: 4.5	
Msep	: 6.6	(at h=32 km)



3.6 Conclusions & Recommendations

Conclusions

When applying photographic scaling and by using a ratio of two scale factors (λ_{eng} and λ_{tot}) it is possible to design a launcher that will meet the specifications.

With the assumptions made, the launcher-design consists of the Winged Cone Reference Vehicle scaled with a factor 1.275 and the adapted HORUS 3B.

This adapted version of the HORUS 3B has an improved payload of 5 Mg and a total take off mass of 100 Mg.

The scale factors that are necessary for the first stage to meet the requirements depend on the values of the 'correction parameters'.

Higher values of drag components result in a larger engine and thus in a higher take off weight.

The use of precompression reduces the size of the engine considerably and will most likely be necessary in order to achieve a reasonable thrust to weight ratio.

The value of the cruise range has a large effect on the necessary amount of fuel and therefore on the weight and volume of the launcher.

In order to design a launch vehicle within a limited time starting points have to be made. This may reduce the commonality of the results, but enables the deliverance of data that describes the performance of the launch vehicle.

Recommendations

In order to design a launch vehicle in more detail, more accurate prediction models are needed.

Especially in the field of aerodynamics and propulsion it is recommended to spend more time in developing models that are generally applicable.

Some modifications of the geometry of the WCRV can be conducted in order to deliver a more optimal design. For example an elliptical body can produce more lift and two vertical tails will cause less



stability problems.

The effects of the second stage, especially on the total drag, should be examined further. This will result in more accurate values of the 'correction parameters'.

It should be investigated in more detail what the effects are of the use of precompression.



3.7 References

- [3.1] Management Operational Requirements,
HAR-ORD-002, TU Delft, 1993
- [3.2] Management Functional Requirements Document
System Engineering, HAR-FRD-003,
TU Delft, 1993
- [3.3] Koelle, D.E., Acta Astronautica Vol. 19, No.1, pp 63-
Kuczera,H. -72, Pergamon Press, U.K., 1989
- [3.4] Wakker, K.F. Inleiding Ruimtevaarttechniek, 1r6, TU
Delft, 1987
- [3.5] Chaput, A.J. Preliminary Sizing Methodology for Hy-
perersonic Vehicles, Journal of Air-craft,
Volume 29, No.2, 1992
- [3.6] Broomhead, M.J. Preliminary Calculation of Aerothermo-
dynamic Characteristics of a Space-Plane,
HAR-AER-001, TU Delft, 1993
- [3.7] Mourik, A. van Structural Model for Space planes, HAR-
WEI-001, TU Delft, 1993
- [3.8] Vliet, L. van Performance of engines of a Space plane,
HAR-PRO-001, TU Delft, 1993
- [3.9] Sprenger, M.L.M. Trajectory Analysis for the HARALD
project, HAR-MIS-001, TU Delft, 1993
- [3.10] Cremers, G. Stability and Control considerations of the
HARALD, HAR-STA-001, TU Delft,
1993
- [3.11] Winged Launcher Configuration Study,
MBB, British Aerospace, Rolls-Royce,
MTU, FIAT, VDK and DORNIER.
Final Presentation ESTEC, 10 May 1989



4 Aerodynamics

Abbreviations

C_D	Dragcoefficient
C_L	Liftcoefficient
C_M	Momentcoefficient
C_N	Normal force coefficient
C_p	Pressure coefficient
M	Mach number
Pr	Prandtl number
Re	Reynolds number
S	Surface/Area
T	Temperature
L	Length
mac	Mean aerodynamic chord
x	Length-coordinate measured from nose of craft (dimensionless factor)
α	Angle of attack
γ	Ratio of specific heats

Indices

N	Forebody cone
cp	Centre of pressure
e	Stagnation point area
l	Lift
o	Zero lift
∞	Conditions at free stream



4.1 Introduction

An important research problem in the design of an advanced space launcher such as HARALD is the determination of the aero(thermo)dynamic characteristics (ref.[4.1]), since both theory and experiments cannot be dealt with easily. In this chapter the results of the aero(thermo)dynamic tools for the conceptual aerothermodynamic design of HARALD are presented and the effect of scaling on the aerodynamic parameters is given. As usual in this phase of the design an accuracy of 30 % is pursued.

As a reference for the first-stage vehicle, on which our attention will be focused, a NASA design study of a hypersonic winged-cone vehicle is used (ref. [4.2]). From this study an extensive aerodynamic database is available. Our model for the first-stage vehicle will be a delta-wing/cone-body combination as shown in fig. 4.1.

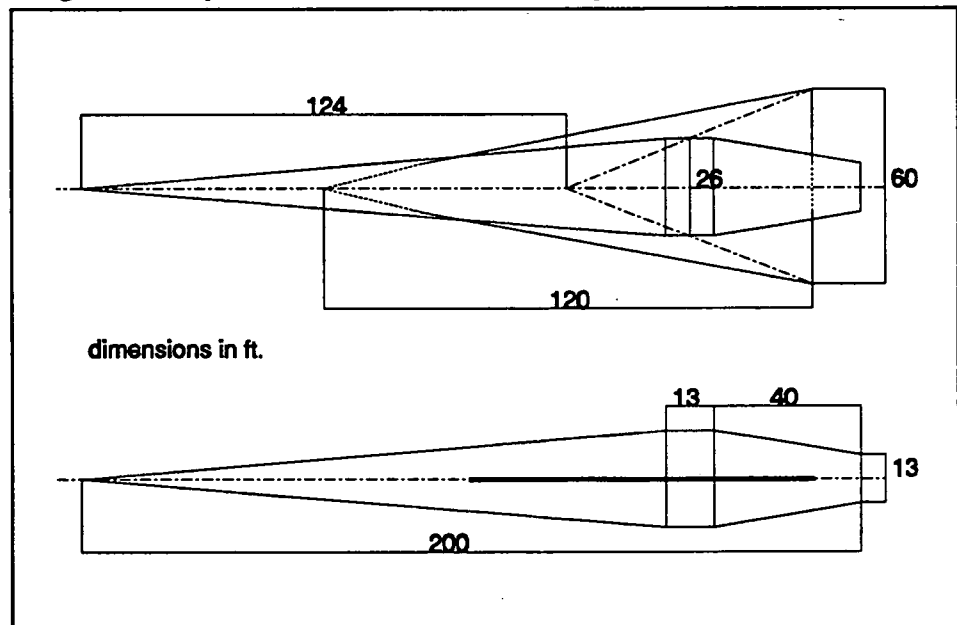


Figure 4.1

*Dimensions of wing-body representation
of Winged Cone Vehicle*

In the case of HARALD's first stage, the speed regime is divided into

- subsonic (0 < M < 0.8)
- transonic (0.8 < M < 1.2)
- supersonic (1.2 < M < 4)
- hypersonic (4 < M < 7)



Prediction methods for the lift-, drag- and pitching-moment coefficients and of the heat-flux have been found in the literature. The results which are found with these methods, except for the heat-flux, are compared and evaluated with respect to the NASA design study.

This chapter is a summarize of work done by the aerodynamics group. A complete coverage of the aerothermodynamic characteristics can be found in ref.[4.9].

4.2 Aerodynamic coefficients

4.2.1 Liftcoefficient

Subsonic

To decrease supersonic wave drag, the wing of the reference vehicle is a so-called delta, consisting of thin, sharp-edged profiles. This wing type induces separation of the flow on the leading edge even at small angles of attack. The flow rolls up into two spiral vortex sheets (fig. 4.2).

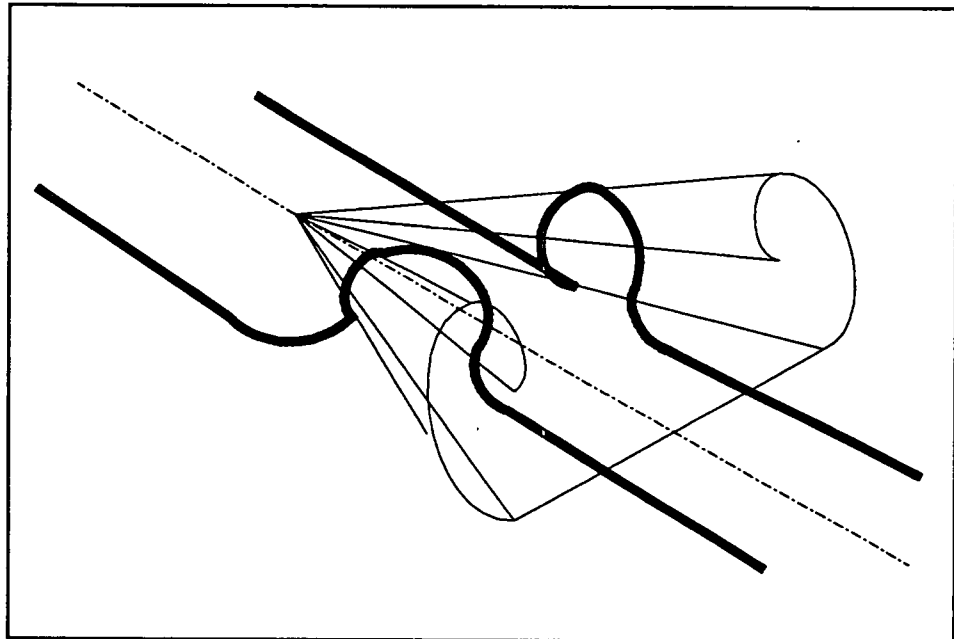


Figure 4.2

Leading-Edge-Vortex Flow

To predict the changes in pressure distribution a method developed by Polhamus in the mid-sixties is used. A detailed description of the



method can be found in ref. [4.8]. In the high subsonic regime compressibility is accounted for by use of the Prandtl-Glauert rule. Two effects have not been studied: the lift of the body and the wing-body interference.

In fig. 4.3 the calculated liftcoefficient for the wing is compared to the liftcoefficient of the wing-body reference for a Mach number of 0.3. This figure shows that the lift is overestimated by 20 to 25 % because of a larger lift gradient. This is probably due to wing/body interference. The presence of the fuselage causes a change in flow angles relative to the wing resulting in an effective change of wing camber.

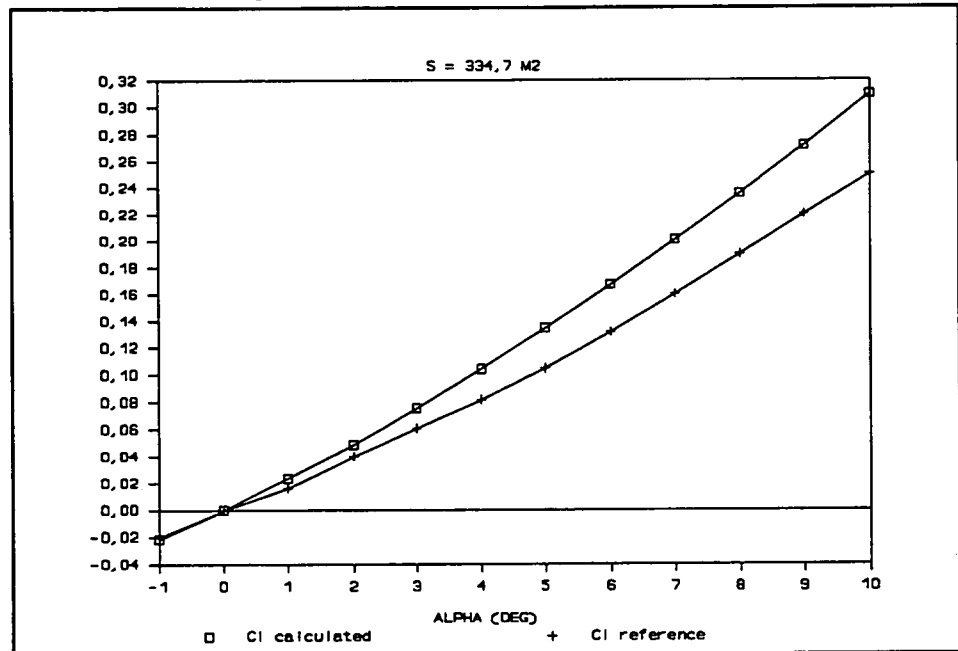


Figure 4.3 Liftcoefficient versus α ($M=0.3$, $h=0$ km SA)

Transonic

It is assumed here that the lift in the transonic region can be calculated using same method as for the subsonic region. Therefore, the results are much like that above.

Supersonic

The main features of the subsonic flow over slender sharp-edge delta wings are maintained well into the supersonic speed range. Polhamus extended his subsonic method to supersonic speeds by introducing the effect of the Mach number and aspect ratio, on which the supersonic



vortex-lift is critically dependent.

The calculated liftcoefficient for the wing-body at a Mach number of 2.5 is compared to the reference liftcoefficient in fig. 4.4. Hereby a wing-body interference factor is used as a correction on the calculated values. It can be seen that there is very little difference between the calculated and the reference liftcoefficient.

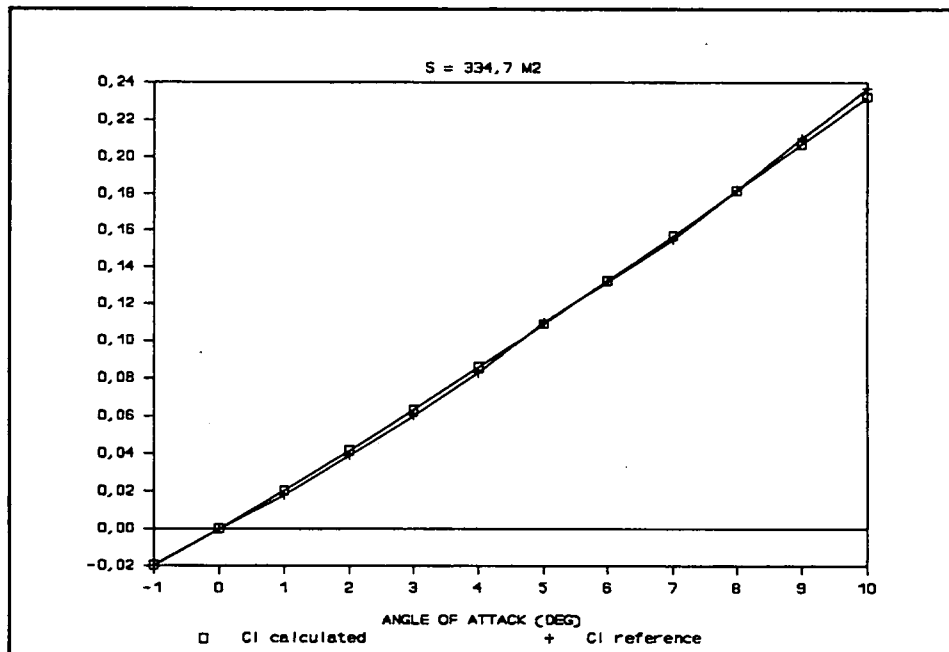


Figure 4.4 *Liftcoefficient versus α ($M=2.5$, $h=15.4$ km SA)*

Hypersonic

The hypersonic liftcoefficient of the wing is calculated with the Prandtl-Meyer shockwave/expansion theory (ref. [4.5]). This theory is only valid for two dimensional flow. But due to the high Mach numbers the disturbances in the flow, which spread backwards over a Mach angle that is very small, can be thought to spread along a streamline, which results in a two dimensional flow.

For the body, the Rasmussen/Newtonian theory (ref. [4.5]) was applied. The Newtonian flow is only valid for infinite Mach numbers and for a ratio of specific heats γ of the gas equal to 1. To use this method for Mach numbers from 4 to 7 and a γ of 1.4, the formula is corrected for with Rasmussen's prediction of the cone pressure distribution.

The body is divided into three parts: the forebody-cone, the midbody-cylinder and the afterbody. In the Newtonian theory it is assumed that



the afterbody does not produce any lift, since it is located in the shadow of the forebody. The lift created by the midbody-cylinder can also be neglected with regard to the lift of the forebody-cone. If the angle-of-attack is smaller than or equal to the cone half-angle the total cone is wetted. If the angle-of-attack is greater than the cone half-angle the lower half of the cone is wetted and the upper half lies in the aerodynamic shadow regime. This results in two different formulas for the calculation of the lift of the forebody-cone. The total liftcoefficient of the fuselage is found by adding the separate lift coefficients of the sections. For example, at a Mach number of six; fig. 4.5:

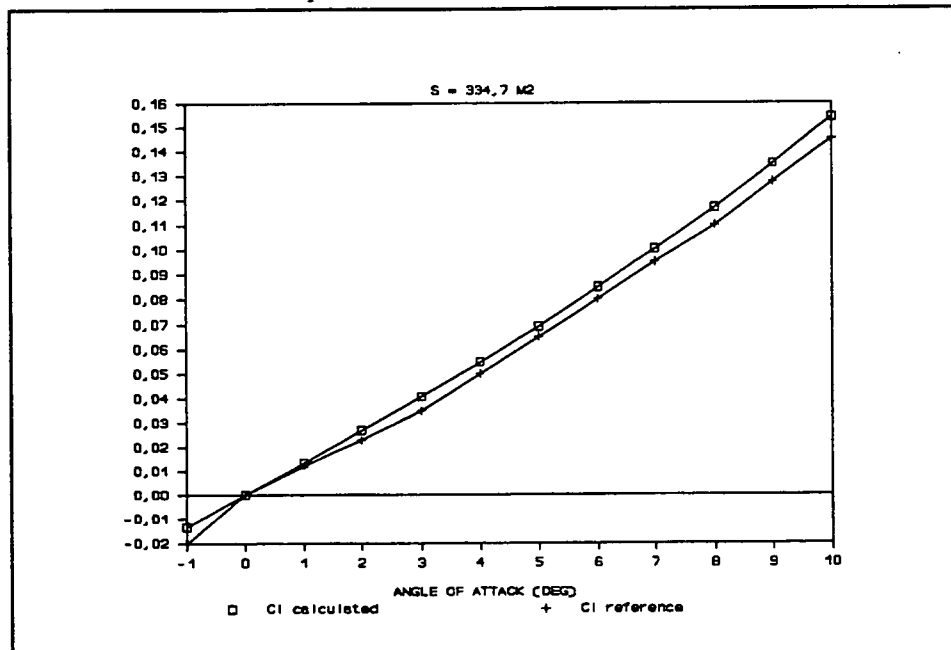


Figure 4.5 *Lift coefficient versus α ($M=6$, $h=29.3$ km SA)*

4.2.2 Dragcoefficient

The total dragcoefficient is built up of two parts according to:

$$C_D = C_{D_0} + C_{D_i} \quad (1)$$

where C_{D_0} is the vehicle zero-lift-dragcoefficient and C_{D_i} is the drag-due-to-lift-coefficient dependent on angle-of-attack.

Subsonic

The zero-lift-dragcoefficient prediction methods presented in ref. [4.4]



are taken from Roskam (ref. [4.6]) and the USAF DatCom Sheets (ref. [4.7]). These methods can be characterized as typical semi-empirical design methods and apply only to 'smooth' surfaces and to flow regimes where the boundary layer is mostly turbulent.

The zero-lift-dragcoefficient of the wing is built up from a wing/fuselage interference factor, a lifting-surface correction factor, a turbulent flat plate skin-friction coefficient, the thickness ratio of the wing, the wetted area, the nett area and the reference area.

The zero-lift-dragcoefficient of the fuselage is built up from a wing/fuselage interference factor, a turbulent flat plate skin-friction coefficient, the fuselage length, the maximum diameter, the wetted area, the maximum frontal area and the reference area.

For the calculation of the drag-due-to-lift use is made of the theory of Polhamus with the assumption that the effects of angle of attack on skin friction are small.

In fig. 4.6 for $M = 0.3$ at 0 km SA the calculated dragcoefficient of the wing-body is compared to the reference. It is clear that the zero-lift-dragcoefficient is independent of angle-of-attack. The curvature of the line is caused by the drag-due-to-lift coefficient. Obviously, Polhamus predicts the trend of the curvature very well. However, the calculated total dragcoefficient differs a constant value from the reference. This is due to a higher estimation of the zero-lift drag than in the reference.

Transonic

As in the subsonic region we use Roskam and DatCom for the zero-lift-dragcoefficient.

The zero-lift-drag consists of friction drag and wave drag, which depends on the wing sweep angle $\Lambda_{c/4}$ at a quarter of the mean aerodynamic chord.

The drag of the fuselage is composed of a wing/fuselage interference factor, the fuselage skin-friction, the base drag due to the afterbody wake and the wave drag. It depends on the fineness ratio (length/diameter) of the fuselage, both length and maximum diameter of the fuselage and the wetted area.

The drag-due-to-lift can be estimated using the same method as that for the subsonic region.



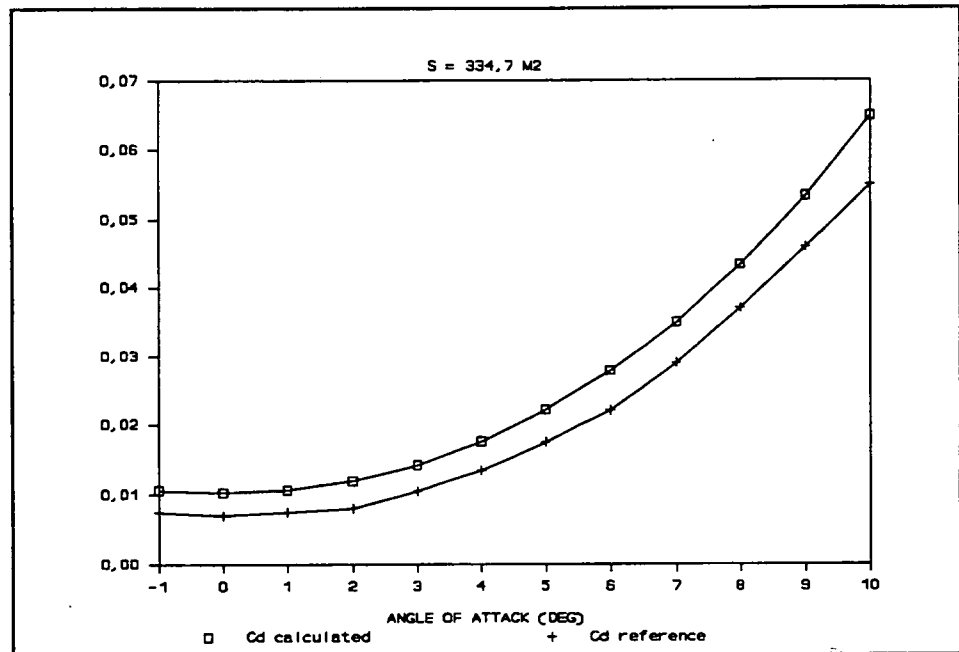


Figure 4.6 Drag coefficient versus α ($M=0.3$, $h=0$ km SA)

Supersonic

Again, Roskam and DatCom are used for the zero-lift-dragcoefficient. The extra wave drag of the wing depends on the leading edge radius and on whether the wing has a subsonic or a supersonic leading edge (the Prandtl/Meyer shock angle is larger than the sweep angle of the wing (ref. [4.4])). The drag-due-to-lift is calculated with Polhamus.

In fig. 4.7 ($M = 2.5$ at 15.4 km SA) the total dragcoefficient is compared to that of the reference vehicle.

Hypersonic

In the hypersonic region the breakdown of the total drag into the zero-lift drag and the drag-due-to-lift is not used. The formulas give the total dragcoefficient as a function of angle-of-attack and, in our case, the zero-lift-dragcoefficient is the total dragcoefficient at $\alpha = 0$.

First, the inviscid drag is considered. Then, the effect of friction is regarded. For the calculation of the wing drag, again the shockwave/expansion theory is applied. This gives a drag depending on angle-of-attack, the thickness-to-chord ratio, the Mach number and the ratio of specific heats of air.



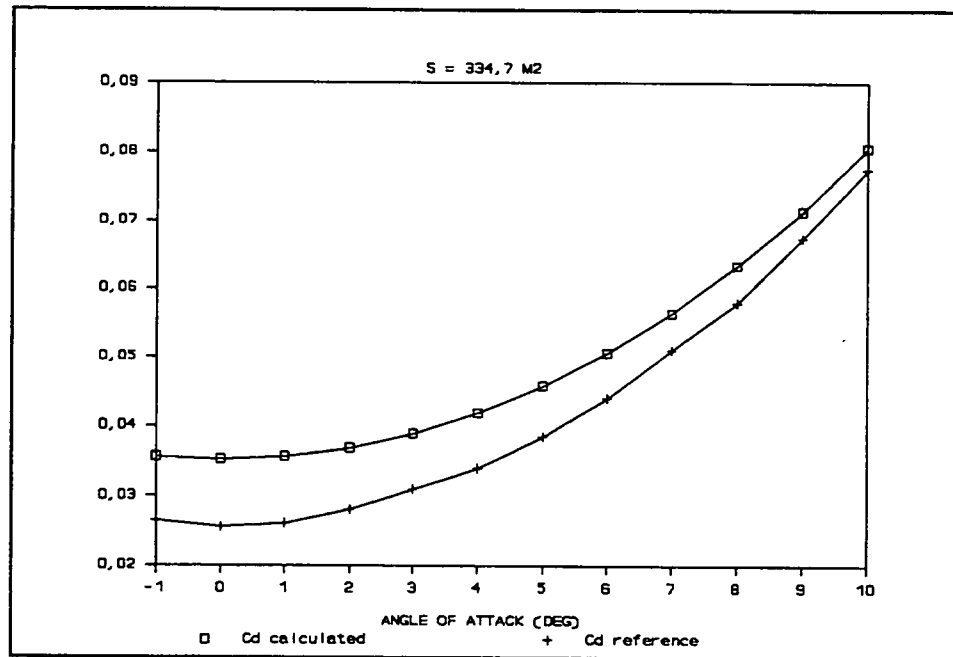


Figure 4.7 Drag coefficient versus α ($M=2.5$, $h=15.4$ km SA)

The fuselage drag uses the Rasmussen/Newtonian theory as does the lift. Because the afterbody is in the aerodynamic shadow regime it has no drag. For the forebody-cone drag the same applies as for the lift with regard to the angle-of-attack and the cone half-angle. The total dragcoefficient of the body is found by adding the different coefficients of the three parts.

In fig. 4.8 ($M = 6.0$ at 29.3 km SA) the total dragcoefficient is compared.

4.2.3 Pitching-momentcoefficient

Subsonic

According to ref. [4.3], the leading-edge-suction analogy of Polhamus has been used by Snyder and Lamar to develop the chordwise load distribution with the corresponding pitching moment of the vortex lift for delta wings. Due to the unique character of the vortex lift, they state that the vortex-lift chordwise loading, rather than being the result of distributed pressure over an area, is better regarded as a force per length distributed along each of the leading edges with a magnitude the same as that of the leading-edge suction force. To evaluate this statement, the vortex-lattice method of Margason and Lamar was utilized to predict the distribution of the potential-flow leading-edge



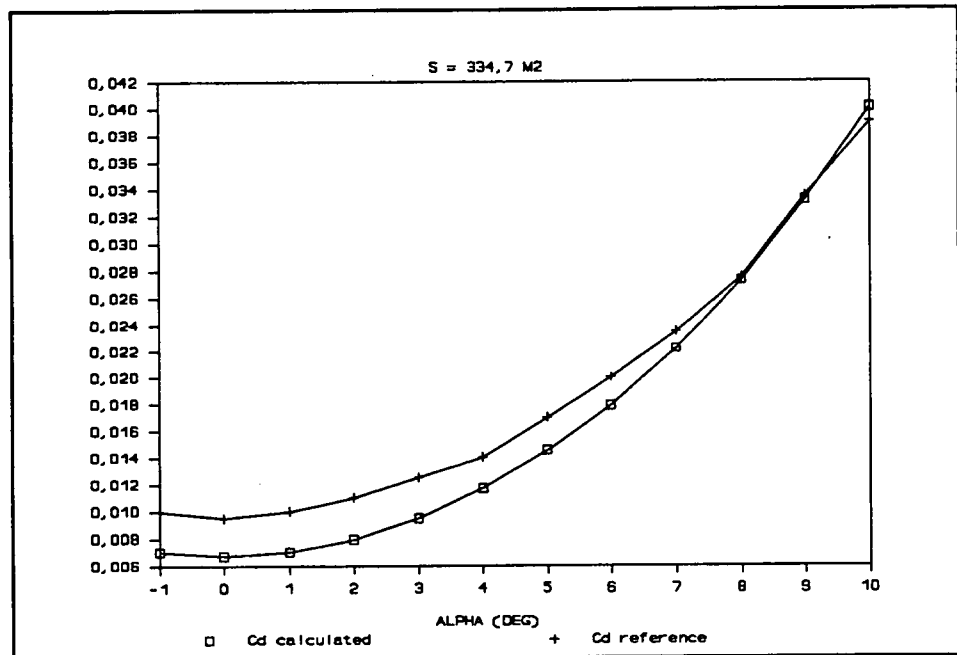


Figure 4.8 Drag coefficient versus α ($M=6$, $h=29.3$ km SA)

suction and then, by use of the Polhamus analogy, the chordwise distribution of vortex lift. In the conceptual stage of a design little information is available about the chordwise pressure distribution of a wing. Determination of the centre of pressure, lift distribution, or pitching moment is therefore not possible, neither for the wing as for the fuselage.

Transonic

For the transonic region the same remarks can be made as for the subsonic region. Despite our efforts, we could not find a simple method in the literature.

Supersonic

The pitching moment coefficient C_M depends on the distance between the moment point x_m and the point of pressure x_{cp} , the point on the wing where the total aerodynamic force acts, according to:



$$C_M = C_N \left(\frac{x_m}{c_r} - \frac{x_{cp}}{c_r} \right) \frac{c_r}{mac} \quad (2)$$

in which C_N is the normal-force coefficient which, when the angle-of-attack α is small, is approximately equal to C_L . For a flat triangular plate with uniform mass distribution x_{cp} corresponds with the centre of gravity x_{cg} .

Hypersonic

With the model for the momentcoefficient C_M (ref. [4.5]) a few simplifications are made: the contribution of the drag to the moment is neglected, because the distance to the moment reference centre is very small, and the normal force coefficient C_N is assumed equal to the liftcoefficient C_L . Both assumptions can be made due to the small angles-of-attack.

With these assumptions made only the lift creates a moment. For the body only the lift of the forebody-cone is regarded as previously mentioned. For the calculation of the momentcoefficient of the body dC_L/dx is needed, in which x is the coordinate from the cone's top to the point where the lift acts.

According to ref. [4.8] this derivative is given by:

$$\frac{d(C_L S_f)}{dx} = 2 \pi x \tan^2 \delta C_L = 2 \frac{x}{l_N} C_L S_f \quad (3)$$

in which δ is the cone half-angle and S_f is the frontal area of the cone which is equal to $\pi(L_N)^2 \tan^2 \delta$. For the momentcoefficient with respect to the cone's top holds:

$$C_M = -\frac{1}{S_f l_N} \int_0^{l_N} x \frac{d(C_L S_f)}{dx} dx \quad (4)$$

Now the momentcoefficient at any point can be calculated.

For $M = 6.0$, the calculated momentcoefficient is compared to the reference (see fig. 4.9). The difference between the calculated and the reference values are due to the fact that the moment of the drag is neglected, and only the lift of the wing and of the forebody make up the moment.



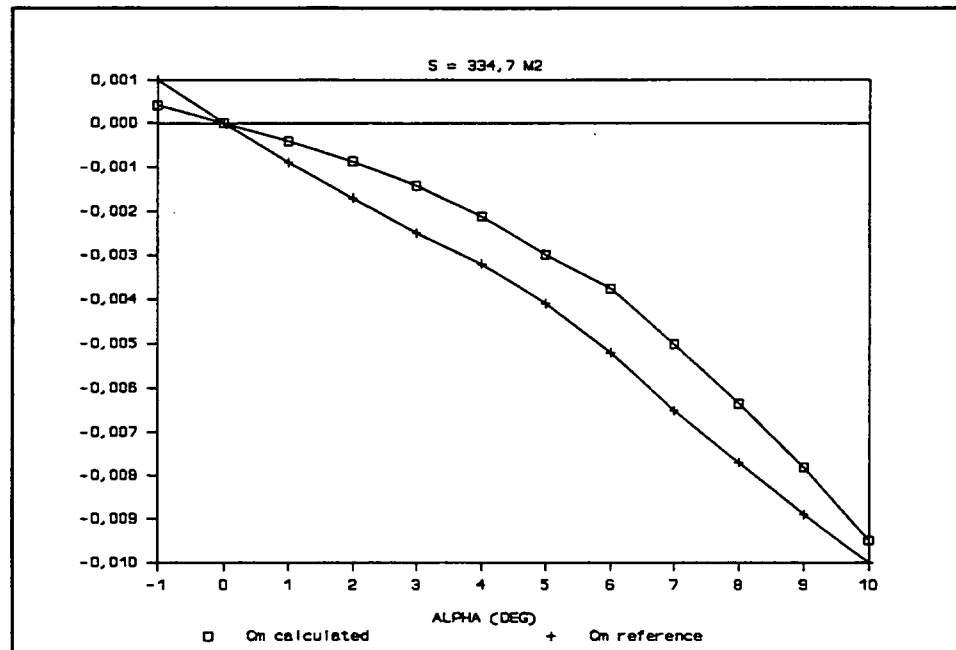


Figure 4.9 *Moment coefficient versus α ($M=6$, $h=29.3$ km SA)*

4.3 Heat flux

At high speeds the boundary layer causes a positive heat flux onto the skin. When only radiation cooling is applied, the construction materials should be able to withstand the high temperatures. These can be determined by considering the equilibrium between the heat supplied by the boundary layer and the heat radiated out of the skin. It is also possible to apply some kind of active cooling, when the heat flux is too high. In this case, the allowable temperature of the skin is given, from which the cooling heat flux can be calculated.

4.3.1 Flat-plate model

The convective heat generated by the boundary layer can be determined by means of the Reynolds-analogy, which relates the convective heat coefficient to the flat plate skin-friction coefficient (ref. [4.4]). To simplify the calculations only the flat plate skin-friction coefficients of a flat plate are looked at. This is a reasonable assumption for the flat wing. In the case of a curved fuselage however, the Reynolds number is corrected for by $Re_{\text{cone}} = 9/4 Re_{\text{plate}}$.

It appeared that the heat flux on the surface away from the stagnation points is not very high.



4.3.2 Stagnation Point

Since the model described in the previous section is not valid in or in the area around stagnation points, an additional method is needed, due to the importance of the stagnation points. In these points the highest temperatures will occur.

Because of material considerations the nose and leading-edges of the vehicle are not infinitely sharp, but have a radius of curvature. Due to this radius of curvature a normal shockwave will be present in front of the body. This results in a subsonic laminar flow region between the body and the shockwave in which the density ρ and the viscosity μ will be approximately constant (ref [4.4])

The trend with Mach number is given in fig. 4.10. If the heat-flux remains within 80 - 650 kW/m² radiation cooling can be applied. Our highest heat-flux occurs at M = 7 and equals 263 kW/m². So passive radiation cooling can be used and no expensive active cooling is needed. A radius of curvature of 0.04 m is taken because this seems realistic.

The Sanger leading-edge temperature equals 1650 K for M =7, which corresponds well with our method which gives a temperature of 1570 K at radius 0.04 m.

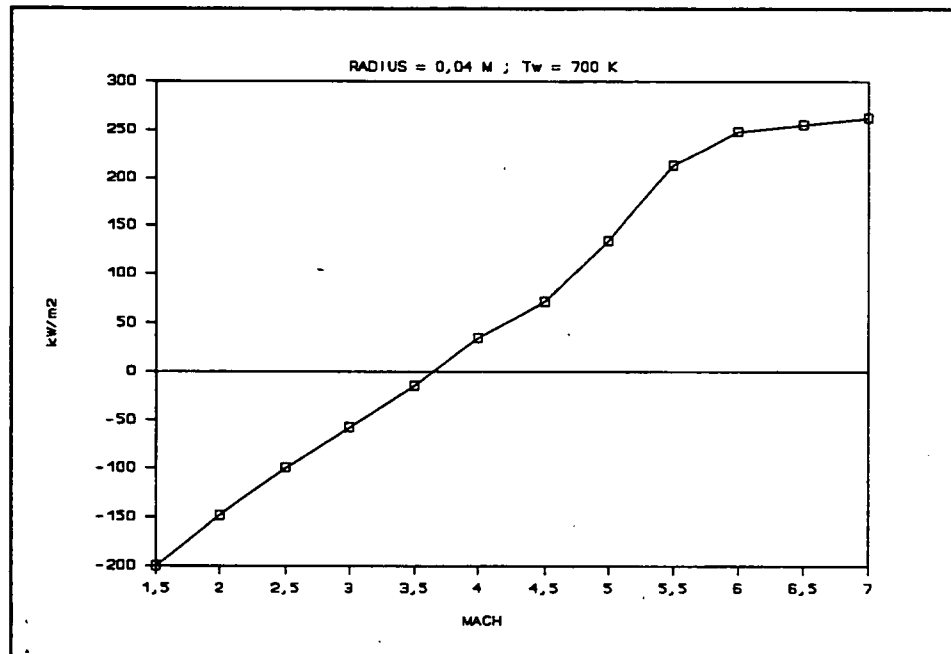


Figure 4.10 Heatflux in stagnation point as function of Mach



4.4 Effect of scaling

It may be assumed that the liftcoefficient, the momentcoefficient and the drag-due-to-lift coefficient are not influenced by photographic scaling. Only the zero-lift drag coefficient is dependent on photographic scaling, due to the change in Reynolds number, that influences the friction coefficient. In fig. 4.11 the effect of scaling the vehicle with a factor 2 on zero-lift drag is presented. It is clear that the influence is very small, especially when compared to the total drag.

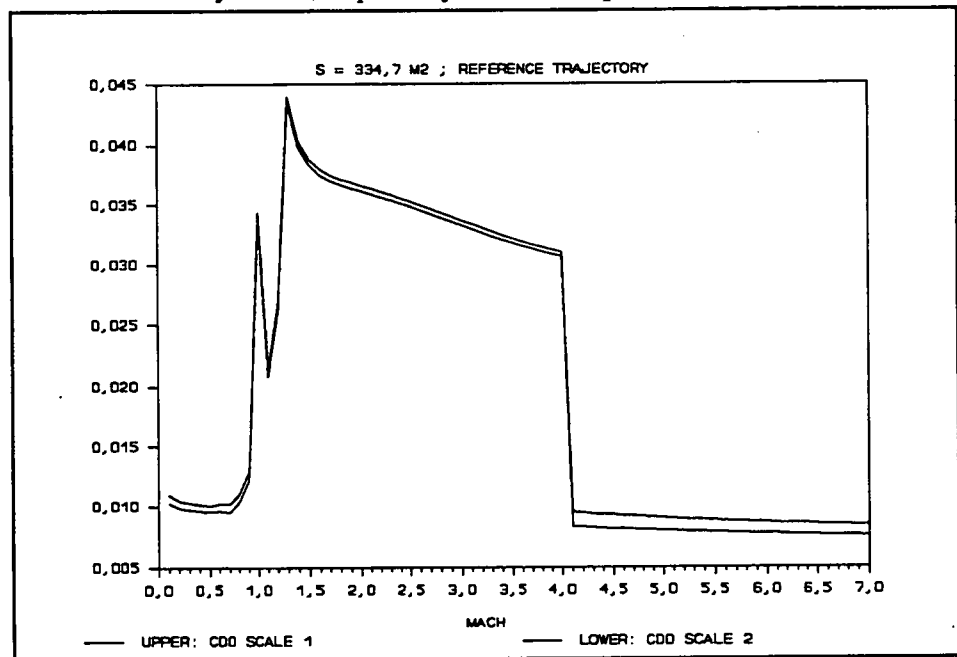


Figure 4.11

Effect of scaling on C_{D0}

4.5 Conclusions & Recommendations

The methods presented in this report are phase 0 / phase A analytical methods, to get a first impression of the aerodynamic forces acting on a space-plane. All methods that are used -except the calculation of the zero-lift dragcoefficient- have an accuracy of 20 to 25% (when compared to the WCRV data).

However, the WCRV data have the same order of uncertainty as our calculated coefficients. This is because the method used in the reference document is, due to its simplicity, normally employed during initial design studies to provide timely analysis of a wide range of



configuration variables. In most cases it predicts correct lift and drag increments due to configuration and Mach number effects. However, absolute levels are not consistently predicted.

From the calculated heat-flux with a wall temperature of 700 K it becomes clear that passive cooling can be used in the form of radiation cooling.

Photographic scaling only effects the zero-lift drag. This effect is not very large and with small scaling factors it is negligible.

The model can only calculate the aerodynamic coefficients of a wing-body vehicle. The influence of other aerodynamic surfaces are not investigated. In future this simple model must be extended to cover these discrepancies.

The chord-wise pressure distribution must be examined so that the momentcoefficient can be calculated and a wing-body interference factor for the subsonic/transonic region must be found to adjust the overestimation of the liftcoefficient by Polhamus.



References

- [4.1] System Engineering Functional Requirements Document Aerothermodynamics, HAR-FRD-004, TU Delft
- [4.2] Hypersonic Vehicle Simulation Model: Winged-Cone Configuration
NASA TM 80062
- [4.3] Pagen, M. Aerodynamic Analysis Methods for Advanced Space Launchers, HAR-AER-004, TU Delft
- [4.4] Buyten, A. Prediction of Supersonic Aerothermodynamic Coefficients of Space Planes, HAR-AER-002, TU Delft
- [4.5] Linden, B.J. van der Hypersonic Flow Model for the HARALD Space Plane, HAR-AER-003, TU Delft
- [4.6] Roskam, J. Airplane Design (Part VI)
Roskam Aviation and Engineering Corporation, Ottawa, Kansas, 1987
- [4.7] Hoak, D.E. a.o. USAF Stability and Control Datcom
Flight Control Division, Air Force Flight Dynamics Laboratory, WPAFB, Ohio, 1978, revised
- [4.8] Polhamus, E.C. A Concept of the Lift of Sharp-Edge Delta Wings based on a Leading-Edge-Suction Analogy , NASA TN D-3767 , October 1966
- [4.9] Broomhead, M.J. Preliminary calculation of aerothermodynamic characteristics of a space plane, HAR-AER-001, TU Delft



5 Propulsion

Abbreviations

TSTO	two stage to orbit
WCRV	Winged Cone Reference Vehicle
NASP	National AeroSpace Plane
JP4	kerosine
LH2	liquid hydrogen
J	Joule
F	thrust
A	frontal area of engine
D	diameter of engine
M	number of Mach
Isp	specific impulse
Φ	fuel to air ratio
α	angle of attack
q	total heat load
m	mass flow
cp	specific heat constant
T	temperature
Lambda	scaling factor



5.1 Introduction

In the Functional Requirements Document (ref. [5.1]) it is stated that the propulsion group should investigate the performance of a propulsion system that could be used for a TSTO launcher. After a literature research it became clear that a turbo-ramjet combination was the only engine configuration that could be realised within the constraints that the engines of the first stage should be fully air-breathing, be designed by current technology and have a short development time.

As the thrust, the specific impulse and the mass of the propulsion system were needed in an early stage of the design process, it was decided to use simplified models for the calculations of the values of these parameters. In a later stage of the project it could then be tried to verify the results of these models by means of more detailed studies.

The first paragraphs of this chapter deal with a possible layout of the propulsion system for this kind of engine. The model for the calculation of the thrust and specific impulse and the verification of this model is discussed in the next two paragraphs. In paragraph 4 a cooling model is derived and in the next paragraph the mass of the total propulsion system is calculated. Conclusions and recommendations are given in the last paragraph.

5.2 Powerplant layout

The parts of the propulsion system that are considered are:

- Turbo-ramjet engines
- Cooling system
- Propellants
- Fuel tanks
- Fuel supply system

An integrated coaxial turbo-ramjet was chosen, because less space is used. Furthermore, an integrated turbo-ramjet is less heavy and has less drag, when compared to a system with two separate intakes, ducts and nozzles. A disadvantage of the system are the high costs and the complexity.

The turbojet is installed coaxial within the duct of the ramjet, see fig.



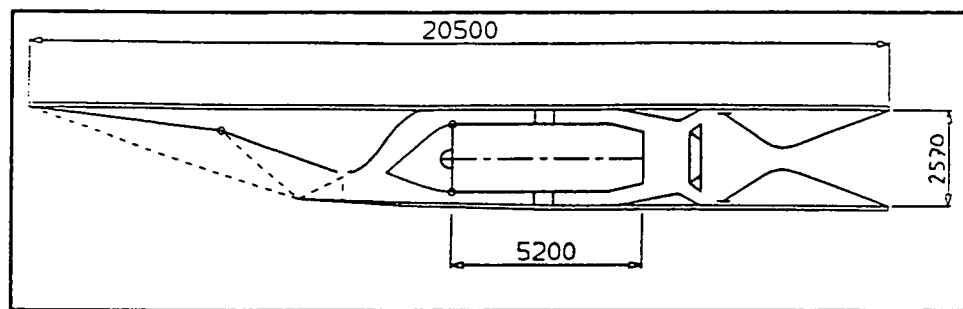


Figure 5.1

Lay out of the engine

5.1. The ramburner is used as afterburner during turbojet operation. The total airflow is led through either the turbojet or the ramjet. Simultaneous operation is not considered and prohibited by closing the ramducts during the turbojet mode and by closing the turbojet during ramjet operation. This closing part has a 2-D configuration and is slowly transformed into a 3-D turbojet entry.

The intake is made up of two adjustable intake ramps in a 2-D layout to create a better compression process at different Mach numbers. An intake air bleed stabilises the perpendicular shock and it could also be used to aid the cooling system after it is regeneratively cooled in a hydrogen heat-exchanger in the nozzle.

The nozzle is 2-D and the throat is adjustable to fit the mass flow during the differing flight conditions.

Layout of the vehicle with engines

The winged cone vehicle has a ring of engines around its body (ref. [5.3]) but, because of the design decisions made by System Engineering, the 6 engines were to be placed underneath the fuselage. This configuration is drawn in fig. 5.2.

It has to be mentioned that a problem will arise when the diameter of the engines becomes too large. Then the engines will be positioned near the wings which will influence the flow around the wings.

Fuel tanks

A requirement was to give the length-to-diameter ratio of cylindrical fuel tanks with either spherical or elliptical ends, see fig. 5.3.

For both JP4 and LH2 the length as a function of the propellant mass were calculated.

With these results the Weight group could fit the tanks in the vehicle.



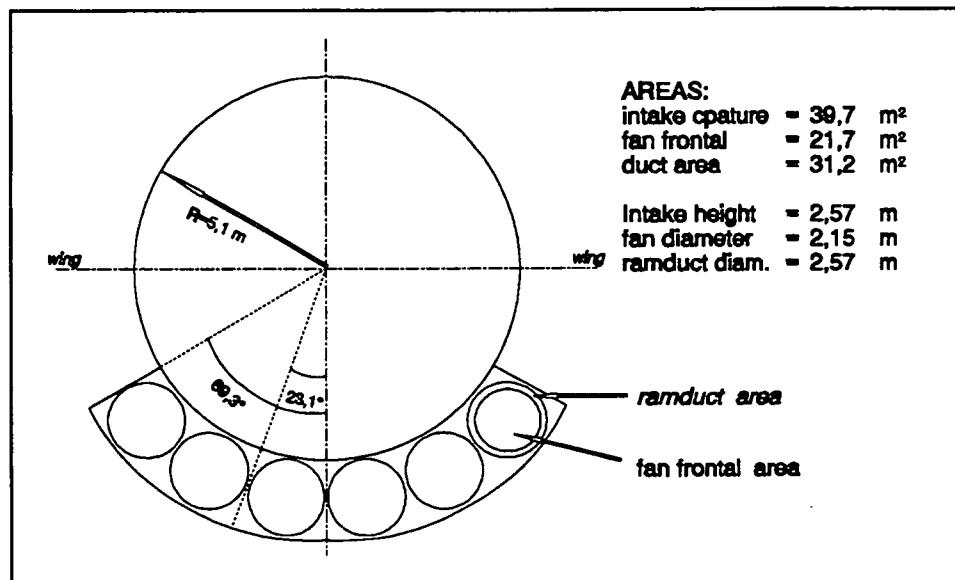


Figure 5.2 Engines in combination with HARALD (front view)

For the fuel supply a pump-feed system was chosen because of the relatively small and light pumps (when compared to a pressurized system). Because the size of the fuel-flow remains within limits, this is possible.

Fuel type

In accordance with the functional requirements only JP4 and LH2 as possible fuel types are considered.

The heat of combustion of LH2 is about three times (2.8) the burning heat of JP4: 120 MJ/kg and 43 MJ/kg. The density however is about ten times less than JP4. This means that the energy density per cubic meter for JP4 is about 3.9 times higher than LH2:

So the advantages of LH2 are that the total mass of the fuel is three times lower than with JP4 and it has a much greater cooling capability. The disadvantages of LH2 are that it needs more space for the tanks, a larger diameter of the fuel pipes is needed and the tanks need thermal protection.

In the case of HARALD it was decided to use LH2.

5.3 Thrust and specific impulse

Because the time was limited, the thrust and the specific impulse could



not be accurately calculated .

In order to deliver the thrust and the specific impulse as soon as possible, the propulsion group decided to use the calculations of the turbo-ramjet presented in J.Propulsion (ref. [5.4]) and to try to verify these.

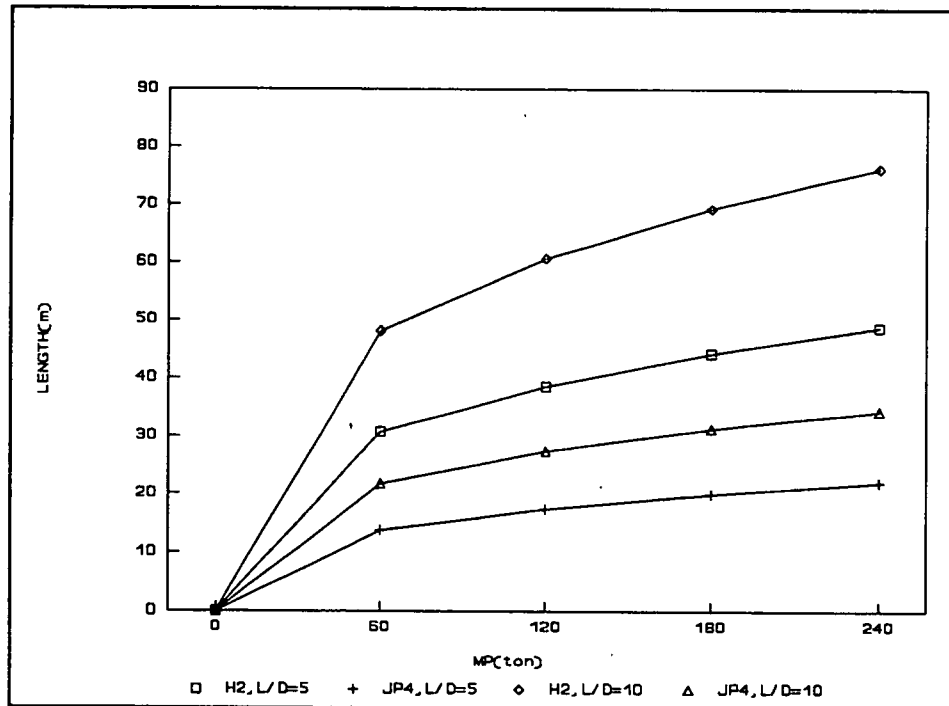


Figure 5.3 *Length of cylindrical tanks with spherical ends
fuel fraction 100%*

5.3.1 The J. Propulsion model.

The model presented in this chapter will be called the J.Propulsion model.

In the J.Propulsion model the thrust and the specific impulse are calculated according to current technology.

In ref. [5.9] a summary of the J.Propulsion model is presented.

Some limitations of the J.Propulsion model;

- target speed of mach 6 and fixed intake ramps above Mach 4.
- lack of precise geometrical data
- dual operation of the turbojet and the ramjet between mach 2 and mach 4.

Out of ref. [5.9] the thrust, related on the fan frontal area of the turbo-



jet and the specific impulse was found. It is assumed that the height of the intake equals the diameter of the ramjet-duct. This should be verified later, to see if there is enough mass flow and to see if no choking occurs in the ram-duct.

The results for a total duct area of 24 m² (= the duct area of the HARALD 1.5), are presented in fig. 5.4.

This figure is distilled from the data of ref. [5.9] (without precompression) and projected along the trajectory of HARALD.

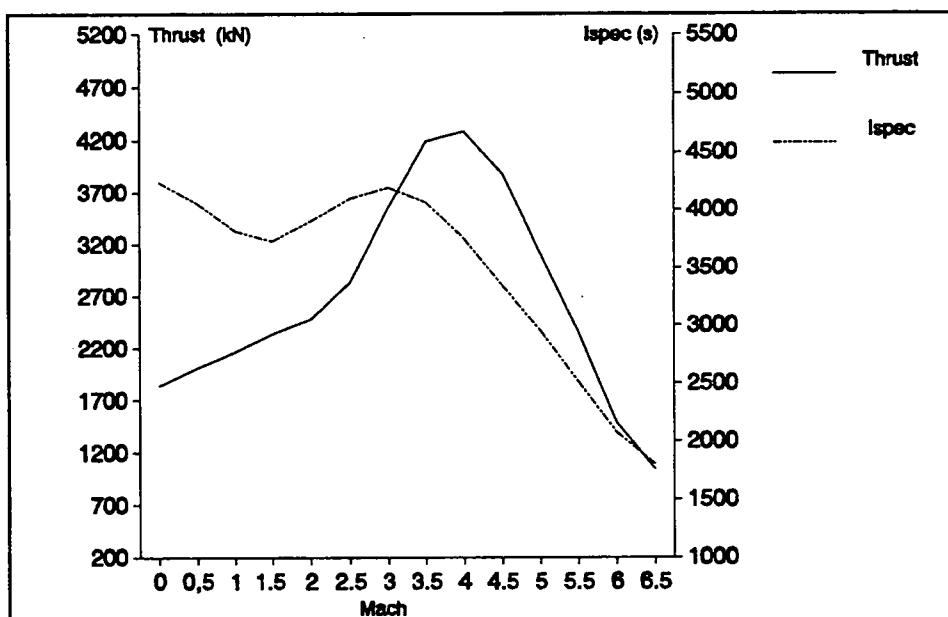


Figure 5.4 *I_{spec} and Thrust versus Mach along trajectory*

Because the engines probably have to be scaled, a simple scaling model for the thrust is used :

$$F/F_0 = A/A_0 = (D/D_0)^2$$

Where A is the frontal area, D is the diameter and the subscript 0 stands for the reference engine.

5.3.2 Verification

It was tried to verify the J. Propulsion model by two models that were developed.

The first model (Turbocalc.) is a turbojet model which was used to verify the thrust and the specific impulse during the turbojet mode.

The second model, Rampro (jointly developed by NLR and TNO), was



used to verify the ramjet mode.

turbojet mode

It was decided to use a modified version of the Olympus 593 of the Concorde (Turbocalc.) as a verification model for the turbojet. This version has a speed regime of Mach = 0 to Mach = 3.5. This model is described in ref. [5.6].

In fig. 5.5 the thrust per area of the J.Propulsion model is compared to Turbocalc..

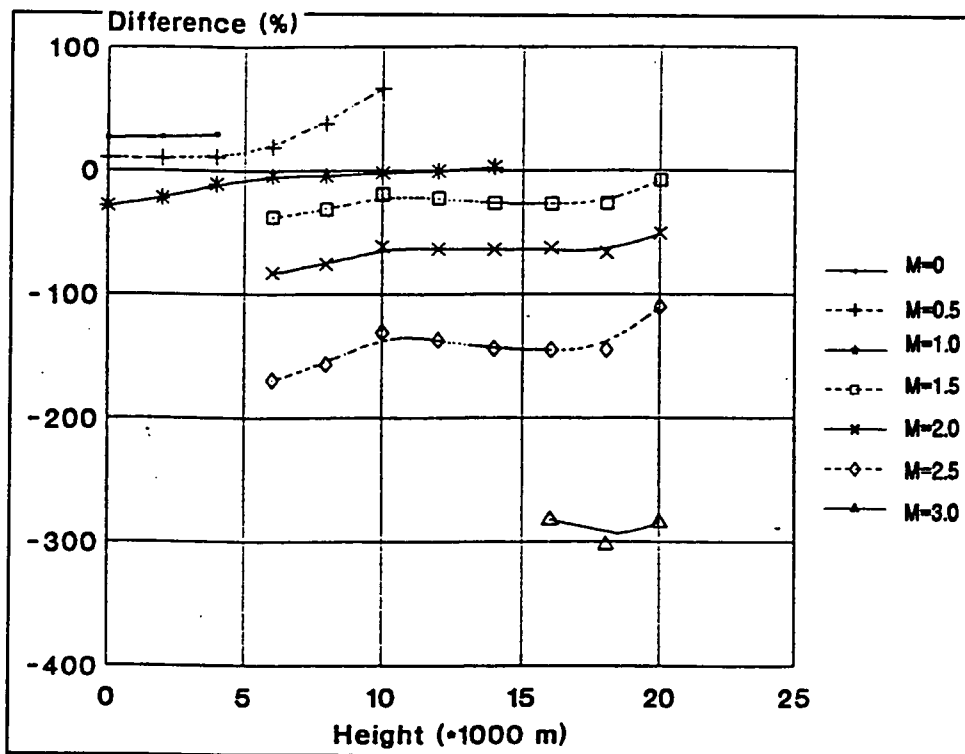


Figure 5.5 Difference in kN/m^2 between Turbocalc. and J.Propulsion $(Turbocalc.- JP)/Turbocalc.* 100\%$

An assumption made is the continuous operation of the afterburner because then the specific impulses were comparable.

In fig. 5.5, it is shown that at high mach numbers there is a very large difference in thrust/m². The thrust given by Turbocalc. is smaller than given by J.Propulsion model.

This could be explained by the fact that already in an early stage the ramjet is working (around Mach = 2).

A difference at the higher mach numbers could also be explained by the possible presence of precompression by the J.Propulsion model.



But also for the low mach numbers there is a discrepancy. This could be explained by assuming that the J.Propulsion model engine has a higher specific thrust (kN/kg/s) than the Olympus engine. So it can put more impulse in less air mass and has a higher thrust per m² fan area, which can be explained by a difference in combustion temperature.

Furthermore, maximum compressor temperatures were not taken into account, which may influence the thrust at higher Mach numbers.

It became clear that Turbocalc. shows, within certain limits, similarity with the J.Propulsion model.

However because better understanding is needed between the differences Turbocalc. was not used in the designing process.

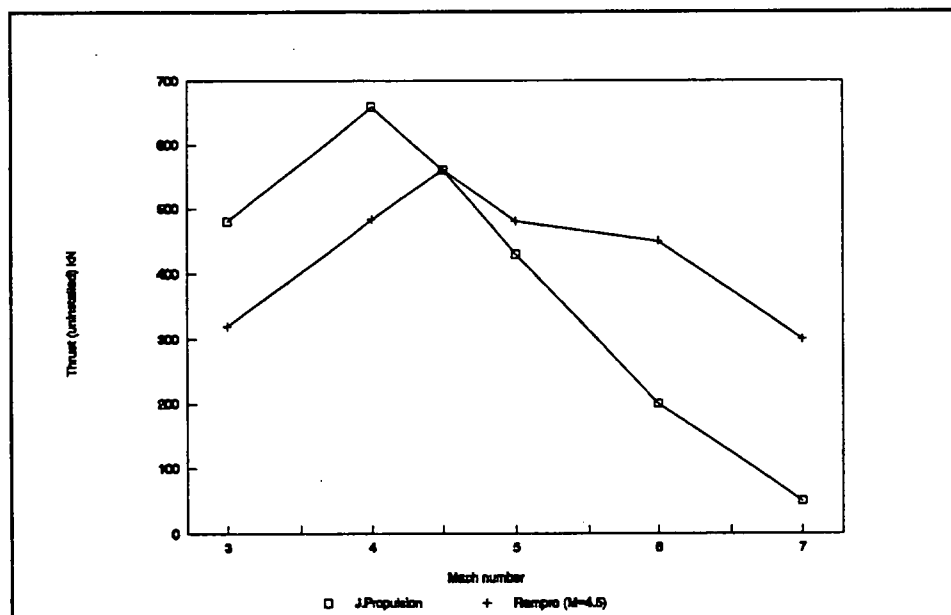


Figure 5.6

Thrust along the Sänger reference trajectory

ramjet mode

The model used to verify the ramjet mode of the J. Propulsion model is Rampro.

Rampro is a computer programme taking only ramjet calculations into account. This model is described in ref. [5.7].

Rampro does not take into account the turbojet, so it is difficult to say anything about the influence of a turbojet placed inside of the ramjet.

First a calculation was made for M = 4.5 see fig. 5.6, because this is the cruise Mach number.

Note that both lines have a maximum.



If the Mach number is lower, the total pressure is lower so the thrust is lower.

If the Mach number is higher, the thrust is lower, because:

- less energy can be added to the air, because the maximum burning temperature is fixed at 3000K
- increasing pressure losses, although the total pressure is increasing
- decreasing density of the air

In fig. 5.6, both lines show the same trend, but the differences are rather big.

The I_{spec} is considered in fig 5.7.

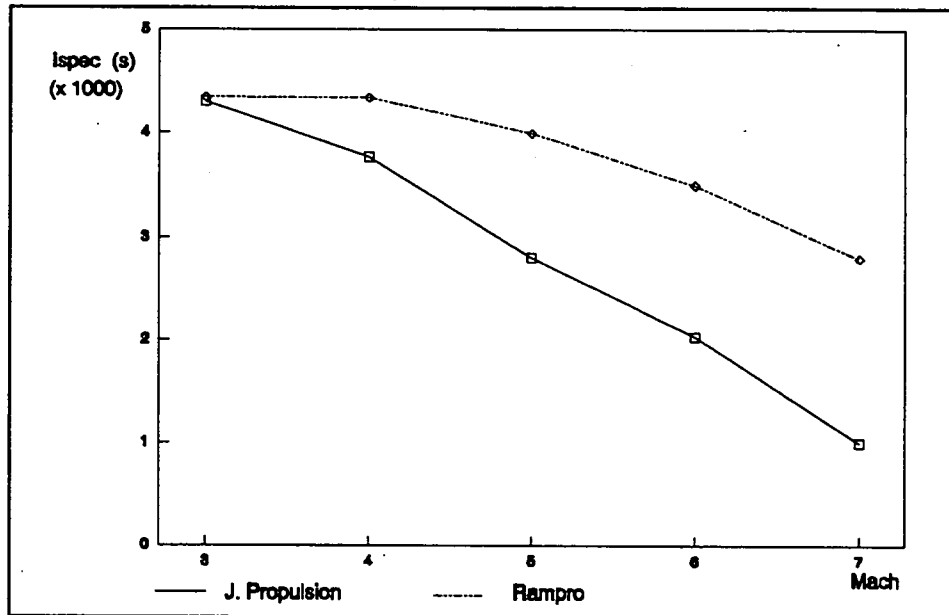


Figure 5.7 I_{spec} along the Sanger reference trajectory

The differences between Rampro and J.Propulsion can be explained as follows:

- Rampro uses 100% combustion efficiency
- different geometries (Rampro does not model a integrated turbojet)
- other pressure recoveries
- precompression can play part
- other FAR 's may be used
- the thrust of J.Propulsion decreases rapidly after $M=4$ because the intake ramps are fixed at $M > 4$.



Because the differences between Rampro and the J.Propulsion model are rather large and not yet fully understood, the J. of Propulsion model for the ramjet is used in the launcher design.

5.3.3 Effects of throttling and angle of attack

Throttling

Because of the required cruising capability of the design the effect of a changing Fuel to Air mass ratio Φ (throttling) on the thrust and Isp has been investigated. The thrust as a function of Φ is calculated for an altitude of 25 km at Mach 4.5, and shown in fig. 5.8.

It can be seen that a decrease in Φ causes a decrease in thrust.

Because less fuel is added, less energy is produced and the thrust will therefore decrease.

It is also noticeable that there is a decline in the increase of the thrust for increasing Φ as $\Phi > 1$.

This is because of incomplete combustion, where unburned fuel has to be heated, which causes heat losses at the cost of thrust.

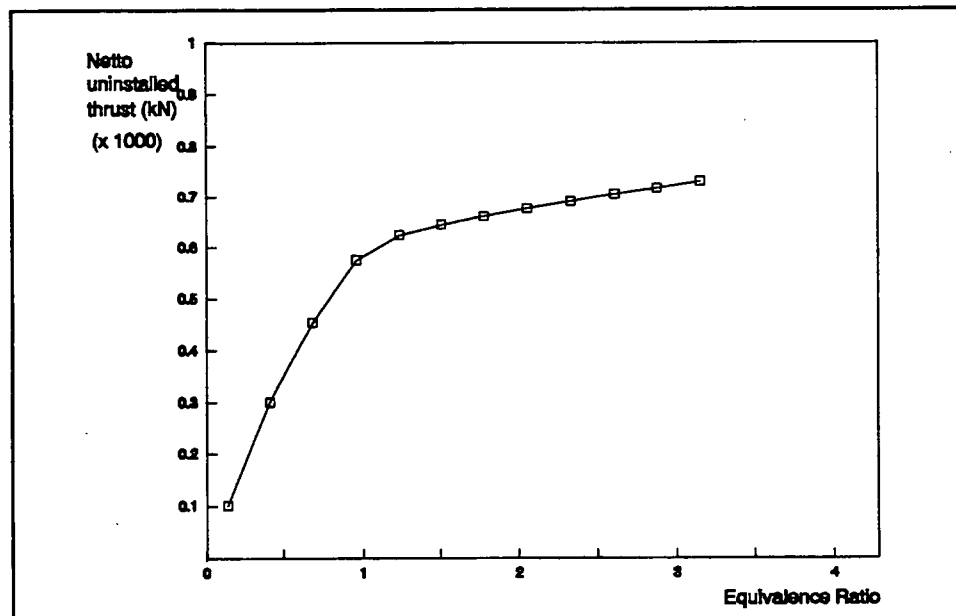


Figure 5.8 Influence of the Equivalence Ratio on the thrust

It can be shown that by increasing the fuel to air ratio, during some flight manoeuvres, the overall fuel consumption can be reduced despite the increase in specific fuel consumption (ref. [5.6]). For a

constant altitude turn, turn time is reduced and for an acceleration-climb at optimum dynamic pressure, climb time is reduced by increasing the equivalence ratio.

The separation flight manoeuvre can be optimized by controlling the mixture ratio which will reduce velocity losses and yield a faster increase of speed and altitude to achieve design requirements.

Angle of attack

Considered is the effect of the angle of attack (α) on the thrust for $M=4.5$ at an altitude of 25 km.

According to the functional requirements the angle of attack will be between $\alpha=-1$ and $\alpha=10$.

It was found that there is an almost linear relationship between the thrust and the α . The thrust decreases with decreasing angle of attack and increases with increasing angle of attack.

This is because of the fact that with increasing α the intake -through its geometry- takes more air.

At increasing angle of attack the deflection through the shockwaves becomes smaller (caused by the geometry) which causes a decreasing pressure loss.

This causes an increase of the pressure recovery factor, which in return gives increasing thrust.

Choking of the ramduct

Because the turbojet is installed in the ramduct, choking can occur in the duct.

Considered is a transition point at $M=3$ from turbojet mode to ramjet mode of the engine with a ramduct diameter of 2 m.

After the perpendicular shock in the intake-throat there is a speed of $M=0.9948$ and a throat height of 1.48 m.

The area per engine is $1.48 * 2 = 2.96 \text{ m}^2$. This causes a mass flow of 1324 Kg/s. The mass flow must pass the ramduct with an area of 1.21 m^2 , the speed becomes then 1094.76 m/s ($M=2.4$) -> supersonic !

possible solutions :

- the turbojet has to take 828,5 Kg/s to prevent choking
- a less ideal pressure recovery factor to cause greater speeds before the perpendicular shock, so that the speed after the perpendicular shock is lower. It has to be $M=0.3$ to prevent



- choking.
- The ratio of the ramduct and the turbojet diameter has to be changed.
 - The intake height must be reduced.

5.4 Cooling model for the engines

The turbo-ramjet engine will need cooling in a number of places. As the first stage must be reusable, ablative cooling is undesirable. For HARALD a direct regenerative cooling system is used. Here the hydrogen is led around the engine through a great number of channels or a jacket covering the whole engine surface.

In ref. [5.5] the heatflux of the combustion chamber and nozzle of the ramjet of the WCRV was found. This is used to calculate the total heat load which must be transferred to the fuel flow resulting in an increase in fuel temperature. In this paragraph the last results are given.

The engine is divided in four main areas: the front part, the combustion chamber, a throat area and the nozzle. The mean value of the heat flux (from ref.[5.7]) for this regions is multiplied with the corresponding area on which they act, giving a total heat load of **70.8 mW**. (A detailed calculation is given in ref. [5.8])

This heat load must be transferred to the coolant. The required mass flow hydrogen per engine can be calculated from;

$$m = q / c_p (T_2 - T_1)$$

where c_p is the specific heat capacity, T_1 the end temperature and the T_2 the start temperature of the fuel. The end temperature of the coolant must remain below its boiling point to avoid local hot spots on the channel surface.

Assuming an end temperature of the fuel of 450 K a pressure of 34.5 MPa, so that it will remain liquid, and a mean specific heat capacity of liquid hydrogen at 200 K, ref.[5.3], the required mass flow hydrogen per engine will be **12.2 kg/s**.

Then, with the calculations of ref. [5.8], the inside wall temperature at the throat becomes **546 K**



The mass flow of the cooling system will scale linearly with the scaling of the engine with the intake, as the total surface area will also scale linearly, as a first approximation, and the heat flux will remain the same.

Verification of the cooling mass-flow

As a verification for the size of the mass-flow, the NASP is looked at (ref. [5.3]), where the total mass flow is about 15 kg/s depending on the materials used for the cooling system. The NASP mass-flow is greater because of the higher heat-load encountered at Mach 18. The total heat-load of 70.8 mW is about one third of the NASP heat-load of 190 MW.

However, the fuel consumption at Mach 7 with an altitude of 35 km is about 4.4 kg/s per engine. With a calculated required coolant mass flow of 12.2 kg/s, this means that there is a too little mass flow to cool the engines. One way to lower the heat-load and thus decrease the necessary coolant mass flow is to increase the equivalence ratio, though this is already done (ref. [5.3]); or higher the system pressure so the hydrogen can take more heat, without going to boil.

In the calculated mass flow, radiative cooling has not been looked at although this can dissipate 5 to 25% of the heat-load. Also of course the calculation is a very rough estimation because of inaccurate data and data acquisition. It can be adjusted by varying the many parameters.

5.5 Mass of the propulsion system

In order to give an estimation of the total take-off mass of the HARALD the mass of the engines has to be determined.

Cooling system mass

An estimation of the mass of the entire cooling system for the engine is calculated in ref. [5.8]. Chosen is a direct Incoloy-909 active regenerative cooling system using the hydrogen as the cooling agent. The cooling mass scales linearly with the heat load, and as it is about one third of the NASP heat load the total cooling system mass will amount to:



$$W(\text{tot})=453 \text{ kg}$$

This heat load is however given at an equivalence ratio of 1.5, and as a ratio of 1 is being worked with the mass will become higher but this will have to be investigated in a further study.

Engine mass

By the Concorde the intake takes up 2.8% Ref. [5.2] of the Gross Take-Off Mass of 46400 kg and so does the nozzle, the engine and its surrounding body takes up 7.4% .

For an upgraded Olympus engine, including the ramjet and the scaling of the intake and nozzle from 1.4 to 2m in diameter this results (for the HARALD 1.5) in:

$$9350 \text{ kg (per engine)}$$

This includes the ramburner, struts and fairings, but not hydraulics and actuation of intake ramps and nozzle petals. Ramducts include core engine casing and sealing provisions of both intakes.

After a large mass reduction per engine, due to the use of new materials, of 40% (ref. [5.2]), the total engine mass including the cooling system will add up to:

$$W(\text{tot}) = 6030 \text{ kg (per engine of the HARALD 1.5)}$$

Scaling the mass of the engines

If scaling is applied to the engine intake area to increase performance, the two frontal dimensions will both be multiplied by a scale factor Λ . The mass will be multiplied by one factor Λ^2 , as the engine can be seen as built up out of layers. The length of the engine will need to be scaled as the expansion ratios and angles of the intake and nozzle must remain the same to keep the airflow laminar.

We will assume a scale factor f for length equal to the other scale factors as a first approximation. Then the total mass of the engines, of the HARALD 1.5, will scale as:

$$W(\text{tot}, \Lambda) = \Lambda^2 * W(\text{tot}) = \Lambda^2 * 36180 \text{ kg}$$

The scale factor, Λ , is determined by System Engineering (Chapter 3).



5.6 Conclusions & recommendations

Conclusions

The thrust and specific impulse are given as a function of size and trajectory according to the J.Propulsion model. The thrust and specific impulse are also calculated with Rampro and Turbocalc, but there is decided not to use these results for the HARALD because the differences between these models and the J. Propulsion model are not yet fully understood.

The mass of the propulsion system is also given as a function of the size of the engines to enable photographic scaling.

Cooling is needed in several places in the engines, but with our assumptions it is not possible to cool sufficiently just by the fuel mass flow.

With the assumption that the intake height is as large as the ramduct, there will occur choking in the ramduct if there is a transition point at Mach 3.

An error occurred by the assumption that the intake area was as big as the duct area. This is not true, because the ducts have a round shape so that area is smaller by a factor 0.78 than the area of the intake.

It was not until the writing of this report that we discovered that scaling the combustion chamber in Rampro implied changing the diffuser. Unknown are the effects on the thrust and Isp.

Recommendations

Because of the limited time it was not possible to study all the aspects of the propulsion system. Some subjects were only slightly touched or marked. So a few recommendations have to be made for further study.

It is recommended to study the effect of overfueling, to see if this can solve the problem of cooling the engines. The installation of a pre-cooler can also have great advantages (mass reduction, lower temperature), but this should first be investigated.



It could be possible to use a smaller engine. The ratio of the ramduct diameter and the fan diameter should therefore be examined.

The ratio of the intake height and the ramduct diameter should be investigated further to see if choking can be prevented.

The use of a flat belly, instead of a cone, can give a uniform flow condition to the engines. This is a configuration that should be looked at in further studies.

The effect of scaling, on the length of the engine, should be investigated in more detail.



References

- [5.1] System Engineering Functional Requirements Document Propulsion, HAR-FRD-005, TU Delft, 1993
- [5.2] Lowrie, B.W. Future Supersonic Transport Propulsion Optimisation, Proceedings of the symposium of the European supersonic transportation system, Strasburg, 6-8 Nov. 1989
- [5.3] Nasa Technical Memorandum 102610 Hypersonic Vehicle Simulation Model: Winged-Cone Configuration, Nasa Langley Research Centre, N91-12705, 1990
- [5.4] Sakata, K. a.o. Hypersonic Turbomachinery-Based Air-Breathing Engines for the Earth-to-Orbit Vehicle, J.Propulsion VOL.7,NO1 Jan.-Feb 1991, pag.108-114
- [5.5] Winged Launcher Configuration Study, MBB, British Aerospace, Rolls-Royce, MTU, FIAT, VDK and DORNIER. Final Presentation ESTEC, 10 May 1989
- [5.6] Wiel, R.A. van der Turbojet propulsion for the HARALD spaceplane, HAR-PRO-004, TU Delft, 1993
- [5.7] Verduijn, F.F. Ramjet propulsion for the HARALD spaceplane, HAR-PRO-003, TU Delft, 1993
- [5.8] Mijnen, P.W. Cooling, weight and configuration for the HARALD propulsion system, HAR-PRO-002, TU Delft, 1993
- [5.9] Vliet, L.D. van Performance of engines of a Space plane, HAR-PRO-001, TU Delft, 1993



6 Structures

Abbreviations

WTO	Take-off weight
c.g.	Centre of gravity
TPS	Thermal Protection System
MMI	Metallic Multi-Wall
cal.	calculated
m	mass
b	body
w	wing
t	tail
c	canard
fe	fixed equipment
g	gear
pp	powerplant
ft	fuel tanks
pl	payload
f	fuel
to	total
p	power parameter
i	i-th substructure



6.1 Introduction

For the HARALD it is important to know the take-off weight and the centre of gravity (cg). This became the main task of structures.

First it was necessary to break down the structure of the HARALD into sub-structures. After this a mass-prediction model had to be developed. Using this we could establish a model for determining the c.g. of the HARALD. After this we performed a sensitivity-analysis on the model.

These three steps will be shown in this report. We will conclude our report with a list of our conclusions and recommendations.

The results printed in this chapter are based on the first report of the group Structures. New results can be found in ref.[6.9].

6.2 Mass prediction model

After deliberation we decided to use the mass-prediction-model for jet-fighters in ref. [6.7]. The shape and performance (except for the high g-loads) of this class of planes comes closest to HARALD (and Sanger). There are of course a few typical differences between a fighter and HARALD. However, these are dealt with in a relatively simple way, as will be shown.

6.2.1 Mass-breakdown

To use the model, first a mass-breakdown is needed. The total structure will be divided into nine substructures that correspond with ten masses. The tenth mass is the fuel mass. The breakdown is as follows:

→	body	m_b
→	wing	m_w
→	tail	m_t
→	canard	m_c
→	fixed equipment	m_{fe}
→	gear	m_g
→	powerplant	m_{pp}
→	fuel tanks	m_{ft}
→	thermal protection	m_{TPS}
→	payload	m_{pl}



→ fuel m_f

empty mass : total mass minus payload minus fuel mass
 struct mass : body, wing, tail, canard, tps and tanks
 equipment : fixed equipment
 powerplant : 6 engines

We combine the individual substructures to larger substructures in order to make comparison to the literature easier.

6.2.2 Determination of the masses

For most of the substructures the used model gives mass-prediction formulas of the form:

$$m_i = c_i \cdot (m_{to})^{p_i} \quad (6.1)$$

m_i = the mass of the i-th substructure

c_i = factor parameter of the i-th substructure

p_i = power parameter of the i-th substructure

m_{to} = the take-off mass (without payload) of the HARALD.

The mass of the fuel tanks is a function of the volume of the fuel (ref. [6.2]). The total fuel mass as well as the mass of the powerplant are input-parameters. All the mass-prediction-formulas can be found in ref. [6.2].

Before anything can be calculated, a value must either be given to, or assumed for all of the specific parameters. These values were derived either those given in ref. [6.7]. or specified by System Engineering. After putting these values into the mass-prediction-formulas, the masses of some of the substructures can be expressed respectively as a function of m_{to} , others have obtained a numerical value. Now m_{to} can be solved from the following equation:

$$m_{to} = m_b + m_w + m_t + m_c + m_{fe} + m_g + m_{pp} + m_{ft} + m_f + m_{TPS} \quad (6.2)$$

Equation 6.2 can be solved by iteration. When m_{to} is known, the masses of all substructures can be determined.



6.3 Verification, validation and qualification of the model

Verification

The verification of the model is carried out with the non-adjusted model. Data of several jet-fighters are put into the model. The outcomes have been compared to the known masses. We have done so for four different jet-fighters: the F16, the F15, the Mirage and the Harrier. The results of these verifications are shown in table 6.1.

Airplane	M_{to} (cal.) [lb]	M_{to} (real) [lb]	Difference
F 15	38611	42055	- 8.07 %
F 16	20781	25084	- 17.15 %
Mirage	22039	23501	- 6.05 %
Harrier	25903	21982	+ 17.84 %

Table 6.1

Mass-model verification.

As can be seen in Table 6.1 the predicted masses of the airplane are within a range of 18% of the real take-off masses. It was now shown that the model was reasonably accurate in its original form.

Validation

The validation of the model is carried out with the adjusted model. The validation is carried out by putting the data of Sanger into the adjusted model. How the model was adjusted will be discussed in 6.4. The outcome will be compared to the known masses. The results of this validation can be found in Table 6.2. These results show that the take-off mass for the Sanger, predicted by the adjusted model is about 21% too high. This overprediction is probably caused by the fact that the model is based on technology of about 20 years ago. We are now able to produce constructions that are much lighter than those twenty years ago.

Airplane	M_{to} (cal.) [lb]	M_{to} (real) [lb]	Difference
Sanger	705020	660 - 770 $\cdot 10^3$	-6.8 - +8.4%

Table 6.2

Mass-model validation

Qualification



After proving that the model was applicable to HARALD, we still had to qualify it. Therefore the results have had to be guaranteed within a certain range. A safety margin had to be used. After verification and validation it could be assumed that the real mass of the HARALD will be within the range of the calculated mass prediction by a factor 25%. The results of the calculations will be shown in 6.5

6.4 Adaption of the model for the HARALD

Between fighter-jets and aircraft like the HARALD there are some essential differences that need to be examined. If these differences appear to influence the predicted masses, the model has to be adjusted. The differences to be examined are the following.

Bodyfactor

The formula of the body is updated by multiplying it by a factor 0.5, because the influence of the factor L/h is too large. The factor 0.5 chosen because the structure mass then comes more into line with what can be expected from the body mass/total mass ratio.

Material choice

High temperatures cause a drop of the maximum allowable stress in a material. The range in temperatures is large. Because of this, one has to change the material (type or dimensions) or use a thermal protection system. (TPS)

It is determined that a titanium structure can withstand temperatures up to 850 Kelvin without losing strength (ref. [6.5]). It was decided to use a safety margin and prescribed that the temperature of the primary titanium structure has to stay below 700 Kelvin.

The way this problem is solved is described in ref. [6.5]. It is stated there that active cooling will not be necessary. The expected values of the heatflux ($0.5-1.5 \text{ MW/m}^2$) can be dealt with by a passive cooling system.

The TPS of the HARALD will consist of two parts:

- a) the nose cap, the leading edges and the control edges will be hot structures. These kind of structures are usually build of



ceramic materials (like SiC/SiC or C/SiC) or of a carbon-carbon composite (C/C), both with a coating.

- b) the body and the wings will be covered with a TPS that exists of a metallic multi-wall insulation (MMI). Within the range of 500°C to 1000°C this concept leads to the lowest mass per square meter. The MMI will be build out of a cobalt nickel alloy with an internal isolation for those areas where the temperature will rise above 800°C.

The mass of the TPS can be predicted. With a hot structure mass of 1.5 Mg and a metallic-multi layer insulation of 14.0 Mg the total TPS will weigh 15.5 Mg.

This result means that 15.5 Mg has to be added to the take-off mass of the HARALD.

Adaption of model for material choice

In the model used it was assumed that 75% of the structure was made of aluminium and 25% of titanium. The HARALD however totally consists of titanium.

The critical load is assumed to be the Euler-load. The critical factor is Elasticity modulus/(density)³. If the factor for aluminium equals 1, then for titanium it equals 1.34. This gives a total mass-penalty of the primary-structure of about 25.5% ($0.75 * 34\% = 25.5\%$). Therefore the formulas of the body, the wing, the tail and the canard must be multiplied by a factor 1.255 (as shown in ref. [6.2]).

Pressurized cabin

Unlike a fighter's flight deck, HARALD's will have to be pressurized. The effect of this on the masses is examined. This examination is performed in ref. [6.2]. The conclusion here is that the presence of a pressure-cabin has very little influence on the total mass of the structure.

6.5 Internal layout

In order to make an accurate c.g. model, first the position of every sub-structure has to be determined. For the following sub-structures an analysis was done. The rest was specified by System Engineering.



6.5.1 Canard

The canard has to be retractable, as it will give too much drag during hypersonic flight. It was decided that both sides of the canard are retracted into the body almost horizontally where they are positioned on top of each other. In order to make this possible the canard needs to be positioned at 19.6 m of the nose of the HARALD.

6.5.2 Gear

After studying literature a tricycle carriage with nose-wheel was decided upon. This because it is the one used by all big jet-aircraft and during landings the brakes can be fully used.

Also important is its place on the HARALD. It became clear at a later stage in the project that, because of extra tanks, there was no room left in the wing for the undercarriage. So it appeared to be analogous with the undercarriage for the F104 Starfighter. Its small wings also do not allow the undercarriage to fold into the wings. Thus the nose wheel was kept the same, but the main bogies were fastened to the main body of the HARALD and designed to retract into the body.

There are problems with the location of the rear gear. It has to be located behind the c.g. but it can not be situated behind the nozzles of the engines. The only possibility left is the location between the engine and the wing, but here there is not enough room. Further solutions will need to be looked into.

6.5.3 Flight deck

In front of the canard there is enough space left to contain the cockpit plus additional equipment. The only problem will be the visibility. Because of the very long nose with a very small slope the pilots will not be able to look in front of them which is unpractical especially during the landing. This problem needs to be solved for example by installing cameras or a bending the nose.

6.5.4 Fuel tanks

System Engineering restricted the tank-geometry. The tanks had to be cylindrical with elliptical end surfaces. Structures decided to use four cylindrical fuel tanks with elliptical end surfaces. They are situated as shown in ref. [6.2]. The total capacity of these fuel tanks is 1103 m^3



of fuel. For the HARALD liquid hydrogen with a density of 71 kgm^{-3} is used, so the total fuel mass will be 78.3 tons.

6.6 Prediction of the cg-position

The most important variables in calculating the location of the c.g. are the mass of the second stage and the mass and location of the fuel (which varies in time). In order to be able to predict the co-ordinates of the c.g. within a short time at every moment of the flight the structure will be divided into three parts.

Dry structure

- For the body, wing, canard and tail the assumption is made that the mass is equably distributed over the surface. Then the c.g. of these structures can be determined with the standard method (ref. [6.6]).
- The positions of the gear, the powerplant and the tanks are determined in the description of the layout. From this position their c.g.'s can easily be calculated.
- The positioning of the fixed equipment is a problem, because this substructure exists of a number of smaller structures which are located all over the HARALD. However in the lit 6.7 the c.g. of the fixed equipment is often located at about 40% of the fuselage length.

Fuel

The mass and the location of the fuel varies during the flight. By pumping fuel around one can influence the location of the c.g. of the HARALD. In that case however, an extra weight item is introduced. For two situations the c.g. of the HARALD has been calculated: namely for filled and for empty tanks. One has to realise that these two values are not the limit values of the c.g.

In order to obtain the c.g. of the total structure the following formula is used:

$$X_{c.g.} = \frac{\sum X_i W_i}{\sum W_i}$$

with: $X_{c.g.}$ = X coordinate of the c.g. of the total structure



$$X_i = X \text{ coordinate of the c.g. of the substructure}$$

$$W_i = \text{weight of the substructure}$$

The position is measured from the tip of the nose.

The relative positions of the sub-components are listed in Table 4

Substructure	Xc.g./L
Body	0.62
Wing	0.80
Tail	0.97
Canard	0.28
Gear 1/3	0.28
2/3	0.85
Powerplant	0.77
Tanks	0.69
Fuel	0.69
Second stage	0.68
Fixed equipment	0.39
TPS	0.65

Table 6.3 relative positions sub-structures

6.7 Results

The results for the HARALD were gained with help of the computer-programme for the prediction of the take-off mass of the HARALD developed by structures.

Numerical results

For the results of the mass calculations the reader is referred to Table 6.4.



Substructure	Mass [ton]		Mass [ton]
Body	50.7	Powerplant	47.8
Wing	13.6	Tanks	10.5
Tail	2.9	Fuel	78.3
Canard	2.9	Second stage	100.0
Gear	1.8	Fixed equipment	35.5
TPS	11.2		
Total			355.2

Table 6.4

Numerical Results

The calculations for the c.g. then yield the following results.

Condition	c.g. position (%)
full tanks	67.2
empty tanks	61.9

Table 6.5

c.g. position

It is clear that it will be possible to keep the c.g. of the total structure within the range of 60% to 70% of the total length. This is necessary according to Stability in order to maintain a stable flight.

Sensitivity analysis

The sensitivity analysis of the mass-model and the c.g.-model is done by studying the effects that scaling of the structure has on the total mass and the mass of the different sub-systems. With the differing masses of the sub-system the position of the c.g. can be determined. We also looked at the influence that the engine mass has on the total mass.

In fig. 1 & 2 respectively the total mass and the c.g. position with full tanks and with empty tanks is plotted against the scaling factor. It is clear that the total weight increases rapidly with increasing scale. The c.g. position goes towards the nose of the HARALD when the scaling factor increases.



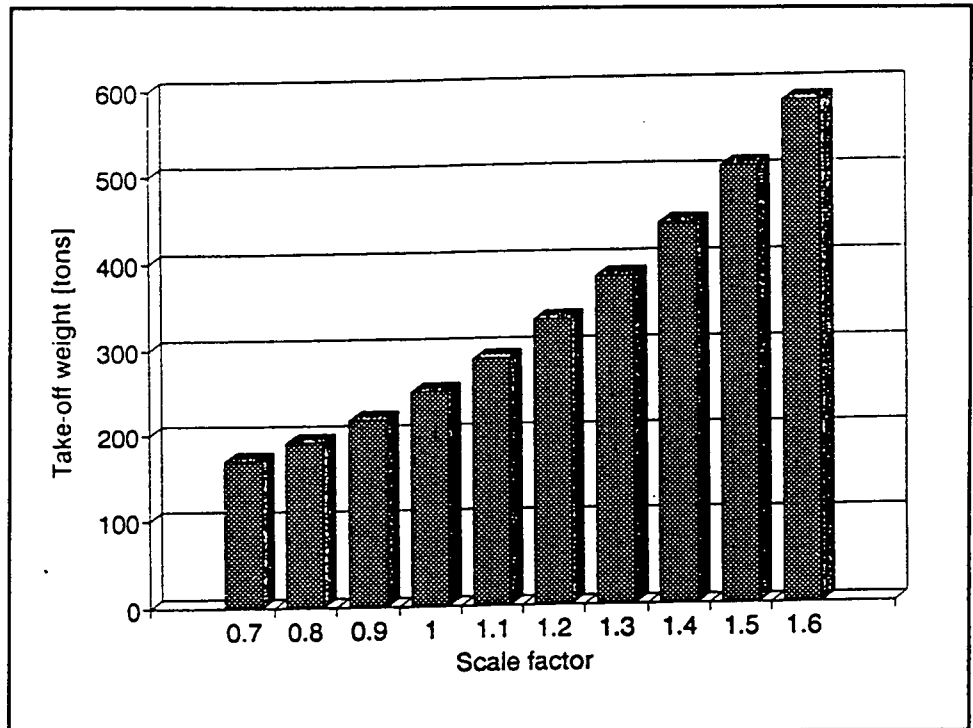


Figure 6.1 *Total mass prediction versus scaling factor (N)*

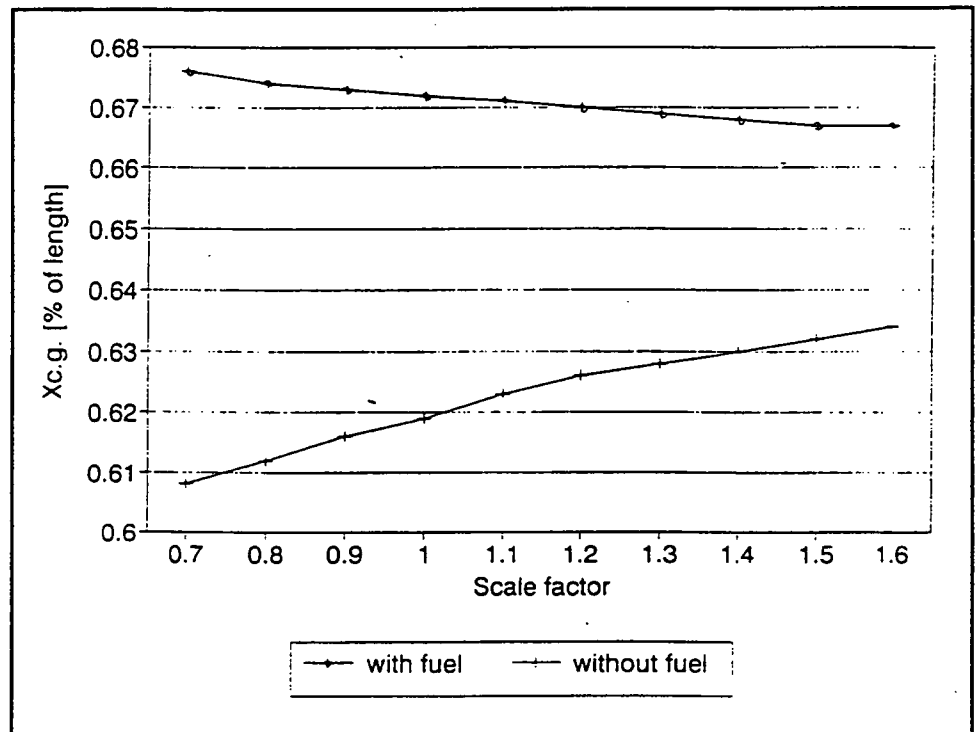


Figure 6.1 *Centre of gravity versus scaling factor*



6.8 Conclusion & Recommendations

Conclusions

Structures has succeeded in producing a mass-prediction model for space planes like the HARALD. After verification and validation the model appeared to be accurate up to 25%. This model has been put in an user friendly computer program which enables the user to calculate the mass of space planes as a function of geometrical parameters like the wingspan, bodylength etc., constants like the fuel-mass and the engine weight, and the photographic-scaling factor. Also the consequences of changes of parameters and/or constants for the (substructure)-mass(es) can quickly be shown with help of this program. The mass of the most recent version of the HARALD comes to 355 tons.

The centre of gravity of the HARALD has been determined with help of the masses, c.g.'s and relative location of the substructures. Some of the substructures like the fuel-tanks did not have a prescribed location. Structures has decided on the internal layout of the HARALD and therefore on the location of those substructures. The calculated c.g.'s of the HARALD with full and with empty fuel tanks are respectively 0.672 and 0.619. Therefore it will be easy to keep the c.g. between 0.6 and 0.7 during the flight which is necessary to allow a stable flight.

Recommendations

The collection of more comparison material in order to validate the model more accurate.

The mathematical aspects of the model need to be examined especially when more variables become constants specified by other groups.

Different tank geometries need to be studied.

The fixed equipment need to be specified in order to make a more accurate determination of the c.g.

The change of the position of the c.g. due to the retraction of the canard needs to be established.

The problem of the positioning of the cockpit (visibility!) needs to be solved.

The critical load for all construction parts needs to be established.



The reason for the high body mass (before correction of the model) needs to be found.

A more accurate temperature distribution needs to be found.

References

- [6.1] System Engineering Functional Requirements Document Structures, HAR-FRD-006, TU Delft, 1993
- [6.2] Mourik, A. van, Brinkman, M.R., Khodaparast, S. Structural model for spaceplanes part 1 Mass model, HAR-STR-001, TU Delft, 1993
- [6.3] Luipen, J.J.W. van, Brinkman, M.R. Structural model for spaceplanes part 2 Computer programme, HAR-STR-005, TU Delft, 1993
- [6.4] Khodaparast, S. Structural model for spaceplanes part 3 Materials, HAR-STR-004, TU Delft, 1993
- [6.5] Boogaard, M. Structural model for spaceplanes part 4 TPS, HAR-STR-002, TU Delft, 1993
- [6.6] Brinkman, M.R. Structural model for spaceplanes part 5 C.G.-Model, HAR-STR-003, TU Delft, 1993
- [6.7] Airframe Structural Design, Lockheed Aeronautical Systems, 1989
- [6.8] Torenbeek, E. Synthesis of Subsonic Airplane Design, Delft, University Press, 1982
- [6.9] Luipen, J.J.W. van, Brinkman, M.R. Structural model for spaceplanes part 2 Computer programme, HAR-STR-006, TU Delft, 1994



7 Stability & Control

Abbreviations

np	neutral point
AOA	angle of attack
arm	length
c	mean aerodynamic chord
cg	centre of gravity
C_D	$D/(qS)$
C_L	$L/(qS)$
C_{la}	lift coefficient of body and wing
$C_{L,dc}$	lift coefficient due to a deflection of the canard
$C_{L,\alpha}$	derivative of lift coefficient with respect to α
C_M	$M/(qSc)$
C_{Ma}	moment coefficient of body and wing
$C_{M,dc}$	moment coefficient due to a deflection of the canard
$C_{M,\alpha}$	derivative of pitch moment coefficient with respect to α
$C_{n,\beta}$	static directional stability derivative
C_N	$N/(qS)$
C_T	$T/(qS)$
$C_{T,n,\beta}$	derivative of yawing thrust-moment coefficient with respect to β
D	drag force
L	lift force
l	length of fuselage HARALD
mrp	moment reference point
M	number of Mach
M	pitching moment
N	normal force
sm	stability margin= $X_{np}-X_{cg}$
WCRV	Winged Cone Reference Vehicle
X_{np}	X location of np
X_{cg}	X location of cg
X_{mrp}	X location of mrp
α	angle of attack
δ_c	deflection of canard
δ_e	deflection of elevon
ρ	air density



7.1 Introduction

Stability and control are two different kinds of disciplines. Stability performs the condition in which an aircraft is due to aerodynamic forces. An aircraft is said to be stable if disturbances of aerodynamic forces will tend to be disabled. The aircraft will be in a new equilibrium. No equilibrium will be achieved when the aircraft is unstable, unless the pilot or a control system manage the aircraft to a desired situation.

The second discipline, control, will perform the deflections of the elevons, canard and rudder to bring the aircraft to a desired point of operation. These deflections will change the aerodynamic forces acting on the vehicle.

So the state of stability has influence on the deflections desired and the overall performance of HARALD.

It was required (ref. [7.1]) that the stability group should therefore determine the state of stability and the deflections needed during the flight. Furthermore, advice should be given to improve the performance by varying the angle of deflection, the position and the size of the canard. Although other aerodynamic surfaces have also have a large influence on the stability and control of the vehicle, it is not within the scope of this project to investigate these in detail.

The static stability is investigated by using a model that determines the location of the neutral point and the location of the centre of gravity along the trajectory. A program has been written to calculate a fuel consumption scheme so that the stability margin is within its requirements.

Another program has been written to calculate the trimmed coefficients along the trajectory with different angles of incidence of the canard.

It must be noted that these models only take the weight of the HORUS into account because no data of aerodynamic coefficients of the HORUS was given.

Our calculations are based on the aerodynamic coefficients of the WCRV.

In this chapter the derivation of the stability margins are given in paragraph 2. In paragraph 3 the model which was used to calculate the trimmed coefficients is discussed. The next paragraph deals with the effects of the canard on the stability and control of the vehicle. Some conclusions and recommendations are given in paragraph 5.



7.2 Static stability requirements

Designing for static stability means that during the whole flight envelope a situation must be achieved where a stable equilibrium condition can be reached, disturbances will be damped out by counter-acting aerodynamic forces and moments and control forces will be acceptable (both in trimmed and out of trim conditions). So

- The aircraft must at least be static longitudinally and directionally stable during its entire flight envelope.
- Control forces and rudder deflections must be minimal during the entire flight envelope.

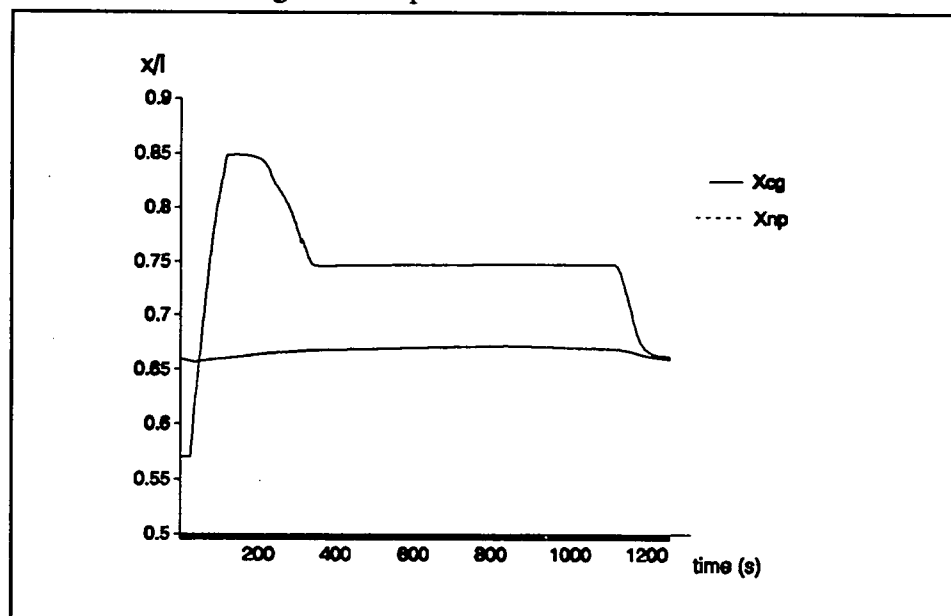


Figure 7.1

x_{cg} and x_{np} along the trajectory

7.2.1 Static longitudinal stability

Static longitudinal stability applies to the response of an aircraft to two kinds of disturbances. The first is a simple disturbance in the horizontal or the vertical speed.

The second, more important kind of disturbance within the scope of the project, is due to a disturbance in pitch. This is normally called the static longitudinal stability. The condition for stability is:

$$C_{m_\alpha} + C_{m_{T_\alpha}} < 0 \quad 7.1$$



This is the well known condition for static longitudinal stability, with an additionally thrust derivative. When this condition is achieved, the aircraft will return to its original trim angle of attack after a disturbance. A positive sign of condition 7.1 means that the handling qualities of the aircraft are deteriorated and an automatic pilot will have to do the control.

The state of static stability is given by the coordinates of the neutral point and the centre of gravity. The results of the location of cg and the location of np is given in figure 7.1. The stability margin is the difference of the coordinates of these two centres,

$$sm = x_{np} - x_{cg} / l$$

a positive margin means a static stable design.

The centre of gravity depends on the way the tanks are emptied due to fuel consumption. The way to empty the tanks depends on the stability margin, so first assumptions are made for the borders of stability margin and then the succeeding tanks will be emptied. We assume the stability margins to be positive near to zero. However as found from the CAA regulations the stability margin may not be smaller than -5% of the mean aerodynamic chord.

A program was written to calculate the order to empty the tanks with the constraints of longitudinal static stability along the mission trajectory.

This program is called HYPSTAT. First it calculates the location of the np (from ref. [7.3]) for each point of the trajectory. After that the program will search for the tank which will lead to the best result for longitudinal static stability. It could be possible that this tank is empty already. If this is the case the program will take the tank with the second best result.

More information can be found in ref. [7.5].

HYPSTAT determines the np, the cg and from that the sm in each point of the trajectory.

The results of the used tank for fuel consumption is given in figure 7.2.



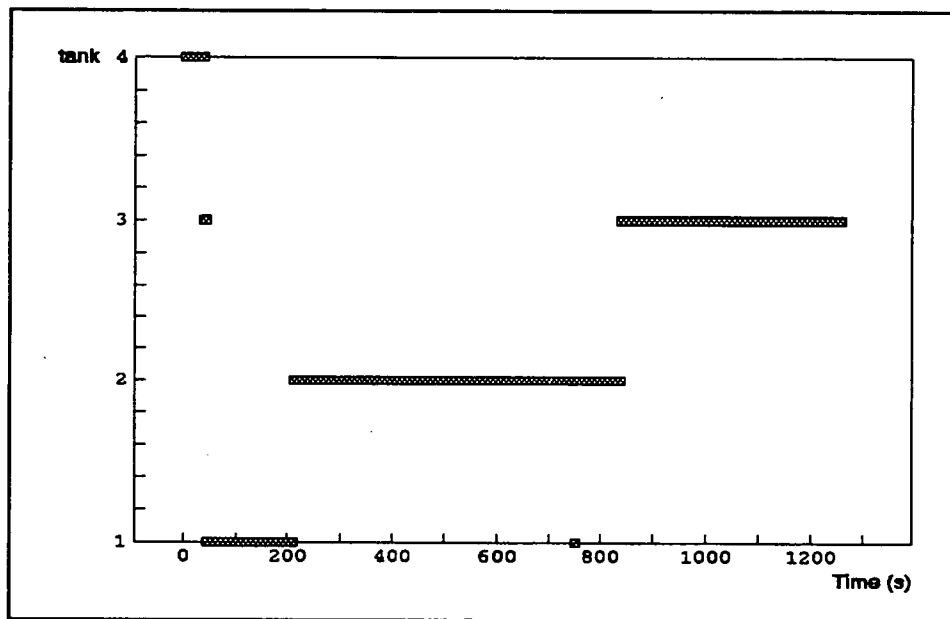


Figure 7.2

Sequence of tank use

7.2.2 Static directional stability

Static directional stability is achieved when the following condition is satisfied:

$$C_{n\beta} + C_{Tn\beta} > 0 \tag{7.2}$$

This directional stability is required, because it gives the aircraft the tendency to return to a straight flight path.

High numbers of Mach and large angles of attack will deteriorate the directional stability considerably. So for the space plane the design for static directional stability will give some very serious problems. The second stage will give rise to additional problems concerning this stability requirement.

As the calculation of the directional stability requires the use of aerodynamic coefficients of separate surfaces, only general remarks could be made regarding this stability, see ref. [7.7].



7.3 Trimmed flight

To drive the vehicle on a straight path, the moment must be zero. The pitching moment equilibrium in the cg is done by a deflection of the elevons and the canard. The canard will operate only in subsonic speeds and is retracted for speeds above Mach 0,9. So in the subsonic speeds, numerous deflections are possible to have a pitching moment equilibrium. The optimal combination of the deflection of the canard and the elevons is thus to have a optimal performance. The performance will be optimal when the lift over drag ratio is at its maximum. We have used data of ref. [7.4] to calculate for trimmed coefficients. So for a given mission trajectory, trust and state of HARALD, and a given centre of gravity an equilibrium will be achieved by the deflections of the elevons and the canard. Finally a program is written to calculate trimmed coefficients.

The program "HYPTRIM" first calculates the trimmed coefficients and deflections along the mission trajectory. The calculations are repeated for speeds below Mach 0,9 with different deflections of the canard. Then the user has to sum up the output for which deflection of the canard, HARALD gives the optimal performance.

A second calculation is done to have a matrix of trimmed coefficients as function of Mach and AOA. The trimmed coefficients in the matrix are corrected for the mission trajectory and thrust. So if trimmed coefficients are needed for e.g. Mach 4 and an AOA, the coefficients in the matrix corresponds to the state of HARALD in the mission trajectory when Mach was 4. This speed corresponds to a specific time in the trajectory and a specific thrust that was acting on HARALD. For detailed information of the "HYPTRIM" program, see ref. [7.6].

In figure 7.3 the change in lift coefficients due to trimming are given as function of the trajectory .

(The time scale in the figures 7.3 to 7.5 has to be multiplied by a factor 2)

In figure 7.4 the change in dragcoefficients due to trimming are given. Figure 7.5 shows the deflections of the elevons needed for trim. It can be seen that these deflections are within the constraints set by System Engineering. So it should be possible to trim the HARALD a long the trajectory.



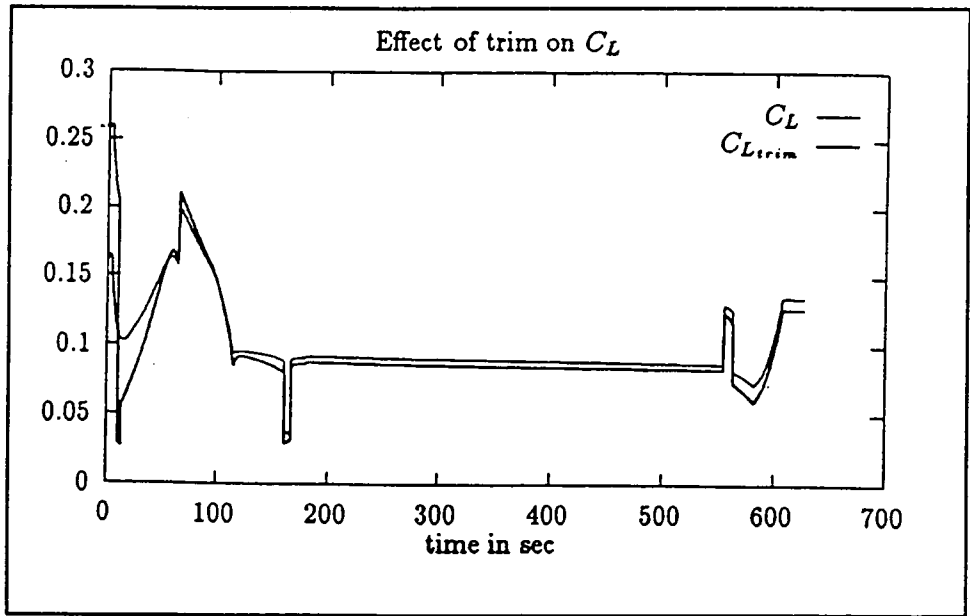


Figure 7.3 *Lift coefficient for trimmed and untrimmed flight*

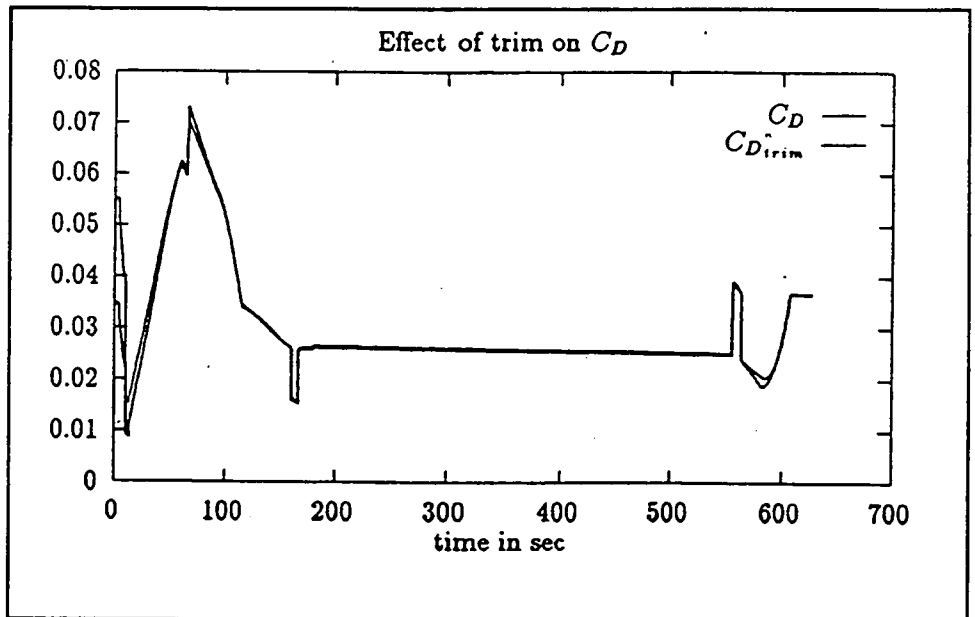


Figure 7.4 *Drag coefficient for trimmed and untrimmed flight*

7.4 Effects of the canard on stability and control

The use of canards may reduce the need of large deflections at low speed. The canard gives an almost neutral stability at low AOA. At higher AOA the canard stalls and there will be increasing pitch stability, however not so strong as for the configuration without canards.



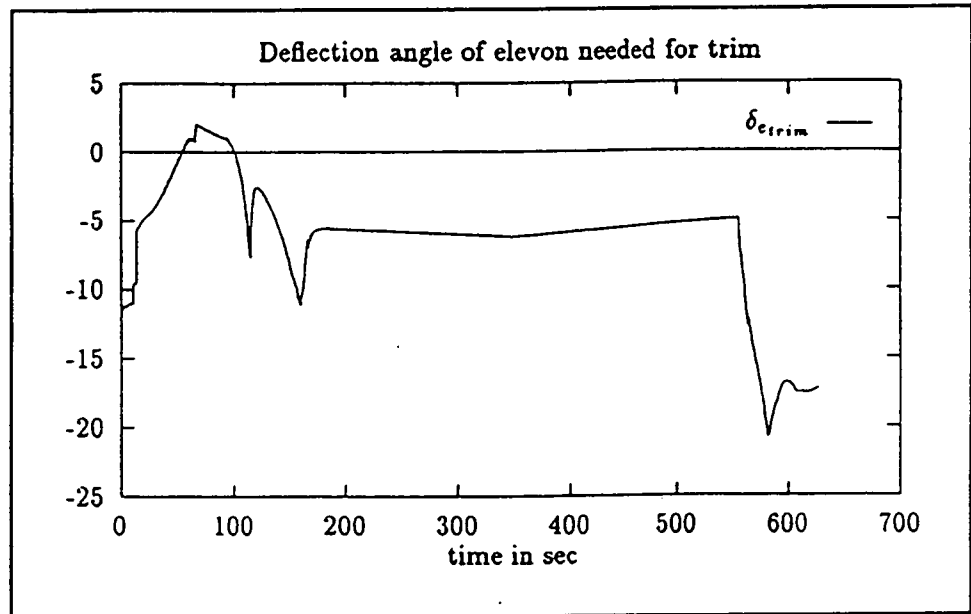


Figure 7.5 *Angle of deflection of the elevon needed for trim*

This configuration requires less rudder deflection and thus less drag penalties. The canard is thus a means for reducing trim drag and stability augmentation. However at high speeds the canard is not necessary for stability purposes.

The canard is placed at the hottest portion of the vehicle. Therefore it was decided to make the canard retractable. In order to do so, the canard had to be repositioned.

More information can be found in ref. [7.7].

Influence of moving the canard

The airfoil section of the canard is the NACA 65A006. This is a symmetric airfoil, so the moment around the np of the airfoil is zero. This means that the moment caused by the canard around the mrp only consists of the lift multiplied with the distance from the canard to the mrp.

While moving the canard, the way C_L changes with α does not change, so C_{L_α} stays the same. Moving the canard hardly influences the place of the np and the change of M_{α} will be neglectable.

One remark must be made here. In flight the canard will influence the stream and a wake will be formed. This wake will influence the stream around the wing. By moving the canard this influence will change and also the stream around the wing. Because of this the lift, drag and moment formed by the wing will change. This influence is neglected.



Influence of deflection of canard

The location of the np is also determined for different deflections of the canard. This was done to investigate the effect of the canard deflection on the sm.

The \bar{x}_{ac} as function of M and δ_c is given in figure 7.6. This figure shows that a deflection of the canard influences the place of the np for at most 5% of the fuselage length.

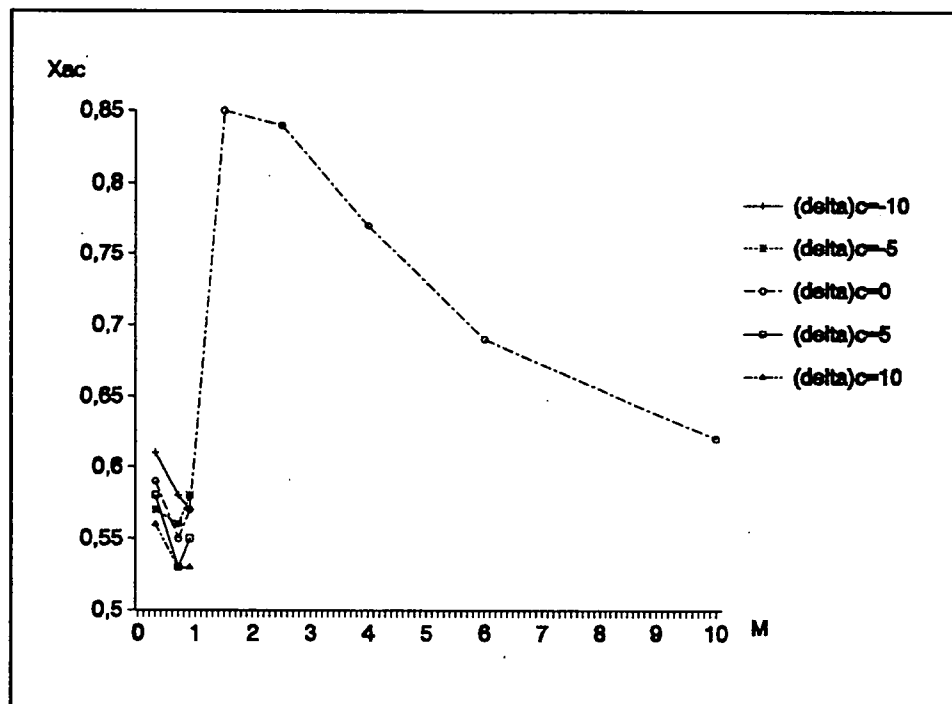


Figure 7.6

x_{ac} as function of Mach en δ_c

Influence of scaling the canard

According to ref. [7.2] dimensionless coefficients are used because scaling has no influence on them. The only condition is that the number of Reynolds does not change significantly. So when scaling the canard the C_L , C_D and C_M of the canard do not change and so the location of the np does not change.

One important effect of scaling is a change of the wake of the canard. This influences the flow around the wing and so the C_L , C_D and C_M of the wing will change. As explained earlier this influence is neglected here.



7.5 Conclusions & Recommendations

Conclusions

The stability margin for the supersonic part of the mission is maintained within its constraints with the use of the fuel consumption scheme. In the subsonic part, the vehicle is expected to be statically unstable.

A trimmed flight condition can be achieved within the deflection limitations of the elevons.

The centre of gravity lies at about 67% of the fuselage length, thus the cg requirement is met. When placing the HORUS considerations must be made of the exact position of placement.

The use of canards will reduce the stability margin and offers more control possibilities. A deployable canard is recommended to avoid heating problems in the high speed region.

Scaling or small movements of the canard will not influence the location of the np.

Giving the canard a deflection influences the place of the np for at most 5% of the fuselage length.

Recommendations

As the influence of the second stage, mounted on top of the HARALD, on the stability and control is not yet known, it is recommended to investigate this configuration in more detail.

Investigate the effects on trim when using other fuel consumption schemes.

A study of other than aerodynamic controls can be made to improve performance during some part of the flight envelope.

A more accurate trajectory can be determined when the values in the thrust and specific impulse matrix are extrapolated. This means that the trim and mission models should be integrated.



References

- [7.1] System Engineering Functional Requirements Document Stability, HAR-FRD-007, TU Delft, 1993
- [7.2] Gerlach, O.H. Vliegeigenschappen I, Part 1 and 2, TU Delft, Faculteit der Luchtvaart- en Ruimtevaart, Dictation D 26-I and D 26-II, 1981.
- [7.3] Shaughnessy, J. Hypersonic Vehicle simulation Model: Winged-Cone configuration, report nr : NASA TM-102610, NASA Langley Research Centre, 23665-5225, 1990.
- [7.4] NASA2, File with formulas of lift, drag and moment coefficients as function of AOA and deflection of the controls of W.C.R.V.
- [7.5] Kolk, C.B. van A first calculation of the static longitudinal stability of HARALD, HAR-STA-002, TU Delft, 1993.
- [7.6] Cremers, G.G.J. Handleiding van twee basic programma's die trimberekeningen uitvoeren aan het spaceplane HARALD, HAR-STA-001, TU Delft, 1993.
- [7.7] Gastel, P. van Stability characteristics of a conical spaceplane design, HAR-STA-003, TU Delft, 1993



8 Mission

Abbreviations

D	aerodynamic drag force (kN)
g	gravitational acceleration (m/s^2)
h	height (km)
I_{sp}	specific impulse (s)
L	aerodynamic lift force (kN)
M	mass (kg)
m	mass flow (kg/s)
S	ground-distance (m)
S_w	wing surface (m^2)
T	thrust (kN)
t	time (s)
V	velocity (m/s)
W	weight (kN)
γ	flightpath-angle (degrees)
θ	pitch angle (degrees)
μ	roughness-coefficient runway
ρ	air density (kg/m^3)
0	beginning of mission
1	groundrun part of take-off
2	transition part of take-off
3	climb part of take-off
c	climb
e	empty
f	fuel
lof	lift-off
land	landing



8.1 Introduction

Now that all characteristics of HARALD are known, the next step is to check whether it is able to meet the specifications (ref. [8.1]). The objective is to transform all of the known data into a single figure of merit by calculating the amount of fuel required to reach the target height and velocity. This quantity can be compared to the fuel available in the tanks. Also, the engine limitations can be investigated, resulting in a flight corridor through which it is possible to accelerate. Within the boundaries of this corridor an optimal ascent trajectory can be found.

To simplify the calculations the whole of the trajectory is split up into the following flight phases:

- take-off of both stages
- ascent of both stages
- separation
- descent first stage
- landing first stage
- ascent second stage
- descent second stage
- landing second stage

It must be stated here that most of the attention has been paid to the ascent of the first stage. The ascent of the second stage is dealt with briefly but sufficiently. The mechanism of separation is considered to be too complicated in this phase of the study. Also, the descent of both stages is neglected in so far that for the first stage 15% of the total fuel weight is allocated as reserve fuel. Furthermore, it is assumed that there is no problem in landing both stages.

In the literature tools can be found to analyze each of the given phases. Also, suitable computer programs, like ASCENT and COLVET, are available at the Faculty of Aerospace Engineering.

The next section gives a short overview of the methods used together with some results. In section 8.3 the effect of scaling will be dealt with. Conclusions and recommendations can be found in section 8.4.



8.2 Methods and results

8.2.1 Take-off

Since the Kourou launch-site is able to launch conventional, vertical take-off launch-systems only, Cayenne Airport in French Guyana (ref. [8.7])

→	latitude	4° 49' 12" N
→	longitude	52° 21' 52" W
→	airfield elevation	9 m above sea level
→	runway length	3200 m
→	runway composition	concrete
→	runway screen height	15.2 m

In fig. 8.1 a typical take-off is subdivided into three parts

- ground-run
- transition
- climb to screen-height

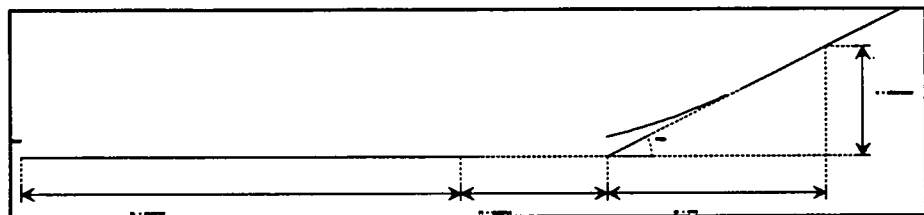


Figure 8.1 *Typical division of take off phase in three segments*

In the ground-run segment the space plane will accelerate from stands-till to a certain lift-off-speed. During this acceleration the vehicle will not only endure aerodynamic drag, but also ground drag as result of the roughness of the runway.

In the transition-segment the under-carriage has lost contact with the ground and therefore the ground-drag diminishes.

The third segment is a linear climb to screen-height, which is nothing more than a safety-prescription. An important requirement is that the required take-off distance does not exceed the available runway. Also, the fuel consumption during take-off has to be calculated.

Since trimmed aerodynamic coefficients with flaps down have not



been calculated, a lift coefficient at lift-off $C_{L,LOF}$ of 0.6 was assumed, which leads to a lift-off-speed of the HARALD combination of

$$V_{LOF} = 148.6 \text{ m/s}^2$$

Now, the different take-off segments can be analyzed (ref.[8.8]), resulting in

→	ground-run	Δs_1	=	1176.1 m
		Δt_1	=	15.9 s
		Δm_1	=	1760.8 kg
→	transition	Δs_2	=	680.0 m
		Δt_2	=	4.2 s
		Δm_2	=	482.1 kg
→	climb to screen	Δs_3	=	15.1 m
		Δt_3	=	0.1 s
		Δm_3	=	10.1 kg
		γ	=	45.2°

For the entire take-off phase this becomes;

$$\begin{aligned} \Delta s &= 1.871.2 \text{ m} \\ \Delta t &= 20.2 \text{ s} \\ \Delta m &= 2253 \text{ kg} \end{aligned}$$

A remark on the high γ : The vehicle probably passed the screen height long before this angle is reached. This has to be examined yet.

8.2.2 Ascent of both stages

After the take-off phase, HARALD begins an ascent to the separation-point from where the adapted HORUS 3B will continue the climb into orbit. The first stage will return to its flight-basis.

The analysis of an ascent trajectory is not something which is easily done by hand. So, two computer-models are applied. First, a look is taken at the flight corridor through which it possible to climb. Only within this corridor an ascent trajectory is feasible. Second, a trajectory is chosen (within the corridor) and the equations of motion (3 DOF, symmetrical flight) along this trajectory are solved.



Energy management

It is obvious that a positive excess thrust (thrust minus drag) is necessary to be able to accelerate and/or climb. In other words, the available (chemical) energy should always be more than the energy required. This form of energy management has been applied in the computer-model EM (ref. [8.3]), which calculates the specific excess power for given ranges of altitudes, numbers of Mach and flight path-angles. The results are stored in a 2-dimensional matrix data file, after which the matrix is displayed in a colour figure called energy-graph EG (see fig. 8.2).

This method has been verified with the help of ASCENT (ref. [8.4] & [8.5]). It can be seen that for every trajectory, which leaves the corridor, the vehicle is not able to climb and at the same time, maintain its velocity. However, it is possible to reach a certain point just outside the corridor because the vehicle can still transform kinetic energy into potential energy. So, it is possible to increase the separation height at the cost of separation speed even when there is no specific excess power left.

EM narrows the field of possible trajectories and so it can deliver considerable time profit in the search for an optimal trajectory.

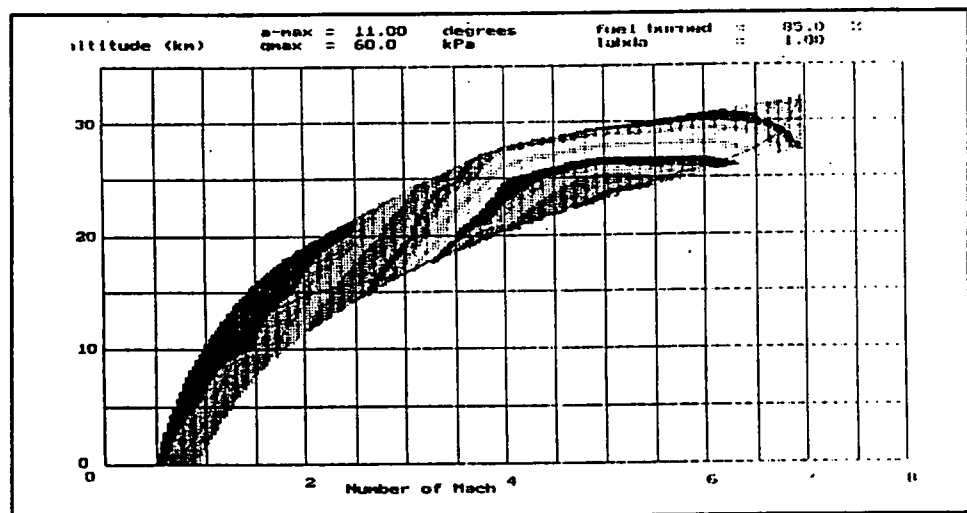


Figure 8.2

Energy graph



ASCENT

ASCENT is a trajectory simulation program especially for winged aerospace planes. It requires a lot of input data:

- vehicle data (geometry)
- environmental data (atmosphere)
- mission data (trajectory)
- simulation data (calculation)

After a simulation all parameters along the trajectory are known, like thrust, drag and weight. The most important results are

- total required fuel weight
- critical points/phases along the trajectory

Figure 8.2 presents the energy-graph of HARALD together with the chosen trajectory from ASCENT.

Results of ASCENT are presented in figures 8.3 - 8.6. In fig. 8.3 the chosen trajectory is displayed with a maximum dynamic pressure constraint of 60 kPa. From fig. 8.4 the total fuel required can be read. A problem is that the thrust of the vehicle is throttled down to very low values; why the available excess power is not used for acceleration, is not clear (fig. 8.5). Finally, comparing fig. 8.5 and 8.6 some critical phases along the flight path can be identified: the acceleration around Mach 2 and the separation point. Since engine cycle transition also occurs around Mach 2, this flight regime should be investigated very thoroughly.



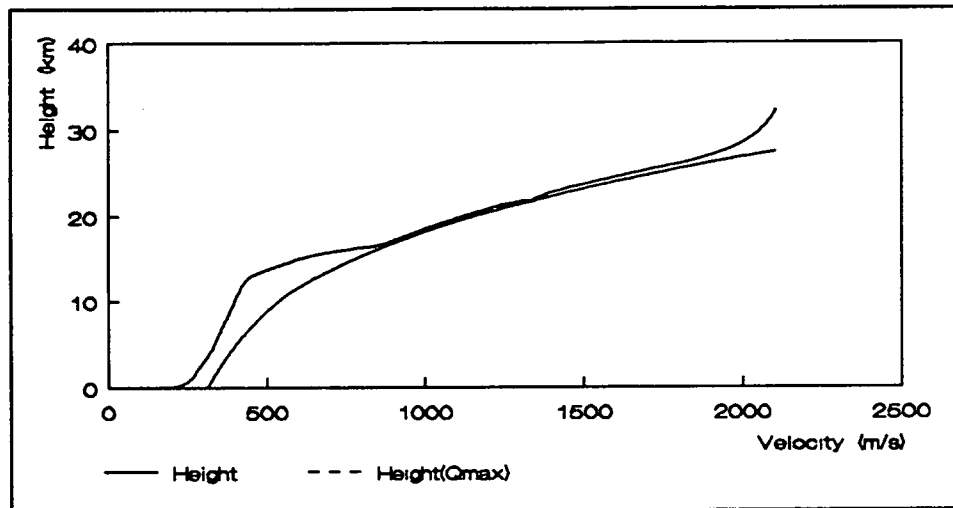


Figure 8.3

Height versus velocity

8.2.3 Ascent of second stage

As mentioned before, after separation the second stage will continue its ascent to a circular orbit, which has been defined as a circular orbit at a height of 1200 km with an inclination of 28.5° . In contrary to the

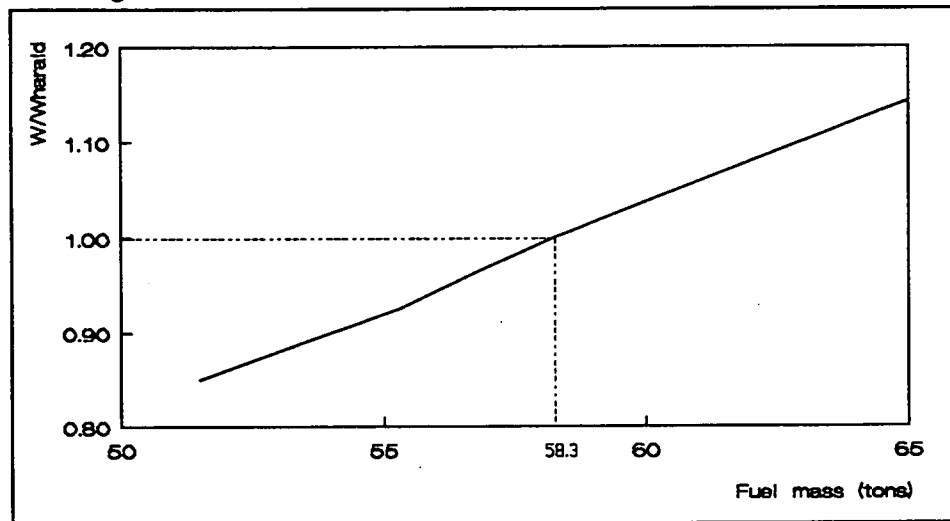


Figure 8.4

Variation of weight versus time

first stage, the second stage uses rocket-engines. Also, the aerodynamic forces are only present in a small part of the trajectory; to keep the analysis simple, they may be neglected. Under these assumptions, three possible kinds of ascent-trajectory were investigated:

- Hohmann trajectory
- constant-pitch-angle trajectory



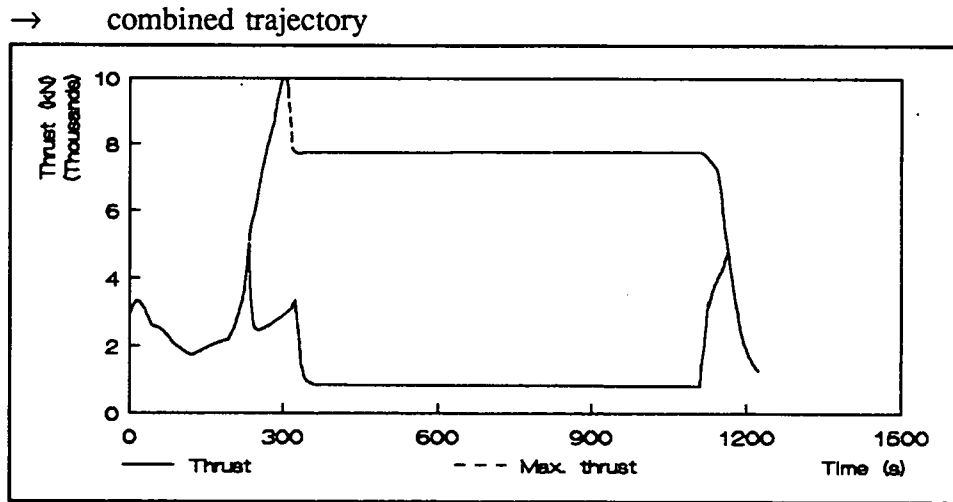


Figure 8.5

Thrust versus time

The Hohmann trajectory is a trajectory of minimum of energy, usually for non-powered flight. So if the vehicle is not able to reach the required height or velocity, it will not with any other trajectory.

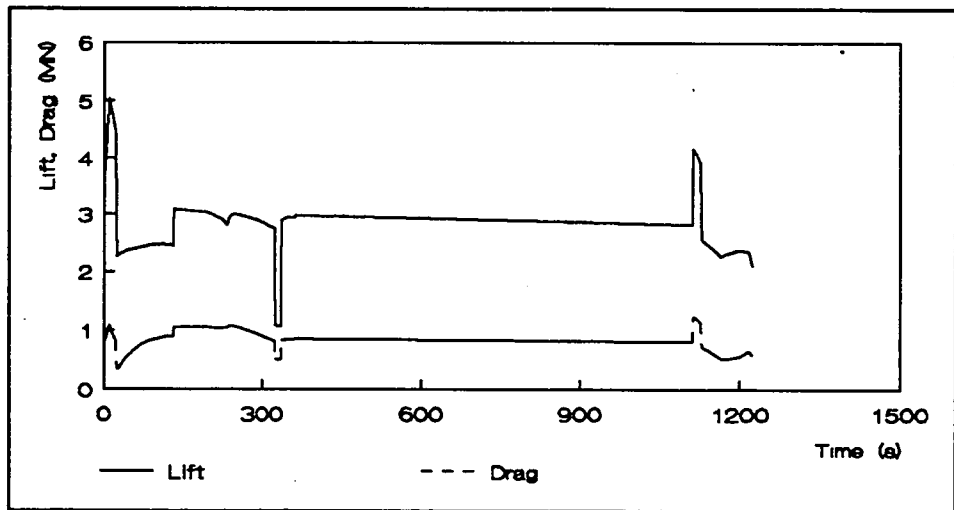


Figure 8.6

Lift and Drag versus time

The constant-pitch-angle trajectory is a powered flight where the burn-out-velocity is a maximum (direct ascent).

Since ASCENT would require data of the HORUS, which is not available yet, the analysis of these trajectories is done with COLVET (ref. [8.6]). COLVET (Calculation Of Launch Vehicle Trajectories) is a computer program for the computation and optimisation of rocket



ascent trajectories and it provides all possible tools to simulate conventional launch systems (remember that the second stage of the HARALD is more or less a conventional system!). Furthermore, COLVET has the possibility to find its own trajectory and corresponding payload when the end conditions of the trajectory are given.

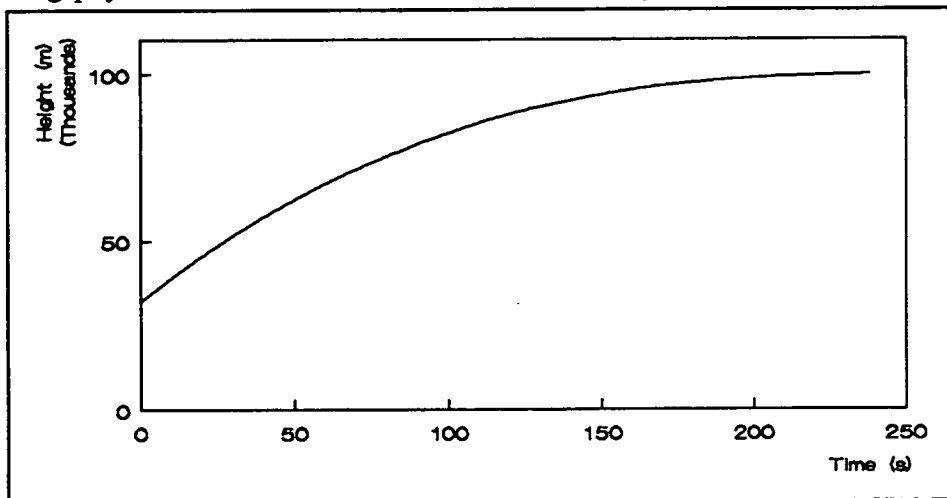


Figure 8.7

Height versus time

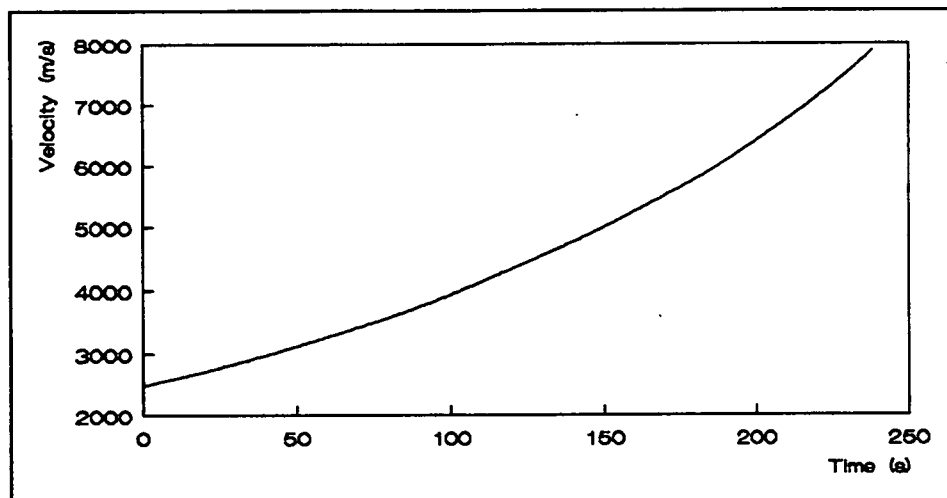


Figure 8.8

Velocity versus time

Here, only the results for the combined trajectory will be given (more results are given in ref. [8.2]). The ascent-trajectory starts with a powered constant pitch-angle ascent up to a height of 100 km and a speed of 7.35 km/s, from where the vehicle will follow an elliptical Hohmann-trajectory by giving two impulsive thrust shots.



Fig. 8.7 and 8.8 give a graphical presentation of height and velocity as a function of time, up to the point where the powered constant pitch-angle trajectory changes into the elliptical Hohmann-trajectory. The different angles are presented in fig. 8.9.

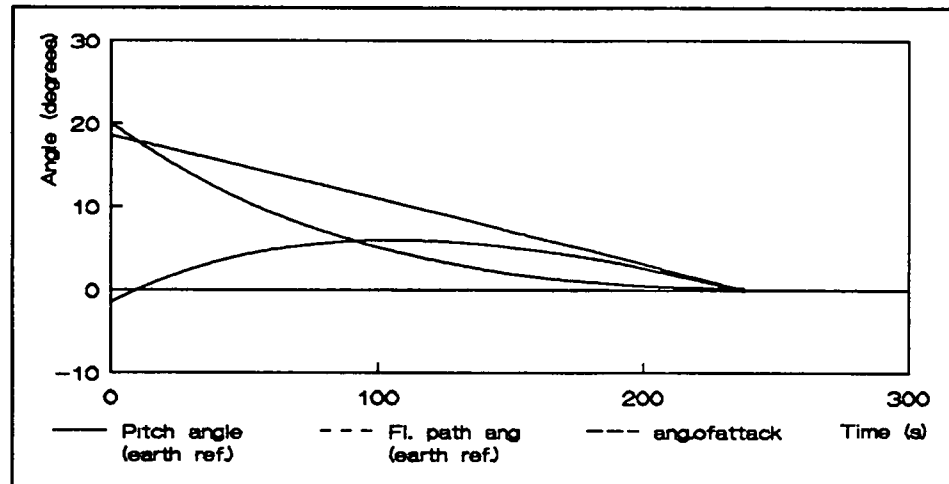


Figure 8.9

Angle in pitch plane

8.3 Effect of scaling

Since it is rather difficult and time-consuming to perform a sensitivity analysis with ASCENT, only the variation in available fuel mass is considered. The result can be found in fig. 8.4.

Variation of the separation point has also been looked at. Since the adapted HORUS 3B is capable of reaching the required orbit from a separation point $M_{sep} = 6.0$ and $h_{sep} = 32$ km, it should be possible to reduce the first stage in size and weight. This should have a positive effect on both operational and development costs.

8.4 Conclusions & recommendations

From the results it is clear that HARALD meets its requirements. Both take-off and landing distances are well within the limits. The first stage is able to accelerate to the desired separation point and the second stage is able to reach the specified orbit.

A considerable part of the mission has not been investigated.



Especially, the separation phase should be examined. Also, the return flight of the first stage and the reentry of the second stage can influence the current design.

Emergency procedures and safety requirements have been neglected, too. They must not be forgotten in the later phases of the design.

Finally, the engine cycle transition point and the separation point should be reviewed and if possible, optimized.

References

- [8.1] System Engineering Functional Requirements Document Mission, HAR-FRD-008, TU Delft, 1993
- [8.2] van der Vorm, P.A. Trajectory computation of first and second stage, HAR-MIS-003, TU Delft, 1993.
- [8.3] Bos, M. Space plane trajectory analysis using the energy management method, HAR-MIS-002, TU Delft, 1993
- [8.4] Korswagen, J.H. ASCENT Trajectory simulation for aerospace planes: development of a simulation program, TU Delft, 1993
- [8.5] Korswagen, J.H. ASCENT User Manual, TU Delft, Report SSR-1, January 1993
- [8.6] Sanders, H.M. The trajectory computation programme COLVET, TU Delft, April 1993
- [8.7] Flight International Airports Guide, first edition, IPC Business Press Information Services Ltd., England, 1974
- [8.8] Sprenger, M.L.M. Trajectory Analysis for the HARALD project, HAR-MIS-001, TU Delft, 1993



9 Costs

Abbreviations

C	costs
CEMR	cost estimation model Roskam
DOC	direct operations cost
EAS	equivalent air speed
GOC	ground and flight operations cost
LCC	life cycle costing
m	mass
NRC	non recurring cost
T	thrust
V	speed
VRC	vehicle recurring cost
W	weight
disp	disposal
l	launch
man	manufacturing
max	maximum
ops	operational
rdte	research, development, testing and evaluation
s	separation
to	take-off



9.1 Introduction

Developing such an advanced space launcher as HARALD, is bound to result in not only high research & development costs, but, due to the non-conventional shape, materials and fuel, also high manufacturing costs. Thus, it is of the utmost importance to get an understanding of these costs in a very early design phase (ref. [9.1]). In the literature one often finds the method of Life Cycle Costing (LCC), which is defined as

a method of expenditure evaluation which recognizes the total sum of all costs associated with the expenditure during its Life Cycle of development, production, ownership and disposal

In our case *ownership* involves servicing, support, maintenance and operational use, whereas disposal costs are negligible. There are four major factors concerning LCC (ref. [9.3]):

- *energy intensiveness*
all cost types should be looked at when the anticipated energy costs are high
- *life expectancy*
development costs tend to become more important when the product is made to last longer
- *efficiency*
the efficiency of operation and maintenance can have a significant impact on overall costs
- *investment cost*
the larger the investment the more important LCC becomes

Another important factor is the current value of money. The discounting process, which is able to predict the worth of money in the future, is particularly important in life cycle cost analyses, because it facilitates the translation of future values to present values. For reasons of comparison, the costs will have to be given using so-called *compatible dollars*, the value of the dollar on a certain moment in time. Here, the results will be presented in 1992 U.S. dollars.

When the life cycle cost prediction has been completed, a sensitivity



analysis should point out the effect of changes in the design. This is done by varying one design aspect and perform the calculations again, while the other input factors are held constant.

While studying the literature, several cost estimation models have been found. The first model used is the *Cost Estimation Model Roskam (CEMR)* (ref. [9.6]). This is a model for cost estimations of airplanes. As the first stage HARALD can be seen as a very modern and improved version of airplanes like the Concorde and the B2, it was assumed that this method was valid for our purposes. But to be sure, the method has been verified by using it to calculate the known costs of existing vehicles and comparing the results to the actual data.

After a few months another model was acquired. *TRANSCOST* is a preliminary cost estimation tool especially made for space transportation systems. Based on a 30 year experience with space launchers, the accuracy of this model is said to be within 25%.

In this chapter only the costs of the first stage are considered because it may be assumed that the second stage HORUS 3B will be bought from elsewhere. In section 9.2 the model according to Roskam will be presented briefly, together with some results, whereas *TRANSCOST* is dealt with in section 9.3. The results of the sensitivity analysis are given in section 9.4. A break-even-point analysis can be found in section 9.5. Finally, section 9.6 contains some conclusions and recommendations.

9.2 The CEMR model

The Cost Estimation Model Roskam (Ref. [9.6]) is a model for preliminary cost estimation for airplanes. It is based on the evolution of an airplane from design to manufacturing, operation and finally disposal. This so-called Life Cycle can be divided into the following six phases:

- planning and conceptual design
- preliminary design and system integration
- detail design and development
- manufacturing and acquisition
- operation and support
- disposal

The total costs of an airplane life cycle are called the Life Cycle Costs



(LCC). According to Roskam these costs can be divided into four parts:

- research, development, testing and evaluation costs
 C_{RDTE}
- manufacturing costs
 C_{MAN}
- operational costs C_{OPS}
- disposal costs C_{DISP}

As has been mentioned before, the disposal costs will not be considered here. For further information about the method we refer to (ref. [9.7]) The model distinguishes between military airplanes and airplanes for commercial use. Because of the non-passenger and first non-commercial purpose of the HARALD, the military-airplane-model has been chosen and is developed further for our purposes.

The most important factors that determine the costs are

- take-off mass m_{TO}
- take-off thrust T_{TO}
- maximum speed V_{max}
- Number of missions

Now, based on the following data of the, baseline vehicle, HARALD 1.5:

take-off mass	$m_{to} = 424,000$ kg	
take-off thrust per engine	$T_{to} = 220$ kN	(6 engines)
separation speed	$V_s = 609$ km/h	(at sea level)

the first estimation of the research and development costs for the first stage is

$$C_{RDTE} = 2.65 \times 10^9 \text{ (1992 \$)}$$

To verify the method, the Concorde and the Space Shuttle were examined. The actual development costs for the Concorde were 10.80×10^9 (1992 \$), whereas the computed costs were 2.33×10^9 (1992 \$). For the Space Shuttle the actual development costs were 16.00×10^9 (1992 \$), but the model predicted 2.40×10^9 (1992 \$).

It is clear that the development costs as predicted by Roskam are



much too low. The main reason for this might be the maximum speed as used in the model. This speed is to be given as Equivalent Air Speed (*EAS*) i.e. the speed scaled down to sea level. Since separation takes place at high altitudes, the air density is very low as compared to the density at sea level resulting in a low *EAS*.

When looking at manufacturing costs the estimations for an airplane like the Concorde differ not much from the actual costs:

computed	0.58×10^9	(1992 \$)
actual	0.53×10^9	(1992 \$)

For the Space Shuttle however, the estimations tend to be too low again:

computed	0.69×10^9	(1992 \$)
real	2.05×10^9	(1992 \$)

Since the manufacturing costs are depending on the development costs, the difference is probably due to the large error in the development cost estimation.

9.3 The TRANSCOST model

TRANSCOST is a statistical-analytical model for cost estimation and economic optimization of space transportation systems. This method splits the total costs into

- Non Recurring Cost (*NRC*) (development $\equiv C_{RDTE}$)
- Vehicle Recurring Cost (*VRC*) (manufacturing, assembly and verification cost $\equiv C_{MAN}$)
- Ground and Flight Operations Cost (direct and indirect cost (*GOC*) $\equiv C_{OPS}$)



TRANSCOST is meant as a tool for System Engineering and Management, when optimum economics are more important than optimum performance. It can be used for the conceptual design phase of all propulsive space transportation system elements and engines (conventional launchers included). Except for the engines, no attention is paid to subsystems. Due to its adequate structure TRANSCOST is especially suitable for LCC analysis and it has been used in the SÄNGER project.

The costs are not expressed in dollars, but in *Man-Year (MY)* in order to have an internationally valid reference, independent from annual changes due to inflation and other factors. The Man-Year can be defined as the total costs of a project, divided by the number of productive (directly accounting) people working on the project. The total costs include material costs, travel costs, office costs, computer costs, all overheads and profits. It should not be confused with annual salary or personnel costs.

A detailed description of the TRANSCOST model can be found in (ref. [9.4] and ref. [9.5]).

Development costs

In order to calculate the (total) development cost of the HARALD, the development cost of the vehicle (without the engines) and the development cost of the engines have to be calculated. Based on a vehicle dry mass without engines of 129 Mg and a mass of one engine of $47.82/6 = 7.97$ Mg, the development costs of the first stage of HARALD become (see also fig. 9.1)

$$C_{RDTE} = 1.26 \times 10^5 \text{ MY} = 23.7 \times 10^9 \text{ (1992 \$)}$$

Manufacturing costs

As the recurring costs are mainly due to manufacturing, it is obvious that the number of vehicles to be built is an important factor. In the case of HARALD, this number will be about 4. However, to show the effect of this number also 3 vehicles will be considered. Again, the vehicle and the engines are separated. An operating empty mass (i.e. with engines) of 176.82 Mg and an engine mass of 7.97 Mg is used, resulting in the recurring costs for a batch of 3 vehicles including engines (see also fig. 9.2)



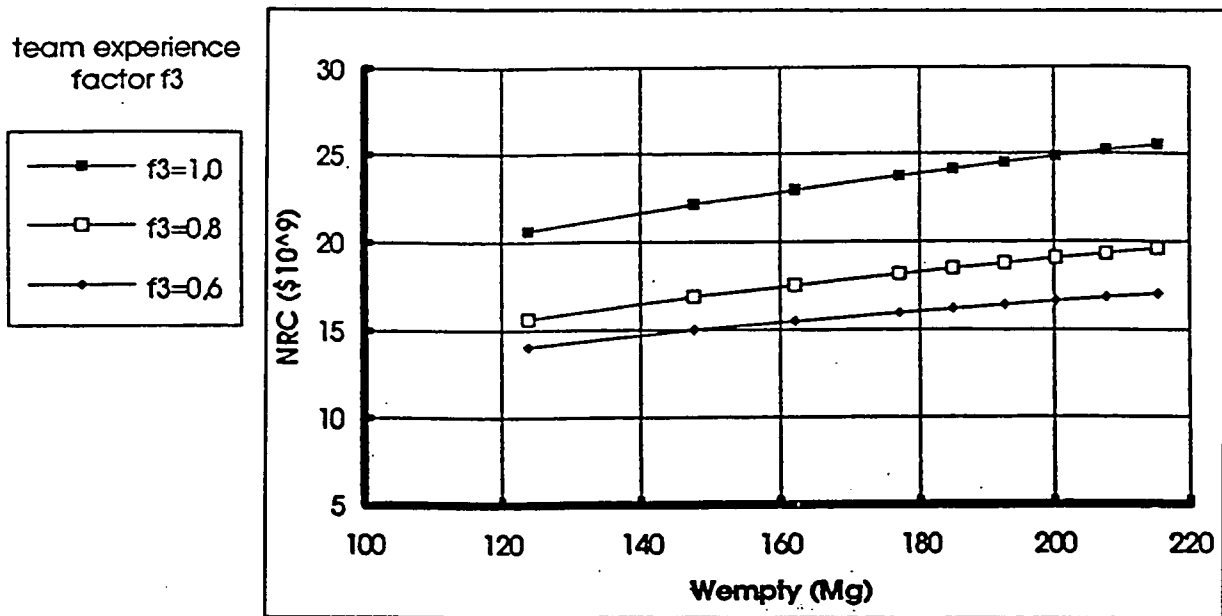


Figure 9.1 Non recurring cost versus empty weight

$$C_{MAN} = 1.37 \times 10^4 \text{ MY} = 2.58 \times 10^9 \text{ (1992 \$)}$$

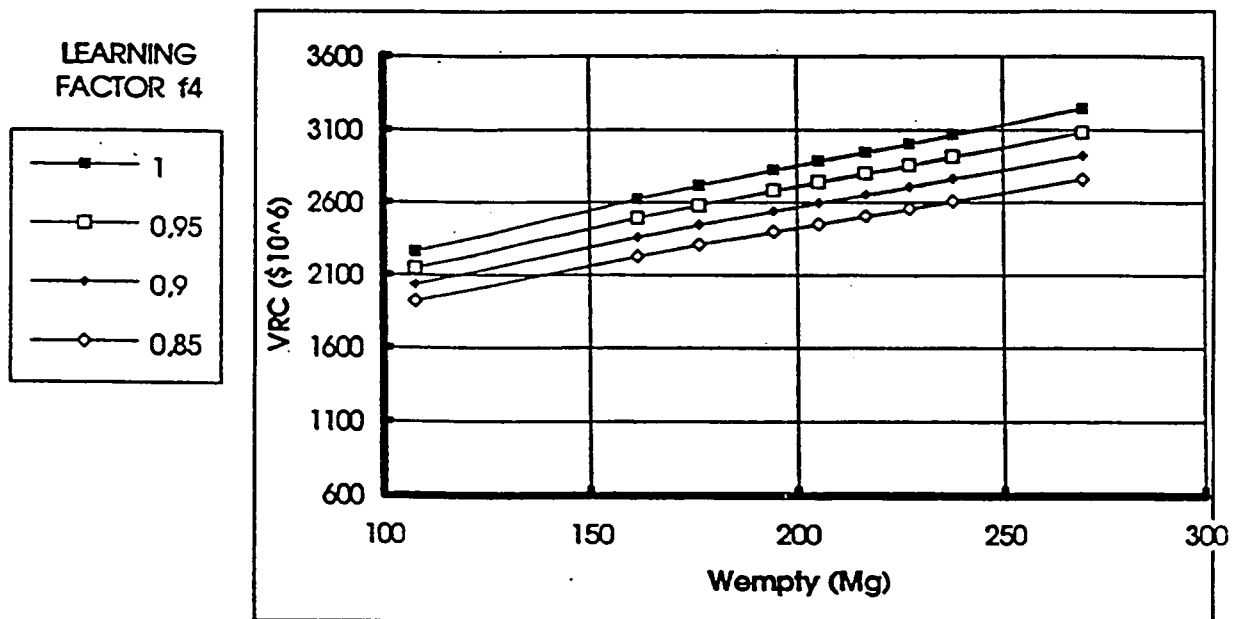


Figure 9.2 Recurring cost versus empty weight

For 4 vehicles the manufacturing costs are

$$C_{MAN} = 1.82 \times 10^4 \text{ MY} = 3.44 \times 10^9 \text{ (1992 \$)}$$



Obviously, the manufacturing costs of one vehicle are 1 billion dollars. Since the number of vehicles to be built is small, the learning factor has no influence and the relation between costs and series number is linear.

Operational costs

Since TRANSCOST is able to estimate the Direct Operating Costs (DOC) only, the other operational items will be taken to be that of the Sanger. The DOC can be divided into four parts

- pre-launch ground operational cost
- launch & mission cost
- propellant cost (for liquid hydrogen this is 0.024 MY-/kg)
- insurance cost

The maintenance cost and the Indirect Operating Cost are assumed to be the same as for the Sanger. When the development cost are amortized, the total launch cost become

$$C_{OPS} = 797.8 \text{ MY} = 0.15 \times 10^9 \text{ (1992 \$)}$$

The development costs of most (advanced) launchers, however, are on the account of the government. Thus, amortization is not necessary, leading to

$$C_{OPS} = 237.8 \text{ MY} = 45.0 \times 10^6 \text{ (1992 \$)}$$

which is low enough to compete with current and near-future launchers.

Fig. 9.3 shows how the operational costs varies with the number of missions for different fuel mass. The reduction in costs for increasing number of missions is clear.

9.4 Sensitivity analysis

First, the development costs versus the empty mass is considered. From fig. 9.1 it can be seen that, when the other parameters are held



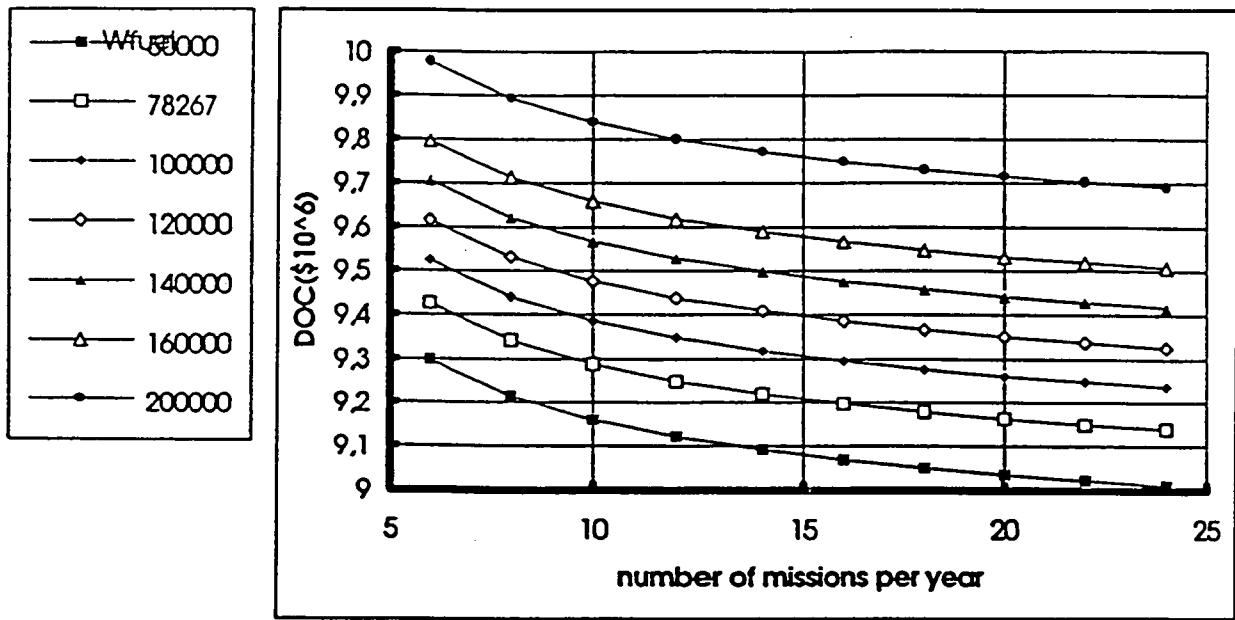


Figure 9.3 Direct operation cost versus number of missions

constant, this relationship is almost a straight line. So, linearization is possible, resulting in

$$C_{RDTE} = 5.11 \cdot 10^4 m_{empty} + 14.6 \cdot 10^9$$

If this formula is differentiated with respect to the dry mass, the slope of the curve is found.

$$\frac{\partial C_{RDTE}}{\partial m_{empty}} = 5.11 \cdot 10^4$$

- For each extra kilogram of dry mass, the development cost grow with approximately 34,200 dollar. When the dry mass of the vehicle grows,
- more constructions and subsystems have to be developed
 - more testing has to be done
 - more people are working on the project

On the other hand, in order to develop the lightest possible vehicle, a lot of extra research and development must be done. In that case a lighter vehicle will cause higher development costs.



For this conceptual design it is assumed that the vehicle designed is the lightest (and thus most economic in operation) possible vehicle. With this assumption, the development costs will increase with increasing dry mass.

Now the manufacturing costs versus the empty mass is considered. Again, according to fig. 9.2 a linearization is possible, resulting in

$$C_{\text{MAN}} = 1.89 \cdot 10^3 m_{\text{empty}} + 0.523 \cdot 10^9$$

If we differentiate this formula with respect to the empty mass the slope of the curve is found

$$\frac{\partial C_{\text{MAN}}}{\partial m_{\text{empty}}} = 1.89 \cdot 10^3$$

The manufacturing costs grow with approximately 1850 dollar per extra kilogram dry mass. The reason for this is that for a higher dry mass

- more material
- more and new constructions
- more people working on the vehicle
- more tools
- more testing
- more (sub)models

are necessary.

9.5 Break-even-point

When the break-even-point, for a payload of 5 Mg, has to be reached before 67 missions (i.e. one third of the total number of missions), the price per kilogram payload has to be (see fig 9.4):

$$C_L/m_{\text{payload}} = 797.8 \cdot 188500/5000 = 30077 \text{ \$/kg}$$

However, when the development costs are not amortized, this becomes

$$C_L/m_{\text{payload}} = 237.8 \cdot 188500/5000 = 8965 \text{ \$/kg}$$



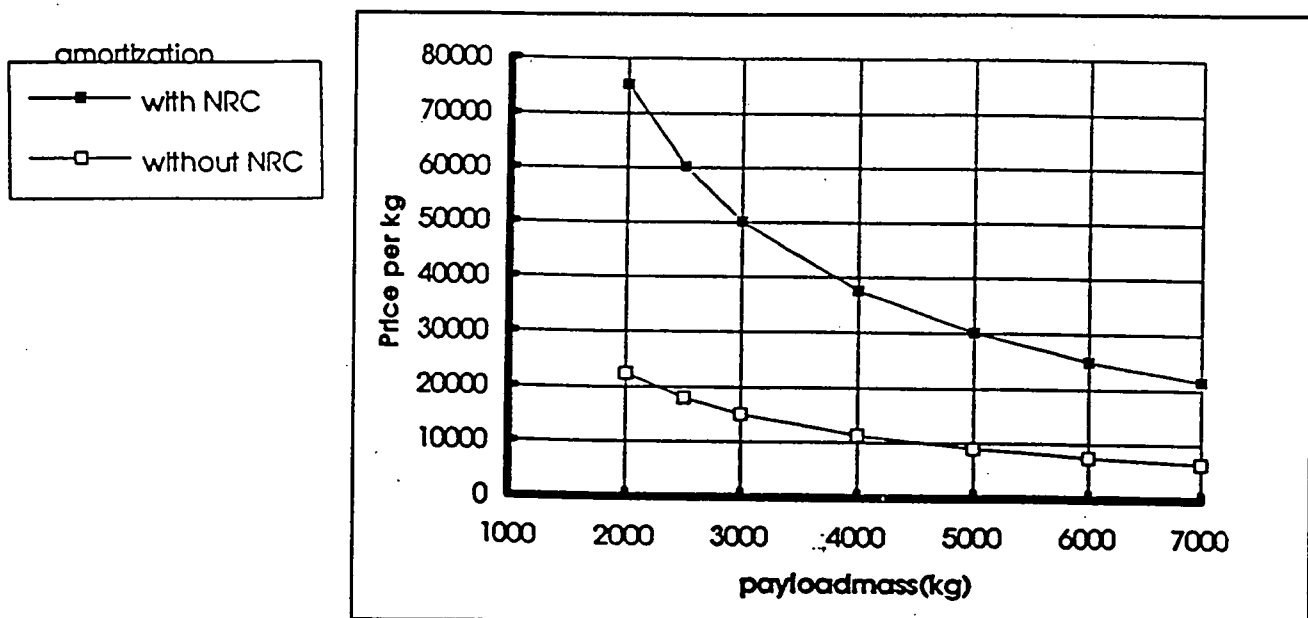


Figure 9.4 Price per kilogram payload versus payload mass

Compared with the price per kilogram payload of ARIANE 44p (30000 \$/kg) the complete amortized HARALD requires the same price per kilogram. But in the case of ARIANE, the development costs are not included in the price per kilogram. When this is applied to HARALD, the operational costs are three times lower, so HARALD will then be a very competitive launcher.

9.6 Conclusions & recommendations

From this study it is obvious that the development costs are very high, because of the advanced concept. Especially the powerplant requires extensive research and development. In contradiction to airplane programs, where the development costs normally are at about 10% of the total production costs, the total production costs are much lower than the development costs, mainly because of the small number of vehicles to be produced. Due to the reusability the operational costs are very low (and the reliability becomes much higher).

For now, it can be concluded that if the financing of the development phase is no problem, it is also from an economic point of view profitable to build HARALD. Since politics and economy influence the space market, more and better market studies must be made.



References

- [9.1] System Engineering Functional Requirements Document
Costs, HAR-FRD-009, TU Delft, 1993
- [9.2] Ashford, D.M., Collins, P.Q. The prospects for European aerospace transporters: part 1&2, Aeronautical Journal, January 1989
- [9.3] Brown, R.J., Yanuck, R.R. Introduction to Life Cycle Costing, Atlanta, 1985
- [9.4] Koelle, D.E. Launch cost analyses for reusable space transportation systems (SÄNGER 2), Acta astronautica, vol. 2 No. 2, 1989, (191-197)
- [9.5] Koelle, D.E. Statistical-analytical model for cost estimation and economic optimization of space transportation systems. TRANS-COST, MBB-report No. URV-185 (1991)
- [9.6] Roskam, J. Airplane design: part 8, Ottawa Kansas, 1990
- [9.7] Punt, P.C. Frenken, G.W.R. Cost of HARALD, a preliminary cost estimation, HAR-COS-001, TU Delft, 1993



Credits

Editors in chief

Bakker, J.
Kraa, A.R.

Co-editors

Kreuwel, W.H.
Oving, B.

Lay-out

Bakker, J.

Authors

Bakker, J.
Bakker, J. & Vossepoel, F.C. & Kraa, A.R.
Kraa, A.R.
Broomhead, M.J.
Vliet, van, L.D.
Luipen, van, J.J.W.
Cremers, G.
Sprenger, M.L.M.
Frenken, G.W.R. & Punt, P.C.

Introduction
Requirements
System Engineering
Aerodynamics
Propulsion
Structures
Stability
Mission
Costs

Special thanks to Skippy Incorporated for the use of their hardware !!



